ADDITIVE MANUFACTURING CASE STUDY AND IMPLEMENTATION STRATEGY

by

Aram Khosh Ettekal

BASc, University of Toronto, Toronto, Ontario, Canada, 2012

A MRP

presented to Ryerson University

in partial fulfillment of the

requirements for the degree of

Master of Engineering

in the Program of

Mechanical and Industrial Engineering

Toronto, Ontario, Canada, 2016

Author's Declaration

I hereby declare that I am the sole author of this project report. This is a true copy of the project report, including any required revisions, as accepted by my examiners.

I authorize Ryerson University to reproduce this project report by photocopying or by other means, in total of in part, at the request of other institutions or individuals for the purpose of scholarly research.

I understand that my project report may be made electronically available to the public.

ADDITIVE MANUFACTURING CASE STUDY AND IMPLEMENTATION STRATEGY

Aram Khosh Ettekal
Master of Engineering
Department of Mechanical and Industrial Engineering
Ryerson University
2016

Abstract

The following report has been created to provide a broad range of information on current additive manufacturing technologies, their present applications in commercial and industrial sectors and predictions for their future deployment in those sectors. The report also examines the ongoing research and development of a variety of 3D printing techniques. The review is divided into three sections. The first section is composed of one to two page summaries of academic journals, thesis papers, consultant perspective articles and company releases. Each individual summary provides a synopsis of the article, as well as what the authors foresee as the future implications of the topic they explored. The second section contains summaries and reviews of technical studies on various aspects of several different 3D printing technologies. Lastly the third section introduces implementation strategy for 3D printed components and presents a study that highlights the effect of part orientation on the structural integrity of the printed components.

Table of Contents

Table of Figures

Nomenclature

A&D	Aerospace and Defense
AM	Additive Manufacturing
AoR	Angle of Radius
BMS	Bare Metal Stents
BVS	Bio-Absorbable Vascular Stents
CI	Carr's Index
DLP	Digital Lighting Processing
DMLS	Direct Metal Laser Sintering
DMMP	Domethyl Methyl Phosphonate
DOPsL	Dynamic Optical Projection Stereolithography
E	Young's Modulus
EMG	Electromyography
FDM	Fused Deposition Model
FR	Flow Rate
HA	Hydroxyapetite
HR	Hausner Ratio
LAM	Laser Additive Manufacturing
LMD	Laser Metal Deposition
LSFF	Laser Solid Freeform Fabrication
NPL	Non-patented Literature
PACs	Printed Active Composites
PCL	Polycaprolatone
PDA	Polydiacetylene
PEGDA	Poly(ethylene glycol) diacrylate
PFTs	Pore-Forming Toxins
PIV	Particle Image Velocimetry
PLGA	Poly-lactide-co-glycolide
PLGA-PEG	Polyethylene Glycol
Ra	Ring's Radius
RHPC	Rapid Hardening Portland Cement
RMM	Rapid Manufacturing Machine
RP	Rapid Prototyping
SEM	Scanning Electron Microscopy
SLS	Selective Laser Sintering
UAS	Unmanned Aerial Systems
VIPr	Variable Impedance Prosthetic
XRD	X-ray Diffraction

1 Introduction

Additive Manufacturing (AM), or 3D printing, is a process which fabricates three-dimensional models through the successive layering of materials. Although developed in the 1980s, it was not until recently that AM gained traction among the media and the masses. The term 3D Printing originally referred to a process of printing layers using specialized inkjet printer heads but has since become an umbrella term for all manufacturing methods involving additive processes. Unlike traditional manufacturing methods, which are subtractive, AM is additive; using up only what materials are needed. This layer-by-layer process, contrary to conventional manufacturing methods which restrict the design freedom, is capable of manufacturing parts with complex geometry. The ease of design and rapid manufacturing associated with 3D printing makes it exceptionally well-suited for rapid prototyping purposes where design changes are frequent and low volumes of parts are required. Given these advantages afforded by AM, it is of particular interest to the manufacturers of commercial and industrial goods.

The objective of this report is to explore different methods and applications of 3D printing that have been utilized in various industries such as aerospace, medical industry, manufacturing and construction. Also some of the technical aspects of the 3D printing process are reviewed by looking at the on-going research in this field. Furthermore, the implementation of 3D printing is demonstrated for an automotive application.

This report is comprised of three sections. The first part is a literature review that examines the methods, applications, and possible opportunities for AM in the future of

manufacturing. From textiles to titanium, this report is meant to educate audiences on the processes involved with AM and to provide introductory, yet detailed, insight into current industries affected by AM and its potential to revolutionize it.

The second part contains elaborated case studies that are related to ongoing research in several different AM processes. Research from multiple academic studies is compiled to provide a snapshot of current AM innovations. The academic journals compiled in this report straddle many different AM techniques and a variety of target industries. The research reviewed focuses on methods of improving 3D printing techniques, utilizing different printing materials and expanding 3D printing to new industries.

The third section describes implementation strategy for 3D printing a part in details. These steps consist of utilizing a computer aided design and 3D printing software to print the part. Furthermore, the provided guideline explains the effect of part orientation on the structural integrity of the part and in order to complete the study, an experiment is performed to demonstrate this effect.

2 An Industry Impact Report

This chapter is an extensive literature review that examines the methods, applications, and possible opportunities for AM in the future. It covers different areas which are affected by additive manufacturing such as the aerospace, manufacturing and medical industries. This section will provide an introductory, yet detailed, insight into the current industries and its potential to revolutionize them.

2.1 3D Printing in the Aerospace Industry

The Aerospace and Defense industry is a major player in the current additive technology market. The ability for additive technology to make customized high strength parts is extremely promising and provides a bright future for the industry.

3D Opportunity in Aerospace and Defense

Additive Manufacturing Takes Flight

"3D opportunity in aerospace and defense" is an article written by Deloitte that discusses the current and future trends in additive manufacturing adoption in the aerospace and defense (A&D) industries. As a pretext to this discussion, Deloitte identifies the unique characteristics of the industry that affect its compatibility with the current and predicted future properties of additive manufacturing. These characteristics include a demand for lightweight and high strength parts, as well as lower quantity production parts that are highly customized for their specific end product. These factors have resulted in the aerospace and defense industries being responsible for 10.2% of total additive manufacturing sector revenues for 2012 [1].

Deloitte describes two factors affected by additive manufacturing that drive its attractiveness to A&D companies. These factors are, “reducing the capital required to achieve economies of scale” and “it increases flexibility and reduces the capital required to achieve scope” [1]**.** Also described by Deloitte are the four paths an aerospace and defense business can follow to utilize additive manufacturing technologies in their business model (these four paths are the same as the ones described in a similar AM automotive sector article produced by Deloitte). These four paths are:

Path I: Companies do not seek radical alterations in either supply chains or products, but may explore AM technologies to improve value delivery for current products within existing supply chains.

Path II: Companies take advantage of scale economics offered by AM as a potential enabler of supply chain transformation for the products they offer.

Path III: Companies take advantage of the scope economics offered by AM technologies to achieve new levels of performance or innovation in the products they offer.

Path IV: Companies alter both supply chains and products in the pursuit of new business models. [1]

The first path is designated as the current most popular path, with companies taking advantage of the cheaper and faster process of 3D printing prototypes rather than making the substantial monetary and time investments required to make prototype tooling. A major development in this path over recent years is the use of AM to produce small volume tooling, as Deloitte cites one company, Advanced Composite Structures, which reported an “overall cost

savings of 79 percent and lead time reduction of 96 percent compared with traditional tooling" [1]. The second path sees companies reducing inventory for spare parts, by instead using 3D printers that have the flexibility to produce many different spare parts on demand. This would significantly reduce the costs incurred by keeping millions of spare parts in warehouses in anticipation of future replacements. The third path is described by companies actively adapting designs to take advantage of the new capabilities of additive manufacturing. In the aerospace sector, this most often means weight reductions and material savings. An important figure was presented by Deloitte that illustrates how strong the drive to reduce aircraft weight is: "removing one pound of weight from each aircraft of a 600+ fleet of commercial aircraft could save about 11,000 gallons of fuel annually" [1].Lastly, path 4 combines the previous three paths approaches, resulting in A&D companies sourcing more and more from suppliers that specialize in additive manufacturing processes (refer to Appendix A-1, Appendix A-2: Framework for Better Understanding AM Paths and Values and Appendix A-3: Potential Application of AM).

Looking towards the future, Deloitte predicts A&D companies will utilize additive manufacturing to bring innovations to both design and supply chains. This will have a large impact on their current suppliers who specialize in traditional tooling and manufacturing, who have little exposure to AM [1]**.**

3D Printing: A Potential Game Changer for Aerospace and Defense

"3D Printing: A Potential Game Changer for Aerospace and Defense" is an article written by Pwc that discusses how new additive manufacturing technologies may change the aerospace and defense industry. The general overview is similar to most discussions of additive manufacturing technology; that it is currently very applicable in rapid, inexpensive prototyping,

and in the future may have the ability to produce a range of parts on demand without dedicated tooling and manufacturing lines. Pwc cites the interest and investments made by large companies and governments as an indicator of the potential of the technology. Boeing, GE, Pratt & Whitney, NASA, and the U.S. government have all made significant investments in additive manufacturing, with the U.S. government creating the National Additive Manufacturing Innovation Institute in 2012 [2].

Pwc goes on to describe the potential advantages and disadvantages of 3D printing in the aerospace and defense industries – focusing on design freedom, materials, costs, and structural integrity. The article describes the geometric freedom that additive manufacturing allows as being a large advantage – allowing designers to utilize geometries not previously possible, to create better products. The range and properties of materials currently available to 3D print with is listed as a disadvantage: "the plastic materials are generally of low quality and not suitable for most production products due to their limited strength, toughness, surface quality, and UV degradation properties" [2]. 3D printing with metal powders is described as an emerging technology, with references to such projects as 3D printing engine blades, but there is no specific discussion of the properties of the 3D printed metal in the article. The article's analysis of the cost of 3D printing focuses exclusively on metals. Cost is listed as another disadvantage due to the fact that metal 3D printers are expensive, the software accompanying them is expensive, and the time per piece produced is very high. In particular, the speed of the metal 3D printer is the parameter that shows the least potential in significantly changing and will be a major hurdle for the technology to overcome in order to compete with current manufacturing methods for full scale production parts. Lastly, the structural integrity of laser

melted metal powders requires research and testing to determine its suitability in different aerospace applications, due to the fact that the grain structure of metals produced in this process is different from metals that are traditionally machined (including the formation of voids). Another metal additive manufacturing method, "electron beam additive manufacturing," is in development stages but has produced grain structures similar to that of machined metals. However, this process requires machining as a secondary step to produce a finished product – increasing costs and decreasing geometric flexibility. Summarizing what this means for the application of additive manufacturing, Pwc discusses the most effective uses for the technology today. Pwc agrees with the commonly held view that current 3D printing technologies are well suited for prototype development. Additionally, low scale, intricate parts are described as a suitable market for the technology, due to the comparable cost per unit with traditional tooling manufacturing methods.

Pwc speculates that the future of additive manufacturing for full scale production is limited by two key factors; product quality and processing speed. As stated before, the grain structure and voids produced with laser melted metal powders significantly limits the range of applications it can be used for, and electron beam manufacturing still requires secondary machining. As with any current application of additive manufacturing, production time is a major concern in the deployment of 3D printing for the aerospace industry. Pwc predicts that within 3-5 years the speed and quality of parts will be suitable for military and commercial aircraft parts, and that in 5-10+ years additive manufacturing parts will be used in high volume weapons and munitions parts [2].

3D Printing Promises to Revolutionize Defense, Aerospace Industries

Yasmin Tadjedeh's article, "3D Printing Promises to Revolutionize Defense, Aerospace Industries", dives into how particular companies within the aerospace industry have used AM to revolutionize the industry. With the acquisition of Morris Technologies and Rapid Quality Manufacturing, General Electric has been working to incorporate AM into its products, focusing millions of dollars into 3D printing research. With the use of direct metal laser sintering, GM has been able to produce engine parts in a single print that with traditional methods would require an incredibly complex assembly of multiple parts [3]. The efficiencies, cost savings, and fuel savings that AM will bring to the aerospace industry are revolutionary, and will bolster the rapid manufacturing of the future.

The AM industry is only becoming more affordable as more advanced printers come out and older printers that would have cost millions are becoming household objects. The usage of these printers has moved from rapid prototyping, to functional prototyping, to complex tooling, and now to making functional parts. Innovation will only continue to rise as prices lower and accessibility to these technologies becomes more widespread.

Lockheed Martin has been using additive manufactured parts across all their business platforms, and has printed parts for satellite manufacturing and other spacecraft programs. These include their Juno satellite, which is destined for Jupiter, or the Orion Multi-Purpose Crew Vehicle, which is envisioned for deep space human transport [3]. Lockheed Martin is also considering using AM to construct small components for their F-35 fighter jet [3]. In the design of spacecraft and fighter jets, where space is a primary concern, AM allows lenient designs that can save space and implement instrumentation without the hassle of invasive brackets.

AM, however, is still just a tool, and full scale production is only a reality in the very distant future. AM "suits small-scale, rapid production innovation" [3], and while it can do tasks in an efficient way that wasn't possible before, it still does not replace traditional manufacturing – "it's a more customizable way to make things, not necessarily a cheaper way to make things" [3]. The large effects of AM are yet to be seen in other transportation industries, but could be applicable, particularly in weight reduction where fuel savings are important [3].

Additive Manufacturing in China

Aviation and Aerospace Applications (Part 2)

In part 2 of Eric Anderson's article, "Additive Manufacturing in China: Aviation and Aerospace Applications", he focuses on China's developments in additive manufacturing in the aviation and aerospace industries. The work of Wang Huaming and a team of researchers on titanium laser additive manufacturing (LAM), specifically laser metal deposition (LMD), has changed the way China manufactures their aviation and aerospace components; putting China at the frontier of this technology [4].

China has printed what they claim to be the world's largest 3D printed titanium component – a four meter long primary load bearing structure that is used in their C919 commercial airliner [4]. Compared to other modern nations, China's titanium manufacturing technology has always lagged behind. The titanium components for the C919 were originally meant to be outsourced to foreign suppliers with a two year manufacturing cycle, but Wang Huaming's team was reportedly able to produce the same component using LMD in only fifty days and at a tithe the price. Performance testing showed that the "printed component

outperformed a traditionally manufactured one" [4]. Beyond the C919 are other Chinese military aircraft that have benefited from the use of titanium components from LAM.

While AM is not yet suited for mass production of parts due its high costs, industries such as defense and aviation, which require small orders of critical parts, can benefit from this technology. Most importantly, this allows China to domestically produce parts they would have otherwise needed to outsource to foreign manufacturers. China's leap in LAM technology will keep them up to speed with global trends and as research develops, they will perhaps play an integral role in the next technological revolution [4]

Additive Manufacturing Trends in Aerospace

In Joe Hiemenz's article, "Additive Manufacturing Trends in Aerospace", he discusses how the aerospace industry has adopted the use of AM and how the trends set by the aerospace industry will impact future manufacturing around the world. The aerospace industry has always been very innovative and inventive, adopting new technologies years before they become common. For aerospace companies whose parts need to be highly customized from very expensive material, AM is an excellent choice for the fabrication, as it allows for better design flexibility and quick turnaround in part revisions. NASA's Mars Rover was outfitted with 70 AM parts [5]. Many tooling and aircraft companies have already begun adopting this technology, taking advantage of the immense time and costs savings of AM. A volunteer company called Connecticut Corsair found it was possible to create complex sheet metal parts by creating plastic molds with AM and then hydroforming the sheet metal to the molds [5].

At the end of all this is full scale production – to produce finished goods using AM. In the commercial and military sector, AM has already begun being accepted in the production of low-

volume parts; fabricating what would take weeks to do in only a matter of days. Unmanned aerial systems (UAS) production is rapidly growing thanks to AM. The complexity, low-volume, and lack of safety regulations makes the use of AM extremely viable and production highly efficient. Aurora Flight Sciences, a manufacturer of unmanned systems and aerospace vehicles, worked with Stratasys and Optomec to combine 3D printed parts with printed electronics. This allowed for much more streamlined production and required far less material and stages to bring a product to completion. Conforming electronics would free up space on the vehicle and improve its aerodynamics.

Nevertheless, there is much to be done with AM that has yet to be seen. The versatility of this technology extends far beyond aerospace and it's only a matter of time before this comes to fruition [5].

2.2 3D Printing in the Medical Industry

From the production of living organs to prosthetic limbs, additive manufacturing could play a crucial role in the advancement of the medical industry. This section provides an outlook on the developments] of additive manufacturing within the medical community.

A Preliminary Investigation into the Development of 3-D Printing of Prosthetic Sockets

This article by Nicholas Herbert, David Simpson, William Spence, and William Ion explores the development of 3D printing methods in the prosthetics industry. Prosthetic lower-limbs require 3 components: the socket, the leg section, and the foot. The socket is considered most important since it must be comfortable for the owner; otherwise, they may not wear it. Correspondingly, the socket and socket ergonomics is the chief focus of this paper [6].

Current prosthetic manufacturing processes are long and inefficient. The method of using plaster of Paris requires many steps to create a final product and all previous data regarding the patient's limb is lost between steps. The addition of CAD/CAM methods have helped to automate this process and retain much of the data that would otherwise have been lost, however, the equipment, especially a CNC milling machine, is very expensive. The entire process still requires the use of plaster of Paris to create a socket, and is a labor-intensive endeavor [6].

New processes include the use of 3D printing to quickly create casts with more precision, accuracy, and data integrity. These methods include stereolithography, selective laser sintering (SLS), and fused deposition modeling (FDM). Stereolithography uses a liquid resin that hardens when in the presence of UV light. The model is held in a vat of the resin and a UV laser produces the model layer by layer as the model descends into the resin. The manufacturing of sockets using this method is slow and the sockets of minimal strength, but demonstrated the potential of rapid prototyping (RP). SLS is similar to stereolithography, except it uses a high powered laser to fuse small particles of plastic, metal, ceramics, or glass powder. SLS produced comfortable sockets that were comparable to traditionally manufactured prosthetics, but were found to be heavier, required many software packages to create and were labor-intensive in design. Researchers are looking into single wall designs in an attempt to control the rigidity of the socket and improve patient comfort. FDM follows a procedure where an extrusion head heats and extrudes semi-molten polymer material through the nozzle and builds the model layer by layer. A collaboration of institutes investigated the manufacturing feasibility of transtibial sockets via FDM methods and created a customized machine for transtibial sockets

called the Rapid Manufacturing Machine (RMM). Since transtibial sockets don't require a high level of dimensional accuracy, they were able to use a wider extrusion nozzle and high working temperatures to reduce build times. Squirt-shape manufacturing is a customized RP process based on FDM methods designed specifically for the manufacturing of prosthetic sockets by Northwestern University. Semi-molten polypropylene is extruded into a continuous helix shape, forming the socket design. Research raised concerns regarding the layered nature of the socket and the anisotropic nature of the material, and long-term trials on three patients were conducted and the most successful case showed an active patient using a socket for over 34 months [6].

Research and trials done with these types of RP methods have proven effective and have demonstrated that RP technology is possible in this industry. Unfortunately, the methods presented are extremely expensive and require a great deal of support and special installation [6].

3D printing on the other hand, is a more cost-effective method, but lacks in accuracy and mechanical properties when compared to the aforementioned techniques. The process uses powdered materials, such as starch or gypsum. A thin layer of powder is first spread over a building platform, where an inkjet printing head extrudes the binding solution onto this layer. When this layer is completed, the process is repeated until the component is complete. While these materials on their own have poor mechanical properties, they can be infiltrated with various resins to improve their strength. In two cases, one transradial and one transtibial, socket casts were created with 3DP and infiltrated with polyurethane resin for improved strength. Both patients agreed that these sockets were as comfortable as the ones made with

traditional methods [6]. The transtibial limb, however, needed to be reinforced with a wrap of 'resin-reinforced carbon fiber material' since the strength of the sockets is widely unproven.

Of all the RP technologies, 3DP has proven to be the fastest, most straightforward, and cost-effective method, but, the strength of these printed materials is still unproven and further studies will be needed to "to assess the dimensional accuracy of the process and the mechanical characteristics of the products compared to the mechanical characteristics of currently used materials" [6].

Bio-Inspired Detoxification using 3D-Printed Hydrogel Nanocomposites

Maling Gou, Xin Qu, Wei Zhu, Mingli Xiang, Jun Yang, Kang Zang, Yuquan Wei, and Shaochen Chen investigate the use of nanoparticles that bind to toxins for detoxification their article, "Bio-inspired detoxification using 3D-printed hydrogel nanocomposites". Pore-forming toxins (PFTs) are 'key virulence factors' of common pathologies and many conventional detoxification methods do not completely neutralize these toxins due to their limited ability to block the PFT molecule [7]. Recent research has developed nanoparticles that can "efficiently bind PFTs and neutralize their toxicity in vivo" [7], however there are some issues caused by toxin buildup in the liver that which risk secondary poisoning to patients with past liver problems. This inspired polydiacetylene (PDA) nanoparticles that are arranged in a "precise 3D matrix with modified liver lobule configuration" [7] with the use of dynamic optical projection stereolithography (DOPsL). This method uses a digital mirror array device which generates dynamic photomasks that can be turned into complex 3D structures via layer-by-layer photopolymerization of biomaterials [7].

This design exploits the hexagonal geometry of the liver which helps to "efficiently remove wastes and xenobiotics from the system" [7]. These PDA nanoparticles work via a cell membrane-mimicking surface which attracts, captures, and neutralizes toxins. Tests were done using lone PDA nanoparticles, red blood cells, and a widely studied PFT called melittin. Red blood cells and melittin were mixed with varying concentrations of PDA nanoparticles and it was found that the more PDA nanoparticles present, the less damaged the red blood cells were. The neutralization efficiency of PDA nanoparticles was found to be approximately 92% [7]. To retrieve the nanoparticles, a hydrogel scaffold was made using poly(ethylene glycol) diacrylate (PEGDA). To attach the nanoparticles to the PEGDA hydrogel, a synthesized diacetylene derivative was used to chemically tether the nanoparticles to the PEGDA hydrogel. By structuring these hydrogels in the shape of the liver, the matrix can very effectively transport PDA nanoparticles and neutralized melittin. This also helps to separate the PDA and PFT from red blood cells, which mitigates any interactions between the red blood cells and the PFTs. The nature of this technology offers a variety of functionalities that have yet to be explored that could lead to many breakthroughs in the development of detoxification methods [7].

3D-Printing of Non-Assembly, Articulated Models

"3D-Printing of Non-Assembly, Articulated Models" is a journal written by a group from University College London that explores the specific topic of creating 3D models that have internal friction components in order to create articulating joints. This capability has direct applications in the medical industry, as the articulating joints in prosthetics are critical to its proper functioning. The processes investigated by the team do not involve any manual modification after printing to create the joints. Every moving part must be a finished product

when it emerges from the 3D printer. Stereolithography and selective laser sintering were chosen as the methods to use when creating these joints due to the higher resolution and part quality they produce when compared to fused deposition modelling. Another important, specific advantage of selective laser sintering is its ability to easily create shapes with overhangs. The team hopes to have a largely automated design and production process, which requires only minimal human intervention to determine the "placement and angular freedom of each joint" [8].

The general joint that was chosen to be the baseline for all of their joints was a ball and joint, with material being added in certain locations to limit movements. To form the ball and socket structure, a very thin gap must be left between the two mating surfaces. To accomplish this in 3D printing, either a thin layer of un-sintered powder or support structure must be left between the two surfaces. Removing the powder or dissolving the support structure can prove to be a challenging task, and the team decided to modify the classic ball and socket design to better facilitate this process. Specifically, the ball was replaced with a cage (a skeletal ball structure) so that there were wide gaps for powder to flow out from. This choice also preserved the smooth, round outer surface of the socket. As previously mentioned, the team desired enough friction at any given orientation for the joint to maintain its pose. This required the skeletal ball, or cage, to be slightly larger than the socket that it mates with. This was not possible with any current 3D printing method, as the two parts would fuse together. To overcome this problem, the team made engraved ridges on the inner surface of the socket so that the cage can be larger than the socket. The tolerances required for this frictional operation are so fine, that a calibration process must be undertaken for each printer before it produces

one of these joints. Once this process for creating a general joint was established, the team set up a process for creating a full, animated body part such as a hand or arm. A mesh was set up for the skeletal/muscular area of the limb, and the joint types and locations were set using 3D modelling software [8].

The major drawback of this process is that as the joint experiences continued use, the surface of the cage and socket are worn away, so that there is less and less friction to keep the joint in a set position. Use of these articulating joints in the medical industry will depend heavily on how this diminishing frictional coefficient can be controlled – since in its current design, these joints rely heavily on a constant and reliable force of friction [8].

Image-Based Analysis of the Internal Microstructure of Bone Replacement Scaffolds Fabricated by 3D Printing

Irsen, Leukers, Bruckschen, Tille, Sietz, Buckmann, and Müller explore in their article, "Image-based analysis of the internal structure of bone replacement scaffolds fabricated by 3D printing", the internal structure of synthetic bone replacements produced by 3D printing methods and post processing procedures. For the 3D printing of ceramic parts, granular material is selectively bonded using a liquid binder, and the final part is created layer by layer. With each layer completion, the building box piston moves down one layer to begin the next. Overhangs need no support since the material is supported by the surrounding unbound powder.

Fine granules of hydroxyapatite are used for synthetic bone grafts. After 3D printing, the scaffolds are fragile and require post processing to optimize mechanical stability. The parts are either sintered in an air furnace at 1250 °C for 3 hours or infiltrated using medical grade

cyanoacrylate and dried for 1 day. The scaffolds are printed larger than the final size to accommodate the shrinkage that occurs in the post processing. Shrinkage of about 25% occurs in sintering [9]. This also reduces the porosity of the scaffold from 52% to 49% [9]. With sintering, the scaffolds lose their re-absorbability. The cyanoacrylate infiltrate reacts with the OH groups in the hydroxyapatite and creates a hard composite [9]. The infiltration closes most of the micro-pores and inter-connected channels within the scaffold. While this is not desirable, it is clear that infiltration could be a viable alternative form of post processing. Changes in the procedure can be made to avoid the clogging of selective pores and channels.

This opens up several opportunities for the fabrication of composite scaffolds with many promising properties for bone replacement [9].

3D Printed Prosthetic Hand with Intelligent EMG Control

Students at Carleton University have prototyped an inexpensive myoelectric hand created from 3D printed parts. Under the supervision of Dr. Leonard MacEachern a team comprised of Alim Baytekin, Alborz Erfani, and Natalie Levasseur, designed and manufactured this highly functional prototype hand. The current cost of myoelectric hands ranges from $15,000 to $50,000, with the affordable hands providing very little functionality and often no more than a single open-and-close-grip. Conversely, the high end ones offer articulate functionality with individually actuated fingers and a wide variety of grips [10]. The need for an affordable and highly functional prosthetic hand has never been greater.

To reduce the cost of creating these prosthetics, new methods had to be developed. Traditional electromyography (EMG) signal acquisition systems were replaced with high resolution analog to digital converters and the signal processing was done on a microcontroller.

A standard commercial FDM 3D printer was used to print components, which costs far less than the traditional way of manufacturing electromechanical hands.

The prosthetic hand contains 4 parts: a 3D printed electromechanical hand, an EMG interface, a microcontroller, and a stable embedded control system. The hand contains over 30 components, including 15 unique printed components, and is actuated with high torque hobby servos controlled by the microcontroller. The EMG acquires muscle impulses from the residual limb, amplifies them, and passes them to the analog-to-digital converter. The signals are then outputted to the microcontroller which controls the actuation of the motors in the hand. A pressure sensor in the prosthetic thumb provides input when the hand grips an object and triggers a haptic feedback system, vibrating in response to a successfully received command [10].

The fifteen unique hand components consist of the finger segments for all fingers and the palm of the hand. Using an FDM printer, these parts take approximately 18 hours to print and are then dipped in a bath of basic solution to dissolve any support material used during the printing. This takes about an hour and the entire printing of the hand costs about $250 [10].

The advantages of using a 3D printed hand are clear. Not only is it inexpensive and affordable, but it offers nearly the same degree of functionality as high end prosthetic hands. As the adoption of 3D printing accelerates and the prices of printing materials decrease, these hands will be printable for only tens of dollars. They are highly customizable and can easily be modelled according to the patient's preference.

The Printer of Youth

Excerpt from "Fabricated: The New World of 3D Printing"

An excerpt from Stephanie Owens' book, "Fabricated: The New World of 3D Printing", entitled "The Printer of Youth" explores the future possibilities and capabilities of 3D printing body parts. She explains a "3D printer ladder of life", where the complexity of body parts increases as you climb up the ladder. At the bottom of the ladder are inanimate body parts that are easily replaced, such as dental crowns of artificial limbs. These are already very common and are widely used by those who require it, from orthodontists to war veterans. Artificial limbs have also become customized to not only be functional, but stylish as well. Bespoke Innovations is a small San Francisco company recently acquired by 3D Systems that designs and 3D prints custom prosthetics. Customers are allowed to select design styles, such as patterns, material plating, and finishing's that go onto the limb. The uniqueness of these limbs allows wearers to be expressive through their choice of design and have become something which gives wearers a sense of pride [11].

Another rung up the ladder is 3D bone implants made from titanium or polymers. Polymers offer properties that titanium or ceramic printed bones would not have, such as the choice to infuse the polymer with bioactive bone growth additives, or antibiotics and anti-inflammatory drugs. In 2012, a titanium jaw was successfully 3D printed for a patient with oral cancer. A CT scan of the woman's jaw was conducted and Xilloc Medical, a medical design company, used computer algorithms to "add thousands of irregular grooves and hollows into the jawbone" [11] with the purpose of allowing her veins, muscles, and nerves to more easily weave and integrate the jawbone into her body. With the speed at which this technology is

developing, it is only a matter of time before the printing of organs and tissues becomes a reality.

3D Printing & the Medical Industry

An In-Depth Analysis of 3DP's Potential Impact on Health Care

Additive manufacturing or 3D printing is a process in which a CAD drawing is taken and used to create a 3 dimensional object through various complex processes. In this article by Nancy Bota, Ethan Coppenrath, Danying Li and Michael Manning, "An in-depth analysis of 3DP'S potential impact on health care", an overview is given on the specific methods and techniques of AM developed throughout the years, as well an insight in the relationship between AM and the medical industry.

In the article, the authors summarize eight different technologies used for AM. The first mentioned is Stereolithography. This process is explained as an additive manufacturing process in which resin or a photopolymer is layered multiple times in a cross section of the original design [12]. Fused Deposition Modeling is a technique where an extrusion nozzle heats polymers and distributes it in small beads, layer by layer [12]. Selective Laser Sintering uses high powered lasers to bond material powders into 3D shapes [12]. 3D Microfabrication is a process in which a desired object is traced in 3D by a laser inside the gel, where the portion of the gel that comes in contact with the laser is hardened [12]. Another method outlined is Electron Beam Melting, where an electron beam melts layers of metal powder together to create solid metal parts [12]. The final method mentioned, 3D printing**,** is a process of AM where layers of powder and binding material are printed across the cross section of a model, similar to conventional 2D inkjet printers [12].

In the medical industry the three largest sectors in which AM can be utilized best is orthopedics, prosthetics and regenerative medicine. Orthopedics AM, specifically 3DP, allows for implants to be customized and fabricated specifically for the customer's needs. For prosthetics, the biggest benefit is the ability to create customizable and detailed parts at a much lower cost. Regenerative medicine is the practice of synthetic organ regeneration and tissue engineering. Currently, there are a small number of firms that have begun printing synthetic organs [12]. The medical industry has demonstrated a large increase in patents as the industry continues to grow in large part due to technologies such as AM (see Appendix A-6).

The most prominent companies in this industry are MIT, Z Corp and Integra. They have not only developed a large amount of the core industry knowledge, but also hold the base IP for the business. MIT specifically has the base IP from which other firms must license or invent around and that's exactly what Z Corp and Integra has done. Bio-Tech firms such as Regeneron, Osiris and Genetech are big players in the regenerative medicine industry, and subsequently have a high degree of interest in AM. With regards to prosthetics and orthopedics, the top firms are mainly comprised of Stryker, DePuy, Medtronic, and Synthes [12].

The value chains of each sector for medical applications will depend on current conventional methods and how the implementation of AM will affect this. Regulations for the technology will affect regenerative medicine due to ethical issues. With this technology moving forward, stem cell research would need to be accelerated as well. With regards to technology in the medical industry, there is no regulatory challenge outside of the normal FDA, which allows firms to quickly implement AM practises. Going forward, the authors offer huge praise for the technology and identify AM immediate benefits in areas such as orthopedic implants, dental

replacements and prosthetics. The adoption of AM as a standard tool in the hospital will be dependent on cost savings and doctors' willingness to embrace it. However, regenerative medicine and organ printing has an uncertain future as it straddles ethical boundaries.

3D – Printed Prosthetics Roll off the Presses

The article authored by Sujata K. Bhatia and Shruti Sharma, titled "3D-Printed Prosthetics Roll off the Presses", offers insight into the process of additive manufacturing and the application's availability to the medical industry. Beginning with an overview on how AM has developed over the years, the author proceeds to analyze the processing methods available in the industry. Stereolithography is an additive manufacturing process in which resins or photopolymers are layered multiple times in a cross section of the original design [13] . The next method described is Inkjet printing**,** which is similar to conventional 2D inkjet printers where layers of powder and binding material are printed across the cross section of a model. Selective Laser Sintering is also outlined. SLS uses high powered lasers to bond material powders into 3 dimensional objects. The final method included is Fused Deposition Modeling**;** a process in which an extrusion nozzle heats polymers and distributes it in small beads layer by layer. A visual depiction of these AM methods may be found in Appendix A-7, Appendix A-8, Appendix A-9 and Appendix A-10.

The authors go on to address the attractions of digital imaging and additive manufacturing. "With the evolution of multi-detector computed tomography and magnetic resonance imaging, high-resolution 3D image data can be acquired within a single breath-hold" [13]. Medical applications for additive manufacturing include vascular networks, bandages, bones, ears, exoskeleton, windpipes, and dental prosthetics [13]. A brief description of how AM

is employed in each of the applications is given in the article. Another significant opportunity mentioned is prosthetics sockets. The overwhelming majority of AM literature is dedicated to this subject, and it is clear that AM is becoming a cornerstone in prosthetic socket development [13].

Looking to the future, various challenges must be met. Printing speeds need to improve, the range of 3D printable material must expand and more research must be conducted on the mechanical properties of AM materials, and how they behave in different environments.

A Variable Impedance Prosthetic Socket for a Transtibial Amputee Designed from Magnetic Resonance Imaging Data

David Moinina and Hugh Herr's report, "A Variable-Impedance Prosthetic Socket for a Transtibial Amputee Designed from Magnetic Resonance Imaging Data", explores the design of a variable impedance prosthetic (VIPr) socket using CAD and additive manufacturing.

Currently, in the production of prosthetics, the construction and modification is based primarily on the non-quantitative craft process, and is dependent on the experience of the prosthetist. This ultimately affects the structural integrity of the socket, as well as how comfortable it is. Initially, CAD is used to interpret data produced from scanning the limb or a generated positive mold. This process relieves pressure by varying the socket wall thickness or adding mechanical features. The article's research relies on quantitative biomechanical data from advanced surface scanning and MRI technology. Polyjet Matrix^{TM} 3D printing technology is the AM method used in creating this VIPr socket. "As a preliminary evaluation of this hypothesis, a VIPr socket is designed, fabricated, and then compared with a conventional prosthetic socket designed by a prosthetist using standard best-of-practice methods" [14].

Since this study is focused on understanding the effects of spatially varying prosthetic wall impedances on socket interface pressures, both sockets were made to have identical internal geometry and shape. The 3D surface image was then transported into SolidWorks after the completion of the surface scan. The use of magnetic resonance imaging through MRI produces an accurate but approximate stiffness of each location on the residual limb from the distance between the bone and the outside surface of the skin.

2.3 3D Printing in the Manufacturing Industry

Additive manufacturing will change how all manufacturing companies operate. This section will discuss the many advantaged and disadvantages 3D printing will bring to the sector.

3D Opportunity in Automotive Industry

Additive manufacturing hits the road

"3D opportunity in the automotive industry" is a paper produced by Deloitte that explores the way in which the capabilities of 3D printing will change the automotive industry due to its competitive advantage, how companies can utilize this new technology, the "drivers" for this change, and the possible hurdles 3D printing has to overcome to be widely adopted in the sector. They expect that the potential of 3D printing technologies can change the design, manufacturing, and distribution methods of the automotive sector. To do this, four paths are outlined through which original equipment manufacturers and suppliers can utilize 3D printing technologies.

The first competitive edge 3D printing provides is an opportunity for "product innovation" [15]. 3D printing allows for flexibility in design and material selection/combination

that cannot be accommodated by current manufacturing methods. When these traditional limitations are removed, designs can be made to improve strength, reduce weight, and lower costs from saving material. The second major competitive advantage of 3D technologies, cited by the article, is the ability to drastically change supply chains. Major capital investments dedicated to single products will no longer be required, which results in the flexibility of different production locations to change from producing one part to an entirely different one very quickly. This would drastically decrease the need to have long supply chains delivering from a single specialized location. As well, replacement parts would no longer need to be produced at the same location and with the same equipment for small quantity orders. Instead, 3D printing equipment would have the flexibility to produce a range of parts in small quantities for spare and replacement purposes (see Appendix A-2: Framework for Better Understanding AM Paths and Values).

Deloitte outlines four ways in which a company can implement this new technology and utilize the advantages it presents:

Path I: Companies do not seek radical alterations in either supply chains or products, but may explore AM technologies to improve value delivery for current products within existing supply chains.

Path II: Companies take advantage of scale economics offered by AM as a potential enabler of supply chain transformation for the products they offer.

Path III: Companies take advantage of the scope economics offered by AM technologies to achieve new levels of performance or innovation in the products they offer.

Path IV: Companies alter both supply chains and products in the pursuit of new business models. [15]

3D Printing and the Future of Manufacturing

"3D Printing and the Future of Manufacturing" is an article written by the Leading Edge Forum that attempts to predict the future landscape of the manufacturing industry after the entrance of 3D printing technology.

The article argues that 3D printing will be a significant disruptive technology in relation to the current large scale manufacturing processes that follows the Ford-inspired mass production model. There are several innovative factors 3D printing brings to the industry that warrants its accreditation as a disruptive technology: flexibility to produce many designs using the same piece of capital equipment, installation and operation in almost any location, capability to produce complex shapes and geometry often not achievable using conventional methods, and the potential to manipulate material properties because of the different material cooling rates possible with 3D printing. The flexibility to create many different products means that large numbers of specialized factories producing specific parts will no longer be necessary – any factory will have the potential to produce almost any part without making any capital expenditures or changes. The fact that 3D printers can be operated at almost any location questions the need to have factories, with large capital investments, producing a specified or limited range or parts. The article forecasts that factories will not altogether disappear, but the way in which they function will have to change to meet the precedent set by the technology's new capabilities and consumer's (both businesses and individuals) new expectations. Examples

of such changes would be the disappearance or downsizing of distribution and warehouse departments [16].

The Leading Edge Forum states that the quality of 3D printed parts still lags that of parts made using traditional manufacturing methods, but that this gap will close. In the same fashion, they expect the speed and cost effectiveness to also catch up with the current manufacturing methods. This disparity is first expected to become less defined in newer product fields such as 'prosthetic limb coverings and vintage replacement parts', and then eventually in established markets as well. Another likely route for 3D printing into the manufacturing industry is through the manufacturing of materials better suited for additive techniques, like titanium, rather than the current subtractive processes [16].

The Leading Edge Forum outlines four distinct 'paths' that 3DP can be incorporated into an automotive manufacturing company. The first, and currently most popular path, has companies exploring the technology by using it to aid in the design process, small scale prototype production, and making custom, low use tools. Path 2 sees companies utilizing the range of products that a single 3D printer can produce, and taking advantage of that by reducing stock inventories and the way in which low-order, spare parts reach the customer. Path 3 is described as 3D printing driving product innovation and design because faster, cheaper changes can be made to prototype products using AM methods than the traditional manufacturing methods used today. Path 4 combines all of the uses of 3D printing described in the first three routes, resulting in a significantly different business model than is seen in today's OEMs [16].

These are the reasons for, and ways in which 3D printing will enter the manufacturing sector, as predicted by the Leading Edge Forum [16].

Disruptive Manufacturing

The Effects of 3D Printing

"Disruptive manufacturing, the effects of 3D printing," is an article written by Deloitte that gives the reader an informational background on the subject of 3D printing, and then explores the benefits and challenges of the technology for current manufacturers. The basic process of utilizing a laser to solidify specific areas of a vat of material is described, without going into major detail. The timeline of additive manufacturing's development is also laid out; from its inception (pioneered by Charles Hull), early commercialization with 3D Systems Inc., research into additive manufacturing organic structures, and high quality-low cost 3D printers geared toward private use [17].

From this brief summary of additive manufacturing's history, the article launches into the topic of how businesses (especially those in manufacturing) can succeed in a marketplace where this technology is present. Deloitte cites a prediction that the "Sales of 3D printers will approach $5 billion in 2017, up from $1.7 billion in 2011" [17]. Deloitte expects much of this growth to occur in the manufacturing sector. Deloitte states as a pretext to this discussion that: "When new technologies emerge, the decline of industries is never rapid, nor is it immediate" [17]. The benefits of utilizing additive manufacturing technologies are: inexpensive prototypes, reduced lead times, hastened innovation process, the ability to use just-in-time inventory systems, reduced inventory overhead costs, ease of customization and increased design capabilities [17]. The challenges are listed as being: often inferior in quality, long cycle times,

limited materials, high material cost and limited size [17]. Deloitte agrees with the prediction that 3D printing will create a revolution similar to the industrial revolution. They state that it is therefore extremely important for a business to recognize the effect that additive manufacturing will have in their sector; failure to do so could lead to loss of market share.

In summary, Deloitte expects 3D printing to have a significant and long lasting position in many established market sectors such as manufacturing, and it is critical for businesses in those sectors to adopt their practices to best utilize the new technology so that their processes do not become obsolete. Deloitte recommends that companies establish the internal initiative within the organization to pursue additive manufacturing. This means investigating and deciding how the technology best fits into their sector and company. Next, they have to follow through with these investigations by investing in their decisions. Thirdly, a network must be created so that the additive manufacturing business units have the resources and connections to pursue the internally established goals. This means changing the organizational structure as needed to accommodate these business changes. In many cases this results in adding skill sets to the company to support the business unit. Lastly, companies should implement and take the changes to market; strategize on how the business unit will function, how will these innovations be brought to market, who is the target market and how profitability will be obtained [17].

Printing Teddy Bears

A Technique for 3D Printing of Soft Interactive Objects

In Scott E. Hudson's paper, "Printing Teddy Bears: A Technique for 3D Printing of Soft Interactive Objects", he explores the applications and methods of 3D printing soft materials, such as felt and yarn, which extends the scope of 3D printing beyond the precise and hard

materials we are accustomed to. He describes his own method of 3D printing soft materials and shares his insight on the techniques as well as the embedding of functional and structural components within the soft materials, such as motors and electric circuits, or plastic meshing for added stiffness and rigidity.

Hudson's printer works very much in the same way as a regular FDM printer – it uses layers upon layers of yarn to create a final product. What's different is a process called *needle felting* where a barbed needle is repeatedly driven into the fibers, pulling fibers from upper layers and entangling them with fibers in lower layers. This is done as yarn is being fed through the printer and is controlled by a feed lock mechanism, which controls the flow of yarn. Tension is kept low on the yarn because of a tendency to pull out previously felted yarn. A low friction lock works best to mitigate this issue. When the printer head is in location it follows several steps: it initiates the punch sequence which performs an initial short needle punch, closes the feed lock, performs *N* (usually 3) full length needle punches, opens the feed lock and moves into the new location to begin this process again. Currently, this results in a printing rate of 2mm per second.

Due to the material being used, there are several issues with geometry that follow it. Printing taller objects was found to be rather difficult. The thinner the base of a relatively tall print (approximately 75mm), the more problems there were with it, due to wobbling (a base diameter of 50mm was printed without difficulty). As with any 3D printing process, the geometry cannot be totally arbitrary, and supports are needed for overhanging elements. With these printing substrates, it can be tricky to determine where to cut the support material without damaging the integrity of the layers above it. Tests were done to determine the

maximum tolerance of an overhang without a support and it was found that for angles of up to 55 degrees, the overhangs would print without fail [18].

An exciting capability of this kind of printing is that it allows for innovative, interactive devices with integrated mechanical and electrical components. Hudson explores five ways of accomplishing this task. *Sew in/on later* is the simplest solution where components are sewn in under flaps or pockets after production. *Deep pocket* embedding is required for larger objects with an approximate void of 20mm and follows the principle of creating voids and pockets within the object to store components. Components are placed into these cavities and covered with a foam slip to allow for good felting over. *Direct felt-over* is used for thin components such as wires and is a literal felting over of these components. Tests have shown that the printer can successfully felt over a 2.5mm wire tie. With c*apped pockets*, components are placed in pockets near the surface of the object and a pocket cap is printed separately and then felted over a lip that overhangs the edge of the pocket. Finally, *nylon braided tunnels* can be directly felted onto the object. Afterwards, fibers within any tunnel are removed with a small screwdriver, allowing wires to freely pass through the tunnel [18].

The fastening of hard, rigid materials to the soft, felted material requires the use of a nylon meshing that is embedded into the hard plastic (created with an FDM 3D printer). The nylon mesh allows for good felting of the soft material and a tight binding of the hard material to the soft material. This technique can easily be used to add joints and articulated features, improving the robustness of the print [18].

Hudson's work here opens up many new possibilities for 3D printed objects and extends the domain of 3D printing from primarily hard and precise objects to include soft and imprecise

objects. However, there is still much future work that needs to be done. In particular, the issues of the physical robustness of the felted objects must be addressed. More work should be spent on the design of new types of mechanisms, structures, and electrical components for use with soft felt like material [18].

Titanium Powder used to 3D Print Automotive Parts

"Titanium powder used to 3D print automotive parts" is an article produced by Phys.org that describes a new, less expensive process for manufacturing titanium powder and the implications this may have on the use of 3D printing in the automotive sector. This new process was developed by a company named Metalysis, and involves the use of electrolysis to turn rutile into titanium powder. This process is less expensive and more environmentally friendly than the traditional Kroll procedure that is currently used to produce titanium powders [19].

When this new titanium powder production process is combined with additive manufacturing methods, further savings are made because of the ability to use less material compared to subtractive methods [19]. Lastly, the new process from Metalysis also allows for more common and easily accessible titanium ores to be used, further decreasing the cost of the titanium powder [19]. The application of this technology also reaches beyond titanium powder production. Members of Metalysis describe the technology as being applicable for other metal powder production (including rare earth metals), and 3D printing metal alloys by combining different metal powder types. This alloying process occurs by mixing metals in their solid state (fine powders) – something that Metalysis claims will allow for the production of alloys not traditionally produced due to differences in melting points and densities [19]. Metalysis claims

that regulating the powder ratios and granular size will allow further control over the final alloy's properties [19].

Metalysis forecasts that these cost savings could result in the replacement of specialty steels and aluminum in many different applications, including in the automotive sector [19]. With the growing pressure to make automobiles more and more fuel efficient, an increased effort has been made to make cars as light weight as possible. Previously, this has meant a greater use of aluminum and plastics, with titanium remaining out of reach due to cost. Metalysis expects their process to reduce costs of titanium "by as much as 75 per cent" [19] and hopes that this newly reduced cost, combined with additive manufacturing techniques, will make titanium a competitive material choice in car design.

Challenges and Opportunities in Design for Additive Manufacturing

In the article "Challenges and Opportunities in Design for Additive Manufacturing", Carolyn Conner Seepersad explains that to realize the full potential of additive manufacturing, designers and engineers must transcend the conventional methods of design and adopt new and innovative ways that take advantage of AM's capabilities. Traditional CAD software follows a subtractive design process, where designers begin with very primitive shapes, such as cubes or cylinders, and remove material until a final product is produced. With AM, the process begins with nothing and only the necessary components are added.

Current technologies are ill-equipped to handle AM based design [20]. Commercial CAD tools are not meant to "represent structures with thousands or even millions of surfaces and geometric parameters" [20]. Topological optimization techniques which help to create intricate and lightweight structures fitting for AM are more optimized for improving "combinations of

weight reduction and linear elasticity and their analogs in the thermal and electromechanical domains" [20].

It is a myth that you can make 'anything' with AM – all AM processes have limits much like traditional design and engineering [20]. Using CAE tools that can support 'Design for AM' knowledge, databases of material properties and empirical knowledge of various processes can be built up and perhaps be used for simulation of AM. New CAD systems that are more AM centered are being proposed such as allowing 3D voxel design or generative design tools that can 'grow' a design from a seed and predetermined rules. Simulation of the AM process would allow designers to repeatedly revise and improve parts, leading to leaner and more reliable products [20].

The public's attention to AM is directed at the "prospect of making things themselves" [20] with the use of personal printers or third party services. The profound effects that AM will have on product design and manufacturing are yet to be seen, but "AM is poised to unleash a wave of innovation with profound implications for the way we design and build our engineered world" [20].

Emphasizing of 3D Printing Technology in Packaging Design Development and Production in Local Industries

"Emphasizing the advantage of 3D printing technology in packaging design development and production in local industries," is an article, written by D. Mohamed and A. Mahmoud from Helwan University, that discusses the use of 3D printing technologies to produce product packaging. Specifically, the article is meant to encourage Egyptian packaging companies (and by extension all packaging companies) to utilize additive manufacturing technologies to create

superior designs and reduce waste. The authors argue that today's consumer is more mindful of the environmental effects of the packaging used in the products they purchase, and this concern affects their purchasing choices – it is therefore in the interest of the producer to use the minimum amount of packaging possible, while still sufficiently protecting the product [21].

Before delving into the ways 3D printing can be applied in the packaging industry, the authors give a brief overview of the different methods of 3D printing. The first is inkjet printing, where a nozzle applies a binding agent to a sheet of powder, layer by layer [21]. The second, Digital Light Processing (DLP) is a process where layers of polymer are sequentially exposed and hardened by light [21]. Thirdly, Fused Deposition Modelling layers molten polymer through a nozzle to create a 3-dimensional structure [21]. Fourth, Selective Laser Sintering uses a laser to sinter a bed of powder, with the unsintered powder acting as a bed to support the structure [21]. Lastly, 2-photon photopolymerization is described as a process where a focused laser traces an object out in a block of gel. This technique can produce parts with dimensions under 100 nm, as well as extremely complex interlocking parts [21]. The article then moves to its main point of focus, analyzing the possibility of using additive manufacturing in Egyptian packaging markets. The authors do this through a questionnaire – asking about current knowledge and future plans regarding 3D printing in the industry. Some of the key results of the questions were: 10% of packaging salesmen had experience with 3D printing, 10% of designers know about the 3D printing technology and use it in developing their packages, and 75% of the designers after seeing the sample believed that they can develop their own package using 3D printing and send the sample to production [21].

The authors conclude that additive manufacturing technologies are currently being used in low capacity at the industrial design phase of packaging production, but have yet to break out of this confined scope of application [21]. Looking forward, the authors see additive manufacturing's role in the industrial design of packaging becoming increasingly large, as its flexibility and low quantity speed are of great benefit. Unfortunately, in its current form, the technology's future in full scale production is much more uncertain due to many large challenges, such as rapid large scale production capabilities.

Multi-Physics Analysis of Laser Solid Freeform Fabrication

"Multi-Physics Analysis of Laser Solid Freeform Fabrication" is a thesis paper written by Masoud Alimardani that explores controlling the physical environment of a Laser Solid Freeform Fabrication (LSFF) process so as to control the final product. More specifically, the author focused on the thermal stress patterns in additive manufactured metals that cause delamination and micro-cracks, and how the physical parameters of the process can be controlled to minimize such effects. The thesis paper begins by briefly describing LSFF – a process in which a laser melts fine metallic particles emitted from a nozzle that is directed downwards towards a moving platform. This melted metallic material quickly solidifies on the platform and creates a 'track' of final material. The author goes on to state that the motivation for exploration of this technology is the transition of additive manufacturing from being solely a rapid prototype fabrication application to being a flexible full production method.

During operation, the laser of a LSFF piece of equipment only needs an interaction time of 10^{-2} to 10^{-4} seconds and operates at a power of 10^{3} to 10^{4} W/mm^2 [22]. One of the main drawbacks of LSFF is the repeated heating and cooling cycles imparted by its exposure to the

laser [22]. Secondly, the laser "develops an uneven temperature distribution throughout the structure" [22] leading to thermal stresses and therefore cracking. The consistency of LSFF results depend on the ability to control the physical parameters of the process; something that is critical if it is to be adopted in industry. To find a method of controlling these parameters, the author attempted to develop a 3D numerical model of the LSFF process to "dynamically predict geometrical characteristics of the deposited additive material, temperature distributions and thermal stress … as a function of process parameters and material properties" [22]. After testing the model, an error margin of 9.30% was found [22]. From the development of this numerical model, the author goes on to explore manipulating the parameters so as to try and control the properties and geometry of the final product. The parameters that were changed were: traverse speed of the substrate, the power of the laser, preheating the metallic material, and the melt pool conditions. By heating the substrate and material that has already been built up, the temperature gradient between the melt pool and surrounding metal is reduced [22]. The result is lower internal thermal stresses created during fabrication [22]. One beneficial aspect of the LSFF process that is often exploited is the fact that the amount of added material is very small. Consequently, the temperature difference between this recently melted material is very large compared to the ambient temperature of the air and substrate, and rapid cooling ensues [22]. As a result, the microstructure of the metal is made up of very small grains, leading to high wear resistance and hardness [22].

The author summarizes what has been learned in the study at the end of the thesis, stating that: the material added per layer increases the farther away from the base the structure becomes, the temperature of the melt pool and surrounding structure decreases

farther away from the platform, and that it is possible to 'define' critical temperatures and stresses during the LSFF build [22]. Also, the rate of cooling and temperature history determines the microstructure of the finished metal, just as it does in traditional metal production [22]. When trying to minimize/control cracking and delamination by decreasing internal thermal stresses, it was found that preheating the substrate (base) and the structure that has been built up greatly aids in achieving this objective by reducing temperature gradients [22]. The path pattern that the laser follows also affects thermal stresses, with offset overlaps shown to create less thermal stress than continuous overlaps [22]. When fabricating multi-material components, the author learned that optimizing the laser power for the different material properties was essential in reducing thermal stresses and therefore the likelihood of cracking/delamination [22]. Looking towards the future of LSFF as a production method, the author foresees: the development of a real time controller that is able to update and adjust building parameters to stay true to the dimensional and stress requirements, development of a path-planning software due to the importance the path has on the properties and geometry of the final structure, more research into the parameters required for LSFF processes involving different materials and their interaction with one another so that multi-material projects are more feasible [22].

Active Materials by Four-Dimension Printing

"Active materials by four-dimension printing" is an article by Qi Ge, H. Jerry Qi, and Martin L. Dunn that explores the fabrication of "printed active composites" (PACs) by "printing glassy shape memory polymer fibers in an elastomeric matrix" [23]. By printing thermo-mechanically programmable lamina into the composite matrix, they are able to create materials

whose shapes are temperature dependent; turning into the desired shape when cooled and returning to its original shape when reheated. The process starts with the design of the CAD file for the PAC which includes the 3D architecture of fibers in the matrix needed to yield the desired active behavior. The matrix "is designed to be an elastomer and the fibers to be a glassy polymer with tailored thermomechanical, including shape-memory, behavior" [23]. They are printed by depositing drops of the polymer at 70^{o} C, wiping them into a smooth film, and then photo-polymerizing the film, which gives a fiber in-plane resolution of 32-64 micrometers, depending on the printing resolution [23]. Printing more film layers produces individual lamina and printing multiple layers of the lamina creates the final composite.

These PAC's are designed to work between temperatures of 15^{o} to 60^{o} C, where the matrix consistently behaves as a rubbery solid (E = ~.7MPa) and the fibers have a modulus of 3.3MPa at 35^{o} C (glass temperature) and 60^{o} C and 13.3MPa at 15^{o} C [23]. This means that between the PAC's operating temperatures, the matrix always remains rubbery while the fibers undergo a glass transition [23]. To activate the shape memory effect, samples are deformed at T_H of 60^{o} and the stress applied is maintained while cooling to T_L of 15^{o} at 2^{o}/min. During cooling, strain in the sample decreases slightly. After holding the sample at T_L long enough for the strain to equilibrate, it is released and the elastic unloading is observed. A fixity ratio that compares axial strain before and after unloading helps to determine the shape memory capabilities of the composite – "Simulations show that fixity increases with increasing fiber volume fraction, as this provides increased stiffness to hold the composite in its prescribed deformation state after cooling" [23]. Fibers were most effective when in line with the load.

Various experiments were conducted involving fiber volume, orientation and the effects on curvature and shape. “In general, the magnitude of the curvature depends on the composite geometries and properties, the applied mechanical load, and the thermal history; all of these are design variables” [23].

The concept of these active composites is well demonstrated in these experiments. Future work would include “spatial variations of material properties and [the use] of computational design tools such as shape and topology optimization to design the layout of the materials in the composite, as well as exploit instabilities to create large configurational changes” [23].

2.4 3D Printing in the Construction Industry

3D printing can provide some unique advantages to the construction industry. From urban planning to building materials, this section analyzes the effect of additive manufacturing.

3D Printing for Urban Planning

A Physical Enhancement of Spatial Perspective

“3D Printing for Urban Planning: A Physical Enhancement of Spatial Perspective” is an article written by T. Ghawana and S. Zlatanova that examines the capabilities of 3D printing for making 3-dimensional city models, based on the parameters of ‘size and resolution’, as well as its overall ability to aid in the visualization city development plans.

The article describes 3D models as being more beneficial for spatial analysis due to the ability to more easily see the entire development. Possible misperceptions that can be created by a virtual 3D model are eliminated (such as artificial depth perception features) much faster

and cheaper than previously possible with handmade models. Urban planning projects often involve small, intricate parts which are a natural fit for 3D printing. The capability to produce both the larger structure of buildings as well as the smaller details of the design means planners can examine and discuss both higher and lower levels of the design at whatever time is convenient. Not only does the physical model allow for higher and lower levels of analysis, it also allows anyone (regardless of training or education) to be part of the planning discussion. This is extremely beneficial since it allows for all members of the community to engage in the planning process. A second suitable application for the technology in urban planning is modelling the topography of the landscape. The current barriers for additive manufacturing methods in urban planning are: the variety of geographic information system data formats that have to be converted into STL for use with 3D printing software, data loss when the conversion is made, cost compared to digital 3D models, and the resolution and accuracy of 3D printers [24].

In summary, the authors of the article foresee that the advantages of 3D printing in urban planning, especially the ability to communicate ideas with community members by taking models to the neighbourhoods themselves, will lead to its increased use within the industry. Making physical models has always had a place in urban and development planning; only previously they were produced by hand. This niche market is therefore primed to adopt additive manufacturing methods [24].

Cost Evaluation of Shell and Compact Models in 3D Printing

Tomislav Galeta, Milan Kljajin, and Mirko Karakašić's article, "Cost Evaluation of Shell and Compact Models in 3D Printing", evaluates the difference in cost between 3D printing solid,

compact models with solid building material and shelled cases of the same models. The shelled cases are made by printing the exterior with a high concentration of binding agent and printing a structural skeleton inside the part. The rest of the model is held together with a low saturation of the binding agent. To improve the mechanical properties of this model, it can be infiltrated with cyanoacrylate, epoxy resin, or wax. Cyanoacrylate is the quickest acting, but most expensive; epoxy resin is somewhat slower, but cheaper, and wax is fast, convenient, and the cheapest [25]. Cyanoacrylate and epoxy resin only penetrates 2 to 8mm while wax penetrates the entire model [25].

Four shell models and four solid models were tested for cost evaluation and each model varied only in base dimension. They began at 50mm and incremented by 50mm up to 200mm. The shelled models had a wall thickness of 4mm. Cost per model was calculated as a sum of the powder, binder, infiltrant, machine, and operator costs. The cost increased as base size increased and the wax was significantly cheaper than other infiltrants when used in shelled models with a base larger than 100mm. When infilitrants other than wax were used, the costs were similar among all models.

If printing cost is more important than model strength, shelled models infiltrated with wax would be the best option. If rapid fabrication is needed, the solid model infiltrated with cyanoacrylate is the best choice [25]. These results may change from printer to printer and from material to material, and as new binding agents and powders are produced, new costs evaluations will be needed [25].

The Scope of Rapid Prototyping in Civil Engineering

"The Scope of Rapid Prototyping in Civil Engineering" is an article written by Harsha N., Sukrutha N., and S. Nagabhushan that discusses the use of rapid prototyping in the design, then construction, of civil engineering projects. Several uses of rapid prototyping are described, and include the development of physical test models to validate predications made by software and calculations, making the chain of information leaner and faster, and the possibility of creating full construction projects through additive manufacturing techniques.

The opportunity to test calculations/predictions using rapid prototyping techniques offers civil engineers a way to both validate traditional designs and experiment with new ones. This offers a greater level of both confidence and innovation in the design phase of a project. The article references an irrigation system designed using digital 3D modelling software and fabricated using additive manufacturing techniques. The author describes the physical prototype as a useful tool in testing and modifying the design on a scaled down version. From this mindset of prototype testing, the authors jump to the exploration of full scale construction using automated, additive manufacturing methods. Methods such as automated concrete layering, directly from digital models, which are still in research and testing stages, are briefly discussed in the article. The majority of the author's focus was on automated subtractive processes, which appear (from the article's description) to have more established applications in the construction industry [26]. The common thread between these two processes is the use of automation. Automation, used extensively to make manufacturing processes leaner, is seen as having the same potential effect in construction. Although the main body of the article may lack specific discussion on additive manufacturing methods, it is a reminder of the important

role that automation and software will play in the development and acceptance of additive manufacturing technologies.

Looking towards the future, the authors see the most important frontier for additive manufacturing/ rapid prototyping in the construction sector as being its use in full scale, complete construction of a building. The following process is seen as a lean and advantageous construction method that can be possible using these technologies: a designer develops plans using 2D and 3D modelling software, creates a scaled down prototype to first analyze and discuss the plan, then uses an automated machine to produce the structure of the building [26].

2.5 3D Printing and Patents

With any new technology there are new regulations that come with it. This section will look at the effect of patents on additive manufacturing.

3D Printing – A Patent Overview

"3D Printing – A Patent Overview" is a journal written by the UK Intellectual Property Office Patents Informatics Team, and it provides an analysis and overview of the patent landscape of 3D printing, giving a sense of the 'space' of 3D printing. It dives into the specifics of where patents are filed, which countries are most active in the pursuit of this technology, and top inventors for the industry.

A worldwide dataset of 3D printing patents yields over 9000 patent publications and over 4000 patent families which can be further reduced to those patents that concentrate on 3D printing in the more modern sense [27]. When plotted, this showed that the development of 3D printing was something that grew over time rather than being a product of some scientific

breakthrough, as shown in Appendix A-81: Comparison of Granted Patents and Published Patent Applications by Publication Year.

But it was not sufficient to only observe the amount of patents that were being applied for, since most patents are published "without any presumption of whether or not a patent may be granted based on that application" [27] – the amount of patents granted would better determine that status of a technology. Some countries may also catalogue their applications in exclusive fields where no patent is allowed, therefore reducing the number of patents from any given country. Although some patent applications may appear in one country, it does not necessarily mean that the research which led to that patent originated from the same country, which is frequently seen amongst multinational companies. Viewing the patents by priority country makes for a more reasonable list that indicates where most innovation is taking place (see Appendix A-82: Priority Country Distribution for Top Countries).

A look at the companies that hold patents gives better insight into the space of the 3D printing industry, the timescale of the technology, and how each company is contributed patents over time. Fujitsu is shown to have the highest amount of patents; however, many of these patents are due to expire soon. Most companies are relatively new to this technology and have only been begun applying for patents within the past 2 decades. The top companies have almost the same amount of patents; suggesting that the success of a company may not be dependent on the amount of patents held. It also found that nearly all the patents held by any company were not created through any collaboration and that the companies themselves are the sole applicants of their patents in this field.

Looking at the location of each inventor is another good indication of where innovation is taking place, since publishing a patent can be done is any country that is most convenient. The amount of academic interest a technology is also a good indicator. Although 3D printing has been around since the 80s, it has not gained much recognition until recently, and this may be why academic interest in it is still on the rise (as well as the use of rapid communications and the openness of the internet).

There is a method of determining the quality of a patent by using citation analysis, where the most frequently cited patents are used as an indicator of quality. “During the patent examination process, a patent examiner will list all those patents which are considered to be relevant to the wording of the claims in the patent application” [27], therefore an early patent that is frequently cited is an indicator of a high quality patent. A drawback in this method is that more recent patents will not have had enough time to gain the amount of citations that an older patent may have. Therefore the results of this method do not provide ‘the whole picture’ when judging the quality of a patent.

To visualize the technological space of the industry, a ‘patent landscape’ was created with a keyword filtering of about 30,000 published patents. This allowed for the grouping of patents that shared these representative keywords in their titles and abstracts, giving an idea of what the largest fields of interest are in 3D printing. This was also done for non-patented literature (NPL), and it was found that the key areas of interest are in biomedical applications, circuits, and electrode fabrication [27].

Downloading Infringement

Patent Law as a Roadblock to the 3D Printing Revolution

Davis Dohetry's article, "Downloading Infringement: Patent Law as a Roadblock to the 3D Printing Revolution", explains how widespread patent law infringement could arise from the use of commercial 3D printers and he proposes law modifications similar to the Digital Millennium Copyright Act that would safeguard patentees and members of the DIY community who may have unknowingly infringed on a patent. Currently, DIYers are able to freely share their own 3D designs on the Internet on websites like Thingiverse, allowing other designers to use or improve on designs, or websites like Shapeways, which allows consumers to order printed user-designed objects and have them shipped to their homes. Both these services can potentially host, intentionally or unintentionally, patented material, thus making it possible to generate patent infringement worldwide.

Unlike copyright infringement, showing of an independent invention does not relieve the creator of patent liability, making it more than likely for a DIYer to design an object that's already been patented. Because of this, there are three possible lines of patent infringement: liability for the one who creates the patented invention, liability for the one who induces the infringement, and liability for the one who sells patented material. The hosting sites like Thingiverse would not be subject to direct infringement since they are only passive hosts and the inventor of the patented invention would not be liable either unless he/she printed copies in the process of the design [28]. The buyer, however, is liable once he/she prints the object at home [28]. Sites like Shapeways are also liable since they would be the ones printing and selling the patented product. Thingiverse and the inventor may be liable to induced infringement,

since they are aiding in another's direct infringement, but this requires that they had the intent to cause another to infringe on a patent. Also, according to a decision made by the Supreme Court, induced infringement requires proof that the defendant had previous knowledge of the patent and "knowledge that infringement would result from [his]/[her] actions" [28]. This does not save the defendant from an act of willful blindness for "if the defendant (1) subjectively believe[s] that there is a high probability that a fact exists, and (2) take[s] deliberate action to avoid learning of that fact, then knowledge will be imputed" [28].

Previous laws pertaining to patent infringement would require all relevant parties to be legally sophisticated. Since most DIYers are not likely to be well orientated with the law and most businesses may find the 3D printing market to be legally unstable, what is needed is a new system of law that allows patentees to preserve their rights while still allowing the benefits of a publicly free domain of shared designs. What may seem simplest is for the patentee to send a cease-and-desist letter to the hosting sites, who will likely comply with the request, since their main source of revenue is not dependent on any single design. But since most online forums operate with pseudonyms, it may take a great pooling of resources to identify the DIYer. If the DIYer feels aggrieved by the removal of his/her design, the DIYer may find different channels to upload the design, thus only publicizing it more. This makes it imperative that the patentee find the identity of the DIYer before any further damage is done. Because of the tremendous amount work required to litigate, most patent infringers needn't worry about infringement. So long as cease-and-desist letters and takedown letters are sent in good faith and websites provide patentees the user's information and DIYers comply with these requests, "such a

system could be sustainable" [28], but as soon as any party attempts to undermine it, there is risk of collapse.

Much like the music piracy crisis of the 90's, consumer-level 3D printing would benefit from something similar to the DMCA. What is needed is a system that standardizes takedown procedures of infringing content that grants safe harbor to hosting sites from liability so long as they didn't have knowledge of infringement and establishes "a limited innocent independent inventor defense that protects DIYers and hosting websites" [28].

The rights of the DIYers ought to be considered too. "In theory, a patent application should fail for lack of novelty or obviousness if a DIYer has previously created and shared a design that is substantially similar to what is being claimed" [28], raising issues of prior art. While hosting sites for these designs showcase and make users' designs available to the public, they face problems with their scope of prior art due to the fact that in order for something to be categorized as prior art, it must be sufficiently catalogued and easily searchable. This makes it possible that "a patentee may monopolize an invention that is effectively part of the common stock of knowledge by way of obviousness" [28].

To counter this, Doherty proposes an Inventive Commons – a nonprofit corporation serving as quasi-governmental role in ensuring that only "truly novel and nonobvious patents are issued" [28]. This self-governing committee, would ensure that "unpatented innovations are quickly and accurately identified as part of the commons, and that no patent applicant succeeds in removing ideas from that commons" [28]. The committee would also continuously index user-generated material to maximize their sphere of analogous prior art and grant both patent agents and applicants access this database.

Intellectual property law has always been outpaced by the rapid developments of digital technology and if the copyright crisis during the advent of digital music is any indication of this, proactive initiatives in legislation ought to be taken to avoid extensive litigation when the 3D printing revolution comes [28].

3 Technical Studies Review

As seen in the previous chapter, additive manufacturing's impact reaches many different industries. The varying technology and materials are what allow 3D printing to be impactful across such a wide variety of areas. This chapter will take a closer look at technical papers and studies about additive manufacturing.

3.1 Technology in the Aerospace Industry

From 3D printed models for aerospace engineering students to forging helicopter parts, this section looks at the additive manufacturing technologies involved with aerospace design.

3.1.1 Literature Review

Enhancing Aerospace Engineering Students' Learning with 3D Printing Wind-Tunnel Models [29]

This 2011 study by Ehud Kroll and Dror Artzi weighs the benefits and drawbacks of using 3D printing to rapidly prototype aerospace models for wind tunnel testing. This research is especially applicable in a post-secondary engineering setting where budgets and time constraints are often limiting factors.

Evaluation of 3D Printing for Dies in Low Volume Forging of 7075 Aluminum Helicopter Parts [30]

This 2005 study, by R. Shivpuri, X. Cheng, K. Agarwal and S. Babu, analyzes the feasibility of 3D printing dies for aluminum helicopter parts.

3.1.2 Theory and Purpose

Enhancing Aerospace Engineering Students' Learning with 3D Printing Wind-Tunnel Models [29]

Wind tunnel testing is typically very expensive. It is costly and time consuming to CNC machine wing structures, given that both the upper and lower surfaces of the wing have specific curvatures. Previous case studies have demonstrated that using RP to manufacture aerospace test models can reduce costs by 5 to 10 times. These studies have had success but also faced challenges due to the limitations of 3D printing. The purpose of this study is to evaluate the merits of RP technology for wind tunnel models, with an emphasis on usefulness in an academic setting.

Evaluation of 3D Printing for Dies in Low Volume Forging of 7075 Aluminum Helicopter Parts [30]

Closed die hot forging requires long lead times to manufacture the moulds. This is not a problem in high volume production, but is concerning for the small orders frequently seen among suppliers for helicopter components. Limited work has been done with using 3D printing techniques to make moulds. However, applications that have been touched on include injection moulding, sheet forming dies and forging dies. This study uses the ProMetal 3D printing method to make intricate aluminum-zinc alloy helicopter components.

3.1.3 Method

Enhancing Aerospace Engineering Students' Learning with 3D Printing Wind-Tunnel Models

3D printing is used to manufacture models of a CERBERUS and an ILAS UAV. The ILAS UAV is printed in sections and assembled with reinforcing rods (refer to Figure 3-1). The

CERBERUS model is similarly printed, but has thin wings and requires stainless steel plates instead (refer to Figure 3-2). Models are fitted with rear strain-gage balance [29].

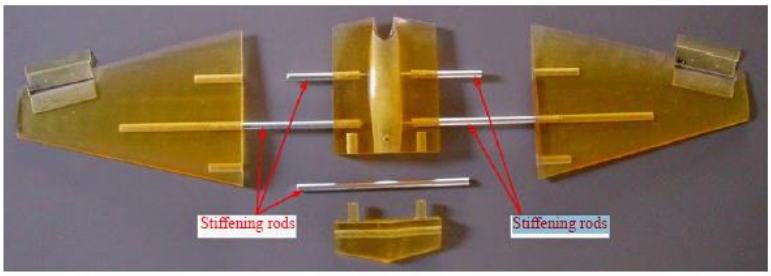

Figure 3-1: ILAS Model Before Final Assembly with Five Reinforcing Rods [29]

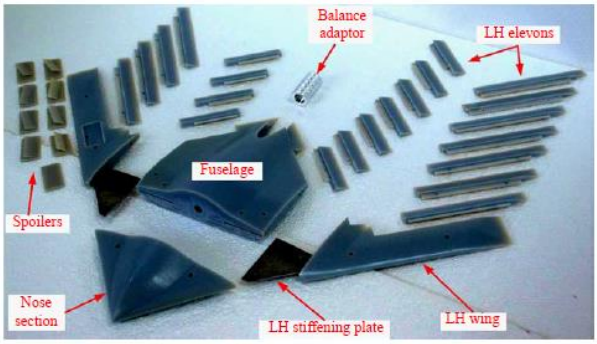

Figure 3-2: CERBERUS Model Parts [29]

Evaluation of 3D Printing for Dies in Low Volume Forging of 7075 Aluminum Helicopter Parts

Two ProMetal dies are printed, cured, sintered and infiltrated as specified by the ProMetal process. One is polished conventionally and the other is done with the EXTRUDEHONE Orbitex process. A third die is traditionally manufactured.

The ProMetal print material is compared to conventional tool steel. A heat transfer comparison between the standard H-13 and ProMetal dies is carried out with thermocouples. Compression testing is conducted using ring testing for friction comparison. Flow stress is also analyzed and the moulds are subjected to forging trials under varying temperatures [30].

3.1.4 Simulation Results and Discussion

Enhancing Aerospace Engineering Students' Learning with 3D Printing Wind-Tunnel Models

Advantages of Wind-Tunnel Testing

This study found that the 3D printed model's costs were drastically lower than traditional models. The cost savings were even greater when hollow models were used. Extra cost savings can be implemented to make and test variations that would not have previously been permitted due to monetary limitations [29].

3D printing a sizeable and complex UAV model took only one to two days, compared to the weeks required if it was to be made out of metal. The model was also able to be geometrically complex. Sections were hollowed out to reduce weight, and it was then possible to take internal pressure measurements. This is not feasible using a CNC machine [29].

The density of the RP polymer was much less than steel or aluminum, which allowed more sensitive force balances to be used in the tests [29].

The horizontal resolution of the 3D printer was 0.1 mm or better, and the layer thickness was 16 microns. This was consistent with traditional models. However, the CAD software approximates curved surfaces as planar ones, which caused some inaccuracies. The RP had suitably fine detail. This study didn't employ this advantage, but 3D printing is capable of manufacturing moving parts without secondary processing [29].

Disadvantages of Wind-Tunnel Testing

The 3D printed polymer offers 55-60 MPa of tensile strength and 79-84 MPa in compression with a modulus of elasticity of 2.7-2.9 GPA. These are much lower than metals. These strengths are for forces parallel to the layer and drop by roughly 50% when forces act

perpendicularly. 3D printing orientation of the UAV must be taken into account due to these directionally variant properties [29].

Wind-Tunnel Testing

No model deformation was seen during testing. Models displayed excellent compatibility with test theory. This testing affirmed confidence in these RP models.

Tolerances for RP parts hampered the seam where the wings and the fuselage meet. CNC machining is still superior in this department. The models' surfaces were adequate, despite the fact that this aspect is often criticized in 3D printed parts. The drag and lift coefficients generated by the testing maintained a linear relationship with their theoretical values. This would not have been the case had stiffness been an issue with the RP model; deflection would have produced non-linear or quadratic discrepancies in these values when correlated with their calculated counterparts [29].

Evaluation of 3D Printing for Dies in Low Volume Forging of 7075 Aluminum Helicopter Parts

Refer to Table 3-1 for a material comparison of ProMetal (420 stainless steel with bronze infiltrate) and conventional tool steel.

Table 3-1: Physical & Mechanical Properties of ProMetal Material as Compared to H-13 Tool Steel

Property	Conventional tool steel	420 + Bronze
Hardness	51-55 HRC	26-30 HRC
Ultimate Strength (Mpa)	1034	683
Yield Strength (Mpa)	793	455
Young's modulus (Gpa)	206	138
Elongation	9 percent	2.30 percent
Thermal conductivity (W/m. ^{o}	24.4	8.22
Density (g/mm^3)	7.8	8

Thermal testing calculations indicate a heat transfer coefficient of 2.84 W/m^2*°C for ProMetal and 19.3 W/m^2*°C for H-13 steel at 232°C. ProMetal's lower heat transfer coefficient is beneficial to forging as it reduces die chill.

The ring compression testing produced friction factors of 0.18 for H-13 (Ra =0.38 um) and 0.27 for ProMetal (0.57 um). The rougher ProMetal dies will therefore require further polishing.

Refer to Figure 3-3 for flow stress results. In compression, the ProMetal material had a yield strength of 627 MPa at 232°C and 1200 MPa at room temperature. Hot working steel has a yield strength of 779 MPa at room temperature for comparison [30].

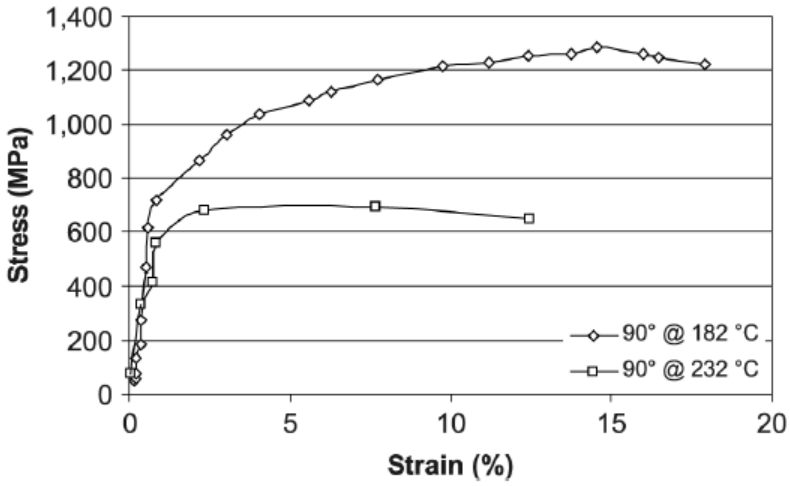

Figure 3-3: Flow Stress of ProMetal at 68°F and 450°F [30]

Both the H-13 and ProMetal dies' simulated performance was modelled to show stress distribution (see Figure 3-4). The ProMetal material was deemed feasible for forging as its yield strength exceeds cavity pressures typically seen during production.

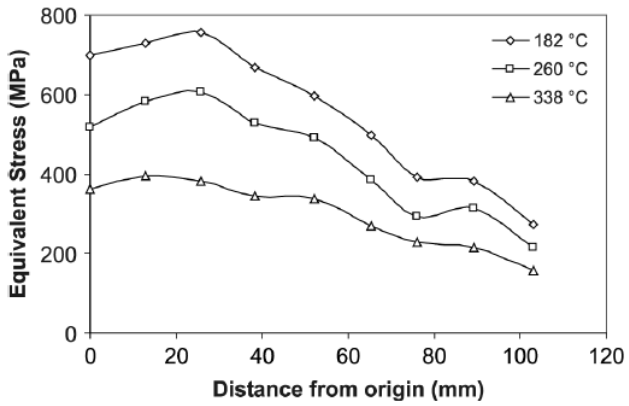

Figure 3-4: Equivalent Stress Distribution in Bottom Die (max stress) [30]

The conventional and the two ProMetal dies were successfully manufactured. The regularly polished Prometal die (Pro-dieA) had a surface roughness of 32-64 RMS, while the one finished with the EXTRUDEHONE orbit (Pro-dieB) had a roughness of 157-160 RMS. Cracks developed in the ProMetal dies during sintering due to the size of the cross sectional area. The sintering cycle was adjusted to reduce crack propagation.

Parts were forged with three dies (refer to Figure 3-5 for sample parts).

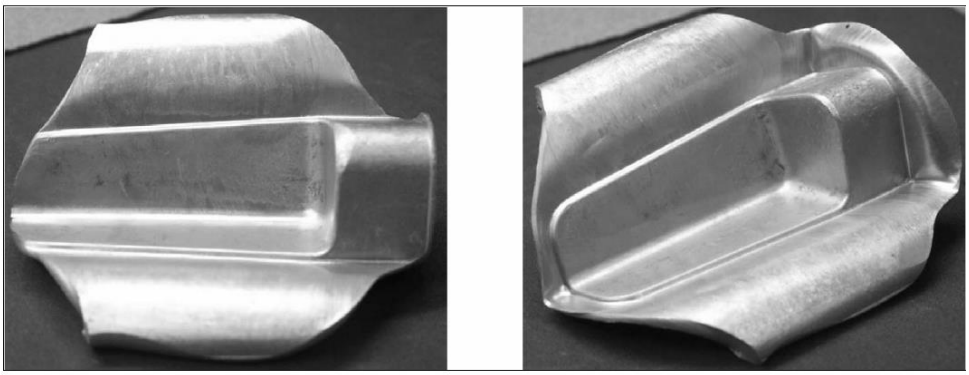

Figure 3-5: Forged Parts (left: forged at 182°C, right: forged at 338°C) [30]

Refer to Figure 3-6 and Figure 3-7 for mould schematics and the measuring positions for components.

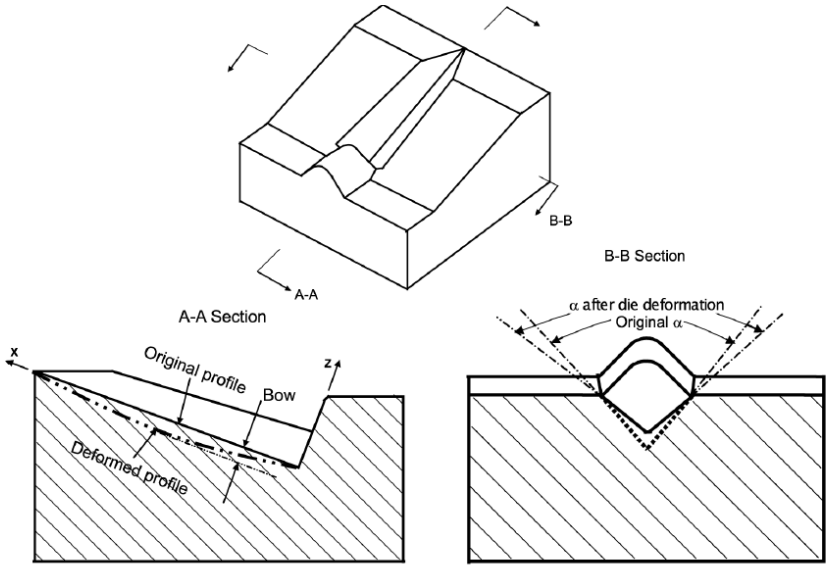

Figure 3-6: Schematics for Die [30]

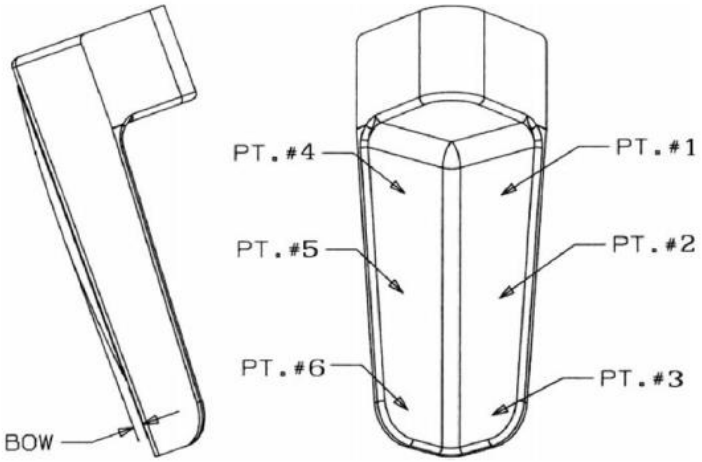

Figure 3-7: Measuring Position for Parts [30]

Part distortion was strongly dependent on the degree of die distortion. However, more pronounced distortion was seen in the parts than the die. Refer to Figure 3-8 and Figure 3-9 for distortion results for the traditionally polished ProMetal die.

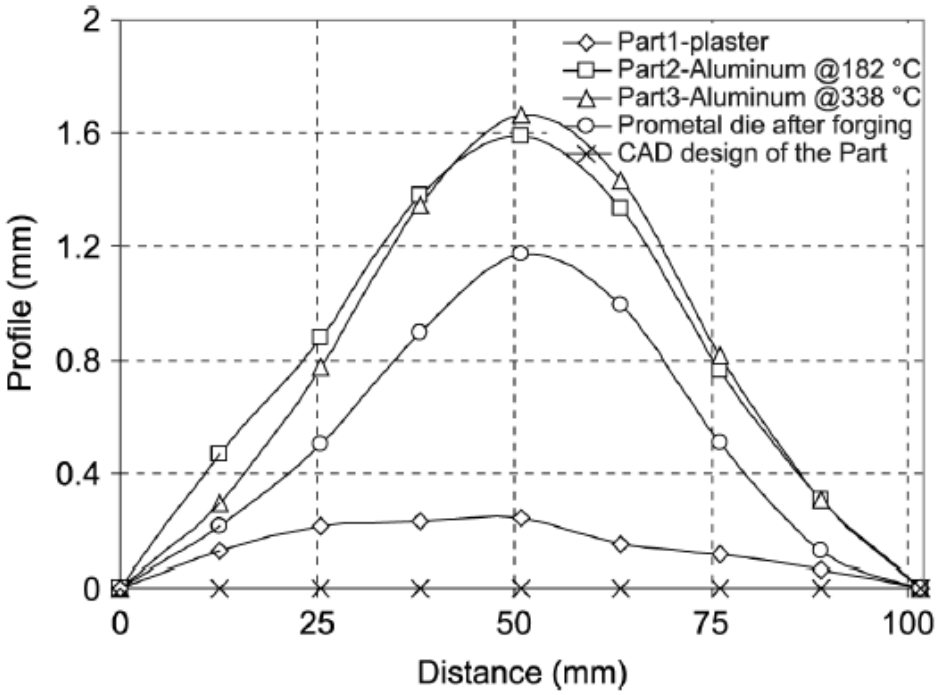

Figure 3-8: Profile Variations (plaster parts were made before actual forging) [30]

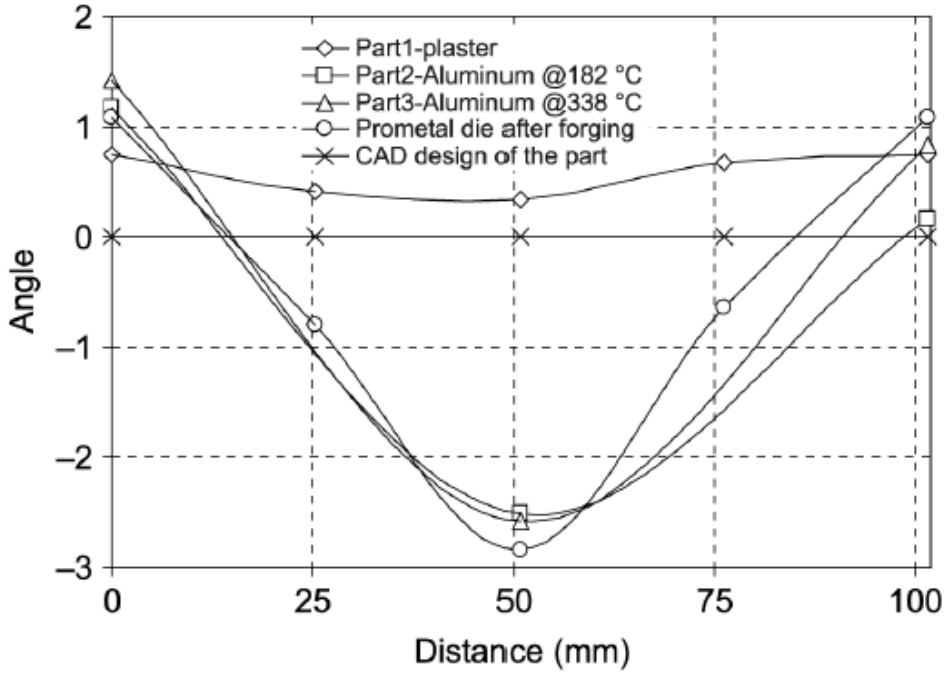

Figure 3-9: Angle Variation [30]

3.1.5 Summary

Enhancing Aerospace Engineering Students' Learning with 3D Printing Wind-Tunnel Models

This testing has validated RP as a good method of constructing aerospace models for wind-tunnel applications. The cost and time savings would be beneficial to student projects. Generally, students finish calculations and designs towards the end of their project time line, which does not permit traditional aerospace models to be manufactured. 3D printing will allow students to quickly produce a model within days of their due date to complement their design. Low costs will potentially give students the ability to alter designs and create several variations for testing. This would have previously been inconceivable at the university level, given the immense cost and time required. 3D printing produced comparable models to those currently used and should be considered when prototyping models for wind-tunnels in the future [29].

Evaluation of 3D Printing for Dies in Low Volume Forging of 7075 Aluminum Helicopter Parts

The ProMetal material has a much lower heat transfer coefficient compared to traditional steel dies. This can be a benefit to the manufacturer as dies can be heated to lower temperatures without undergoing die chilling effect. However, considerable polishing and surface modifications must be implemented to mitigate the rougher die surface on the ProMetal. Aluminum may be forged with ProMetal's hot hardness. The next step is determining a method of building ProMetal dies with larger volumes as they are currently constrained at 305mm diameters [30].

3.2 Technology in the Electronics Industry

New developments in technology will allow the electronics industry to take advantage of the benefits of 3D Printing. This sections looks at technical papers covering the different materials that could be useful for manufacturing electronics.

3.2.1 Literature Review

Liquid Phase 3D Printing for Quickly Manufacturing Conductive Metal Objects with Low Melting Point Alloy Ink

This 2014 study by Lei Wang and Jing Liu examines 3D printing using low melting point alloys. The article explores using liquid metal ink to rapidly 3D print conductive structures.

Embedded 3D Printing of Strain Sensors within Highly Stretchable Elastomers

This 2014 study by Joseph T. Muth, Daniel M. Vogt, Ryan L. Truby, Yigit Menguc, David Kolesky, Robert J. Wood and Jennifer A. Lewis experimentally 3D prints highly deformable strain sensors in elastomer matrices.

Effects of Layer Thickness and Binder Saturation Level Parameters on 3D Printing Process

This 2011 study by Mohammed Vaezi and Chee Kai Chua seeks to rectify problems with 3D printed components' strength and surface quality by examining layer thickness and binder saturation levels.

3.2.2 Theory and Purpose

Liquid Phase 3D Printing for Quickly Manufacturing Conductive Metal Objects with Low Melting Point Alloy Ink

Low melting point liquids with melting points just slightly above room temperature have shown immense promise for technical applications. This study looks to expand upon previous work by using these metals as the printing ink in additive manufacturing. The liquid metal is injected into a printing fluid (air, ethanol, water etc.), cools down and then solidifies. The heat transfer with the previous layer fuses it to the structure. Studying parameters, such as the cooling medium, cooling medium temperature and droplet size, will lead to optimal printing of conductive components using liquid metals [31].

Embedded 3D Printing of Strain Sensors within Highly Stretchable Elastomers

Stretchable electronics are becoming very popular due to their diverse range of uses. However, integrating rigid electronics into malleable bodies is difficult. The interface between the electronics and surrounding materials is often a weak point in the structure. This report attempts to embed conformable strain sensors in a soft matrix using 3D printing. Doing so successfully will validate this new method and improve upon electronics enclosed within a soft body [32].

Effects of Layer Thickness and Binder Saturation Level Parameters on 3D Printing Process

3D printing parameters need to be optimized to achieve the best print quality. Research into this is ongoing and previous studies have improved surface finish by controlling bimodal powder distribution. Drop formation, bleed compensation and powder blends have all been manipulated to achieve better strength and dimensional tolerances. In addition, electrically

conductive components have been manufactured with 3D printing. Despite these technical advances, more research needs to be conducted to better understand these properties. Binder saturation levels and print layer thickness have previously been established as having the biggest impact on both component surface finish and strength. This article's objective is to evaluate the effects of binder saturation and layer thickness on the quality of 3D printed components [33].

3.2.3 Method

Liquid Phase 3D Printing for Quickly Manufacturing Conductive Metal Objects with Low Melting Point Alloy Ink

Printable Metal Ink

This study will conduct trials using a prepared $Bi_{35}In_{48.6}Sn_{15.9}Zn_{0.4}$ alloy.

Liquid Phase Cooling Fluid

This study will compare air, ethanol and water as cooling mediums.

Experimental Devices

A syringe with the liquid metal is used to simulate the printer head in this study. The syringe which dispenses the liquid alloy is regulated using a heater to maintain a temperature just above room temperature, so as not to clog the printing head. The heater is regulated with a temperature controller. The syringe nozzle is submerged in the cooling fluid and monitored with a high speed camera (refer to Figure 3-10). Various parameters are tested to identify their impact on 3D printability.

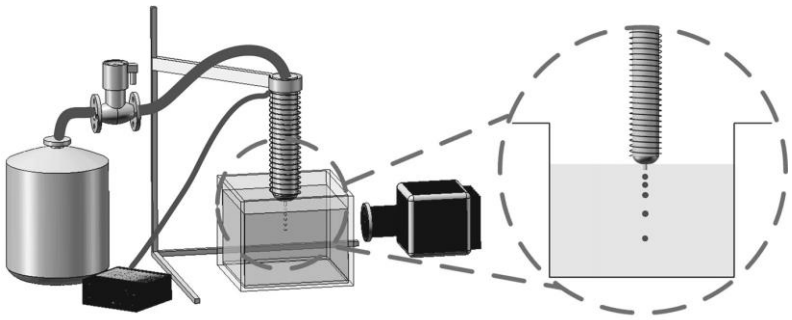

Figure 3-10: Test Set-Up [31]

Embedded 3D Printing of Strain Sensors within Highly Stretchable Elastomers

A specially designed 3D printer is used. A viscoelastic ink is deposited in a matrix in rows of U-shaped filaments and forms resistive sensors (refer to Figure 3-11). The 3D printing nozzle disturbs a portion of the matrix as it moves laterally and results in a network of voids. The void is then packed using a filler fluid, and both the matrix and fluid are cured while the ink remains in a liquid state.

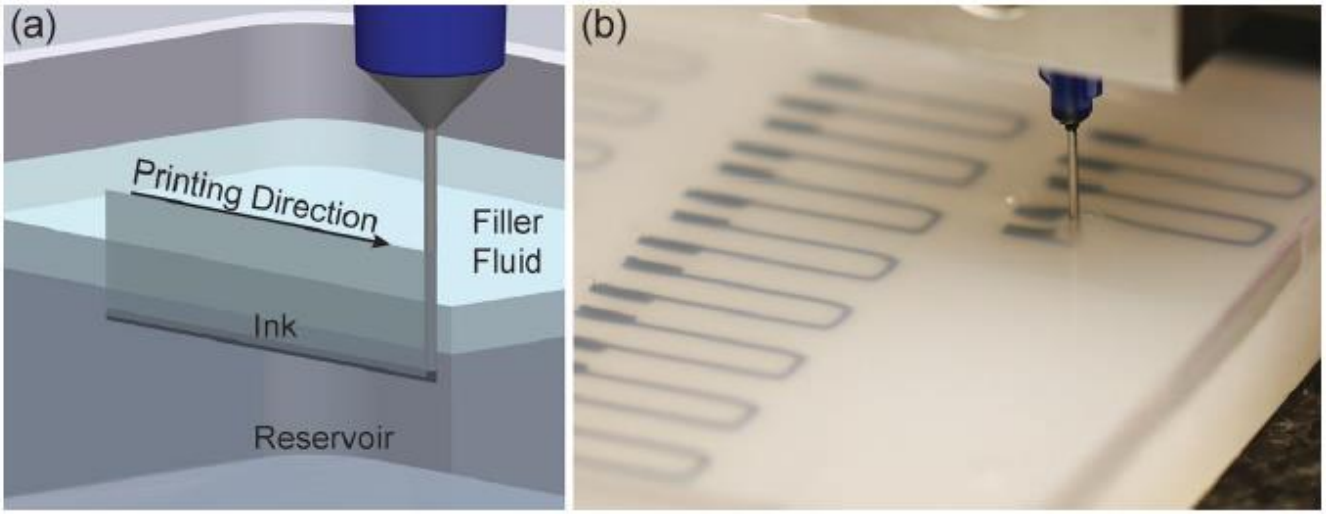

Figure 3-11: Embedded 3D Printing Process

a) e-3DP Process

b) Planar Array of Soft Strain Sensors [32]

The ink, matrix and filler fluid must be chemically compatible and have specific rheological attributes. This study uses conductive carbon grease as the active ink due to its physical properties. The addition of a thinning agent to the filler fluid produces almost Newtonian behavior. Print speed and ink mixtures are varied to determine an optimal combination. The 3D printed composite structure is then subjected to a number of strain tests. Wearable objects with embedded strain sensors were also e-3DP'd to prove the flexibility of this technology [32].

Effects of Layer Thickness and Binder Saturation Level Parameters on 3D Printing Process

Two different layer thicknesses of 0.1 mm and 0.087 mm are both tested at two binder saturation levels of 90% and 125%. The four different combinations are used to print test samples (see Figure 3-12), which are then subjected to tensile and flexural tests.

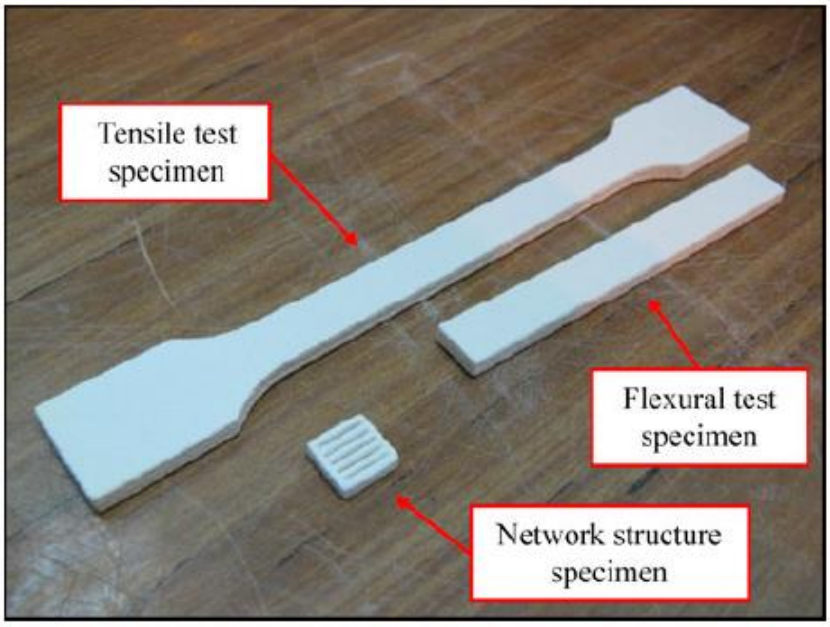

Figure 3-12: 3D Printed Test Sample Geometry [33]

3.2.4 Simulation Results and Discussion

Liquid Phase 3D Printing for Quickly Manufacturing Conductive Metal Objects with Low Melting Point Alloy Ink

The physical properties of the printing alloy were analyzed (refer to Table 3-2).

Table 3-2: Typical Physical Properties of $Bi_{35}In_{48.6}Sn_{15.9}Zn_{0.4}$ [31]

Density (g/cm)	Melting point (^oC)	Supercooling degree	Melting enthalpy (J/g)	Specific heat capacity (J/(g.^oC))
7.898	58.3	2.4	28.94	0.262 at 25 ^oC

The air pressure, printing nozzle diameter and drop ejection velocity were varied while creating several different structures (refer to Figure 3-13).

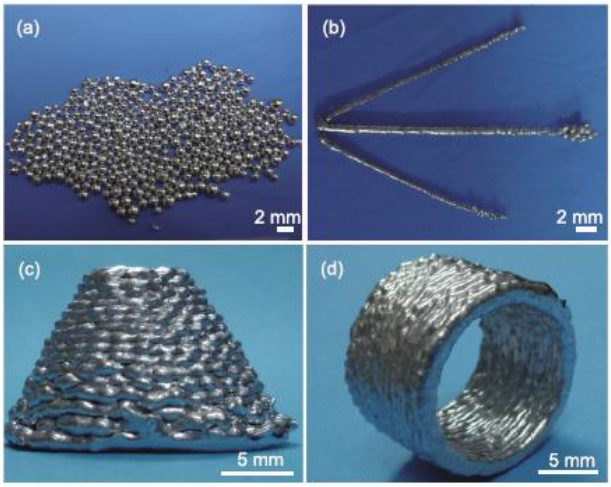

Figure 3-13: Typical 3D Metal Structures Made by Liquid Phase 3DP [31]

(a) Liquid metal balls; (b) liquid metal rods;
(c) frustum of a cone structure; (d) cylinder structure.

If droplets cool in air (conventional 3D printing), cooling times are much longer. Metal oxidation is found in greater quantities than with water or ethanol. This weakens the final structure. In

addition, the metal sustains its melted state for a longer period of time, and it forms a globule, instead of the beads produced when ethanol is used as the cooling fluid (refer to Figure 3-14).

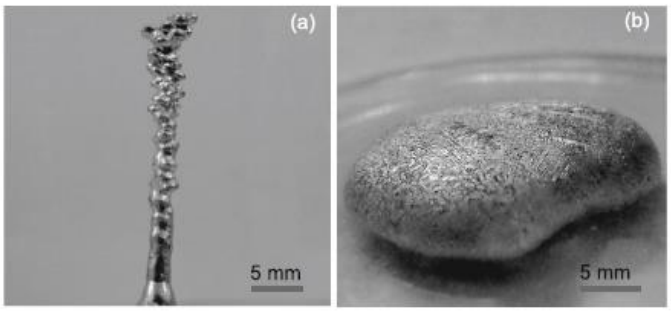

Figure 3-14: Comparison Between Ethanol Cooling and Air Cooling Printings

(a) Column formed by the ethanol cooling method; (b) molten globule formed by the air cooling approach [31]

The upward buoyancy of water and ethanol, as well as their relative thermal conductivities and specific heat capacities, are much higher than air (refer to Table 3-3). These thermal properties quickly cool the liquid metal beads; preventing oxidation and yielding rapidly prototyped structures [31].

Table 3-3: Properties of Water, Ethanol and Dry Air at 100 kPa, 20°C [31]

	Liquid Phase/Cooling fluid		**Gas phase/Cooling fluid**
	Water	**Ethanol**	**Dry air**
Thermal Conductivity (λ, W/(m.K))	0.597	0.24	2.59×10^{-2}
λ/λ_{air}	23.05	9.27	1.00
Density (ρ, kg/m3)	0.998	0.7893	1.205
ρ/ρ_{air}	828.22	655.02	1.00
Viscosity (η, Pa.s)	0.001	0.0012	17.9×10^{-6}
η/η_{air}	55.87	67.04	1.00
Heat capacity (c, kJ/(kg.K))	4.1818	2.42	1.005
c/c_{air}	4.16	2.41	1.00

The temperature of the cooling fluid must be carefully monitored. If it is too warm, the liquid metal will not cool fast enough and melt as a globule. If it is too cool, the droplet will solidify too quickly and will not have enough time to fuse to the previous layer through heat transfer.

The air pressure within the syringe and needle diameter must also be controlled. Too much pressure, or too small a head, will result in smaller droplets. These smaller droplets have a tendency to exit the nozzle following adjacent drops too closely. It this occurs, jetting may result (refer to Figure 3-15 and

Figure 3-16).

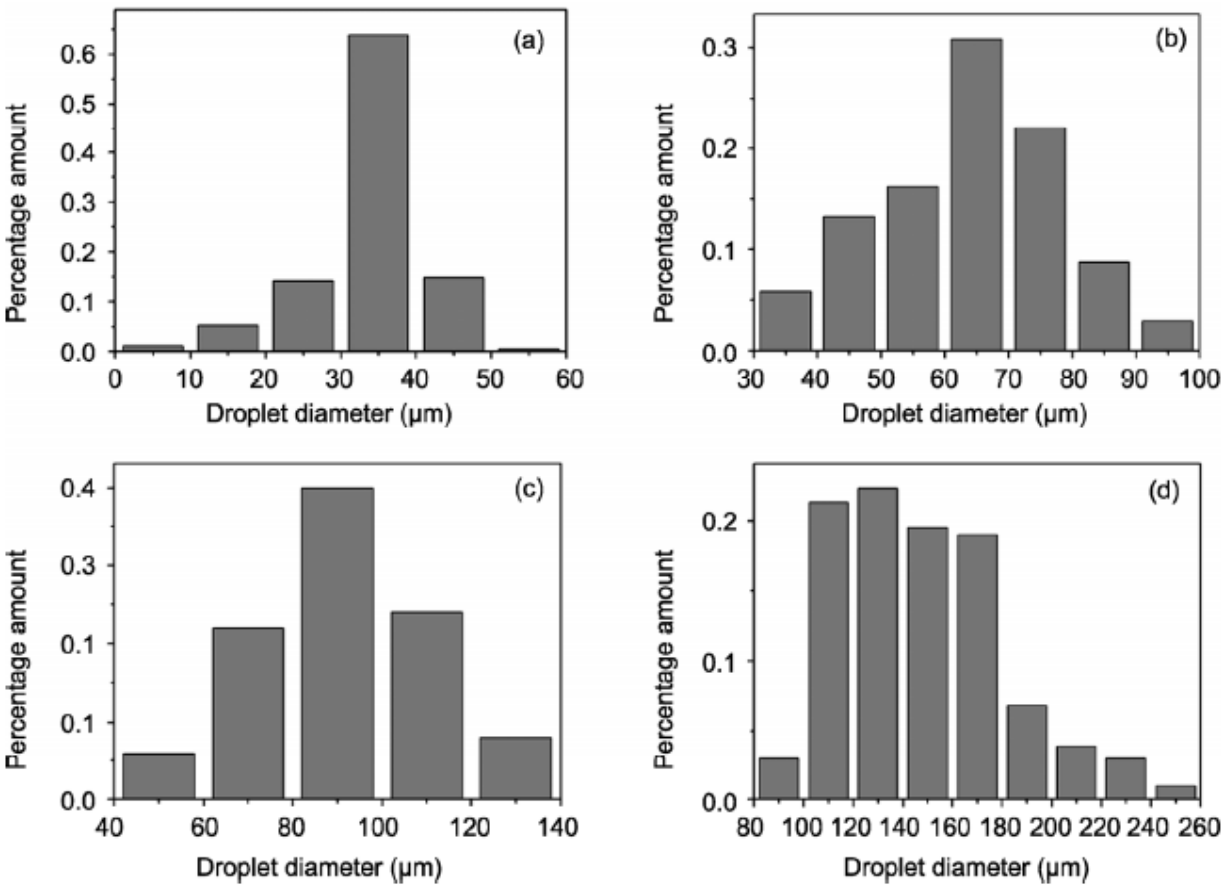

Figure 3-15: The Size Distribution of the Droplets Produced with Syringe Needles (inner diameter) of:

0.16 mm (a), 0.34 mm (b), 0.51 mm (c) and 0.84 mm (d) [31]

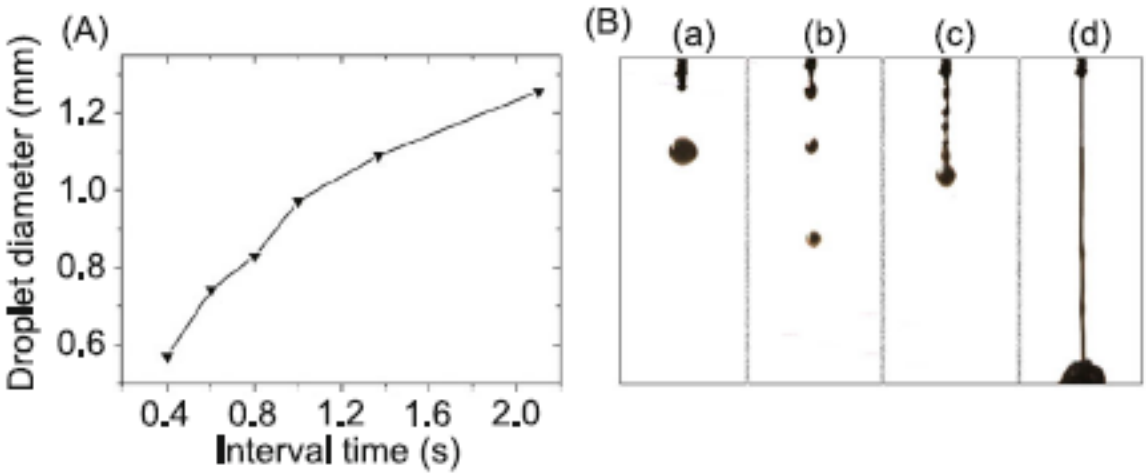

Figure 3-16: The Relationship Between the Droplet Diameter and the Interval

(A) Statistical results by using 0.26 mm inner diameter needle with ethanol cooling method; (B) the process (from a to d) when the interval time changes from 2.1 s (dripping) to zero (jetting) [31]

Embedded 3D Printing of Strain Sensors within Highly Stretchable Elastomers

This e-3DP method was successful in embedding strain gages in an elastomeric matrix. The ink retained its position and remained stable inside the matrix. The curing process yielded very extensible and functional sensors. 900% elongation at failure and a Shore Hardness of 00-30 was achieved. These properties make this component desirable for applications requiring a conforming soft sensing device.

The cross sectional area varied with the printing speed. With a nozzle diameter of 410 um and a print pressure of 50 psi, the cross section went from roughly 0.71 mm to 0.066 mm as the printer's speed increased from 0.5 mm/s to 4 mm/s. The decrease in area led to a rise in the sensors' electrical resistance from approximately 11 kohms to 60 kohms. The ink remained

electrically stable in the e-3DP component. These higher printing speeds resulted in increased sensor sensitivity (due to a smaller cross section), as well as more rounding in the corners of the U-shaped sensors [32].

Hysteresis occurred when the sensors were subjected to strain cycling. The sensors did not achieve their initial resistance value upon relaxation after strain cycling, but it was within 10% of the starting resistance.

Sensors produced predictable responses up to approximately 400%, and then became inconsistent from 400% to 700%. Beyond that sensors began to fail. When embedded sensors ripped at failure strains, they tore where the external wire connects with the sensor and not at imperfections produced during the printing process [32].

Effects of Layer Thickness and Binder Saturation Level Parameters on 3D Printing Process

Refer to Figure 3-17 and Figure 3-18 and

Table 3-4 and Table 3-5 for tensile and flexural testing results.

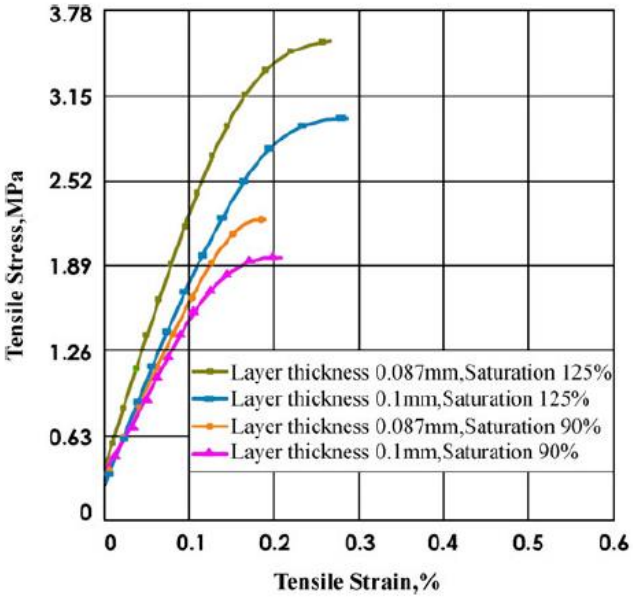

Figure 3-17: Tensile Stress-Strain Results [33]

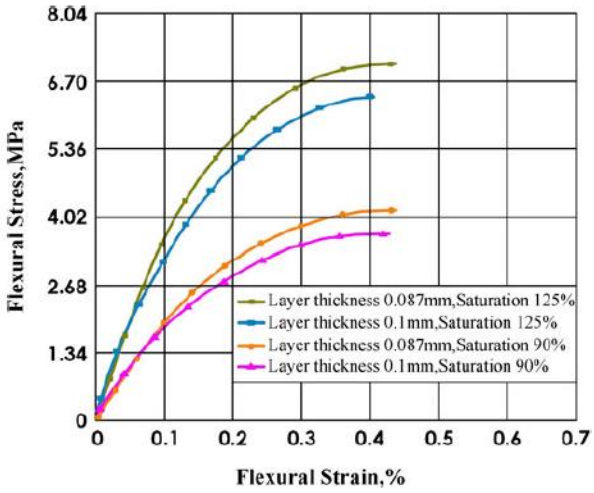

Figure 3-18: Flexural Stress-Strain Results [33]

Table 3-4: Tensile Properties of ZP102 Test Specimens

	Tensile strain (%)	UTS (Mpa)
0.1 mm layer thickness 90% saturation	0.2	1.99
0.087 mm layer thickness 90% saturation	0.19	2.279
0.1 mm layer thickness 125% saturation	0.28	3.048
0.087 mm layer thickness 125% saturation	0.26	3.562

Table 3-5: Flexural Properties of ZP102 Test Specimens

	Flexural strain (%)	Flextural stress (Mpa)
0.1 mm layer thickness 90% saturation	0.42	4.32
0.087 mm layer thickness 90% saturation	0.43	3.83
0.1 mm layer thickness 125% saturation	0.40	7.33

0.087 mm layer thickness 125% saturation	0.43	6.65

Higher saturation levels led to higher tensile and flexural strengths, due to the increased amount of spray binder. Thinner layers resulted in greater tensile strengths in the samples, but a decrease in flexural strengths. Of course, the opposites were true as well.

Under a constant saturation level, a layer thickness decrease also lowered the quality and consistency of the component's surface. This is because the binder is free to spread laterally but struggles to penetrate through layers [33].

3.2.5 Summary

Liquid Phase 3D Printing for Quickly Manufacturing Conductive Metal Objects with Low Melting Point Alloy Ink

This study successfully established a method for 3D printing conductive structures using liquid metal ink. Liquid cooling mediums allow for faster printing times as well as superior print quality due to their thermal properties. The size and exit velocity of droplets from the print nozzle have been identified as variables that affect the integrity of the final structure. The syringe needle diameter, temperature and air pressure can be controlled to optimize these parameters. The liquid phase 3D printer developed and used in this study can be an important tool in expanding the use of additive manufacturing. It could be particularly useful in addressing problems with the lengthy print times that currently inhibit 3D printing from doing large scale production runs [31].

Embedded 3D Printing of Strain Sensors within Highly Stretchable Elastomers

This study established a new approach to 3D printing embedded deformable sensors using a carbon-based ink in a cured matrix. This technology will have many applications in the "soft electronics" industry [32].

Effects of Layer Thickness and Binder Saturation Level Parameters on 3D Printing Process

This study evaluated the impact of layer thickness and binder saturation level on 3D print quality. Samples with the same layer thickness had better strength and integrity at 125% binder saturation than those at 90%. However, the lower binder saturation parts had better overall surface finish. When binder saturation levels are held constant, an increase in layer thickness from 0.087mm to 0.1mm decreased the tensile strength but increased the flexural strength in test samples. The layer thickness increase also improved the surface quality [33].

3.3 Technology in the Medical Industry

Additive manufacturing has enormous potential in the medical industry. This section breaks down studies surrounding printed bones, drugs and medical devices.

3.3.1 Literature Review

Printability of Calcium Phosphate:

Calcium Sulfate Powders for the Application of Tissue Engineered Bone Scaffolds using the 3D Printing Technique

This 2014 study, by Zuoxin Zhou, Fraser Buchanan, Christina Mitchell and Nicholas Dunne, explores blending calcium phosphate (CaP) with the traditional 3D printing powder; calcium sulfate ($CaSO_4$). The composite powder is printed with a water-based binder to maintain good repeatability and to prevent damage to the print head during long term use [34].

Influence of Grain Size and Grain-Size Distribution on Workability of Granules with 3D Printing

This 2014 study by Sebastian Spath and Hermann Seitz assesses the influence of grain size and grain size distribution on the flowability and workability of 3D printing powder.

In Vivo Evaluation and Characterization of a Bio-Absorbable Drug-Coated Stent Fabricated using a 3D-printing System

This 2015 study by Su A Park, Sang Jin Lee, Kyung Seob Lim, In Ho Bae, Jun Hee Lee, Wan Doo Kim, Myung Ho Jeong and Jun-Kyu-Park look at making a biocompatible and biodegradable stent using 3D rapid prototyping technology.

3.3.2 Theory and Purpose

Printability of Calcium Phosphate

Calcium Sulfate Powders for the Application of Tissue Engineered Bone Scaffolds using the 3D Printing Technique

Powder-based inkjet 3DP is particularly desirable for use in the medical field. Inkjet 3D printers use a thermal print head and a binding liquid; liquid bubbles are repeatedly formed and collapsed on the heating surface inside the print head. These bubbles squeeze droplets out of nozzles. These thermal drop-on-demand print heads must use low viscosity binding liquids that do not damage the heating elements. Water based printing fluid is the most gentle on the print head during prolonged use and is currently present in most 3D printers [34].

For medical applications, it would be desirable to use CaP, which is biocompatible and chemically similar to bone. To print a strong product, CaP must be used in conjunction with an acidic binder which would corrode and damage the printhead when used repeatedly. This study

hopes to blend CaP with another suitable medically compatible powder to form a compound that is curable with a water-based binder, thereby saving the printhead for larger scale production runs. $CaSO_4$ is selected given its previously commendable performances in other medical applications. The composite powder's 3D printability is assessed for powder packing attributes, binder drop penetration, wettability and the integrity of 3D printed components using the CaP:$CaSO_4$ blend. [34]

Influence of Grain Size and Grain-Size Distribution on Workability of Granules with 3D Printing

3D printing is emerging at the forefront of bone scaffolding technology. Bone implants are generally composed of hydroxyapatite (HA), given its likeness to human bone. Microporosity is crucial to a well-integrated bone scaffold. Microporosity is dependent on grain size and grain size distribution. However, changes to the grain size and grain size distribution impacts flowability, which is a key parameter in 3D printability. 3D printing powder recoating also requires a certain degree of flowability. The purpose of this study is to examine the relationship between grain size and grain size distribution on the powder's flowability, as well as establish an optimal recoating method [35].

In Vivo Evaluation and Characterization of a Bio-Absorbable Drug-Coated Stent Fabricated using a 3D-printing System

Bio-absorbable vascular stents (BVS) are one type of stent currently used to treat coronary artery disease. BVS have the advantage of completely degrading, and typically see lower instances of restenosis. An optimal BVS should be a strong biomechanical vascular support, have the ability to slowly release medication during vascular healing to prevent

neointimal hyperplasia and disintegrate after vascular repair. 3D printing such a stent has become a reality given advances in the rapid prototyping technology. However, traditional bare metal stents (BMS) manufactured from stainless steel or titanium can cause adverse side effects as they remain in the body even after vascular repair. A 3D printed BVS must be composed of polycaprolatone (PCL) in order to be residue-free. The stent must be spray coated with an immunosuppressive drug (sirolimus). If successful, this would be the first BVS capable of sustained drug release [36].

3.3.3 Method

Printability of Calcium Phosphate:

Calcium Sulfate Powders for the Application of Tissue Engineered Bone Scaffolds using the 3D Printing Technique

Two different types of CaP powders are blended with $CaSO_4$ in ratios of 25:75 wt.% and at 50:50 wt.%. A coarse and a fine powder are made for each blend, thereby making 8 different composite powders. The powder reservoir is carefully controlled. The powder bed packing ratio is calculated using Equation 3.1 [34].

$$\textbf{Powder bed packing ratio} = \textbf{Powder bed} \times \frac{\textbf{density}}{\textbf{CaP} \times \rho_{CaP} + CaSO_4 \times \rho_{CaSO_4}} \qquad \text{Eq 3.1}$$

Drop penetration tests are conducted using a droplet of the water-based binder. The wetting ratio is calculated using Equation 3.2.

$$\text{Wetting Ratio} = \frac{(\text{mass}_{(granula)} - \text{mass}_{(droplet)})}{((CaP \times \rho_{CaP} + CaSO_4 \times \rho_{CaSo_4}) \times \text{volume}_{(droplet)})} \qquad \text{Eq 3.2}$$

A scanning electron microscopy (SEM) is used to examine the powders. An X-ray diffraction (XRD) is performed as well [34].

Influence of Grain Size and Grain-Size Distribution on Workability of Granules with 3D Printing

A 3D printing powder (calcium phosphate) spray-dried with HA particles is segregated into different grain size fractions. Pure HA is mixed with two different grain size groups. Particle size analysis is conducted on all grain size categories using a laser granulometry. Optical examination is done with a SEM. Powder recoating testing is also carried out to determine an optimal recoating method. The fixed blade, fixed roll and rotating roll recoating mechanisms will all be analyzed.

The angle of repose (AoR), flow rate (FR), Hausner ratio (HR) and Carr's index (CI) are all used to measure flowability (refer to Equations 3.3 and 3.4).

$$HR = \frac{density_{tapped}}{density_{\ bulk}} \qquad \text{Eq 3.3}$$

$$CI = \frac{density_{tapped} - density_{bulk}}{density_{\ tapped}} \qquad \text{Eq 3.4}$$

In Vivo Evaluation and Characterization of a Bio-Absorbable Drug-Coated Stent Fabricated using a 3D-printing System

PCL, poly-lactide-co-glycolide (PLGA) and polyethylene glycol (PLGA-PEG) are used to make and coat the stents. 50 BVS PCL scaffolds are made using 3D printing; 25 will be drug coated and 25 will not. The strut size distance is 300 microns while the between strand distance is 1300 microns. The BVS is sprayed with PLGA-PEG 15 and the sirolimus drug using an

ultrasonic spray device. The stents are then sputter coated with gold for 1.5 minutes. Weight gain during drug coating is measured and the stents are subjected to a phosphate degradation test. The stents are tested in male pigs [36].

3.3.4 Simulation Results and Discussion

Printability of Calcium Phosphate:

Calcium Sulfate Powders for the Application of Tissue Engineered Bone Scaffolds using the 3D Printing Technique

Powder Packing

Coarse powders had much higher packing bed densities than the finer blends. Packing ratios were also higher in the coarser powder compared to the finer blend (refer to Table 3-6). The coarser composite powders had smoother powder bed surfaces as well. The finer blends had lower levels of surface homogeneity.

Table 3-6: Powder Properties for Beta-TCP:$CaSO_4$ Combinations [34]

Powder Properties	β-TCP (coarse):$CASO_4$		β-TCP (fine): $CASO_4$	
	25:75 wt. %	**50:50 wt.%**	**25:75 wt. %**	**50:50 wt.%**
True Particle Density ($g.cm^{-3}$)	2.855	2.95	2.855	2.95
Bulk Density ($g.cm^{-3}$)	0.823 ± 0.006	0.763 ± 0.006	0.640 ± 0.009	0.531 ± 0.005
In-process powder bed density ($g.cm^{-3}$)	0.923 ± 0.035	0.898 ± 0.054	0.620 ± 0.063	0.552 ± 0.050
Powder bed packing ration	32% ± 1%	30% ± 2%	22% ± %2	19% ± 2%

Drop Penetration and Wettability

CaP:$CaSO_4$ combinations had faster drop penetration times than pure CaP powder. Coarse $CaSO_4$ powders yielded lower drop penetration times than the finer blends. However, the coarse powders had less vertical penetration (refer to Table 3-7 and Table 3-8).

Table 3-7: Drop Penetration Data (Mean +/- SD) for HA:$CaSO_4$ Powder Combinations [34]

	HA (coarse):$CaSO_4$		HA (fine):$CaSO_4$	
	25:75 wt%	**50:50 wt%**	**25:75 wt%**	**50:50 wt%**
Drop penetration time (s)	1.5 ± 0.16	0.73 ± 0.14	3.88 ± 1.32	4.80 ± 1.4
Granule height (mm)	3.04 ± 0.05	3.46 ± 0.26	4.97 ± 0.21	4.16 ± 0.31
Wetting ratio (%)	1.03 ± 0.04	1.05 ± 0.15	0.66 ± 0.07	0.45 ± 0.03

Table 3-8: Drop Penetration Data (Mean +/- SD) for Beta-TCP:$CaSO_4$ Powder Combinations [34]

	HA (coarse):$CaSO_4$		HA (fine):$CaSO_4$	
	25:75 wt%	**50:50 wt%**	**25:75 wt%**	**50:50 wt%**
Drop penetration time (s)	1.96 ± 0.54	2.23 ± 0.28	5.07 ± 1.07	3.01 ± 0.37
Granule height (mm)	3.37 ± 0.09	2.69 ± 0.11	4.47 ± 0.32	3.69 ± 0.21
Wetting ratio (%)	0.64 ± 0.03	0.42 ± 0.03	0.57 ± 0.12	0.22 ± 0.07

The finer blends demonstrated lower wetting ratios than their coarser counterparts [34].

Analysis of the 3DP manufactured components

Coarser powder blends had a higher green mass than the finer powder blends (refer to Figure 3-19). There were large differences in the green mass for the fine power between the 25 wt.% CaP and 50 wt.% CaP blends. This was not the case with the coarse composite powders.

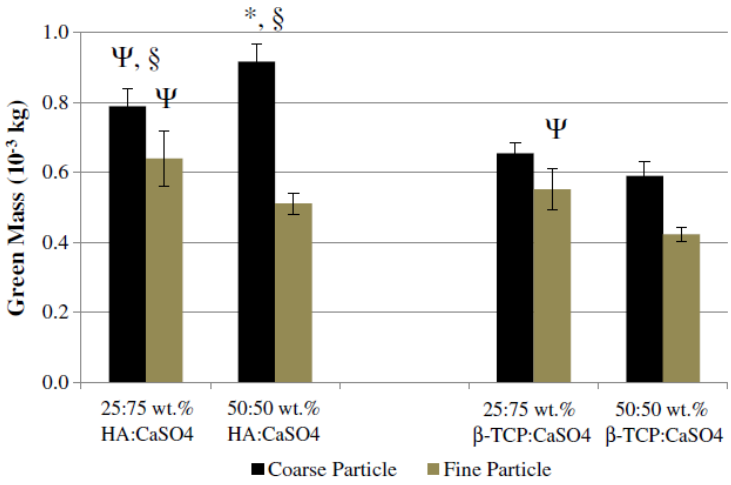

Figure 3-19: Green Mass of Components with Different Powder Combinations [34]

* denotes p-values < 0.05, indicating a significant difference between a CaP (coarse): $CaSO_4$ powder and a CaP (fine): $CaSO_4$ powder; Ψ denotes p-values < 0.05, indicating a significant difference between powders having differing CaP: CaSO4 ratios; § denotes p-values < 0.05, indicating a significant difference between HA: $CaSO_4$ and the β-TCP: $CaSO_4$ powder combinations

Increasing the CaP weight ratio for both the fine and coarse powders decreased compressive strength. 3D printed samples were the highest quality when the 25:75 wt.% coarse CaP: $CaSO_4$ powder was used (refer to Figure 3-20). Solid blocks and 3D porous components were successfully printed in a repeatable fashion [34].

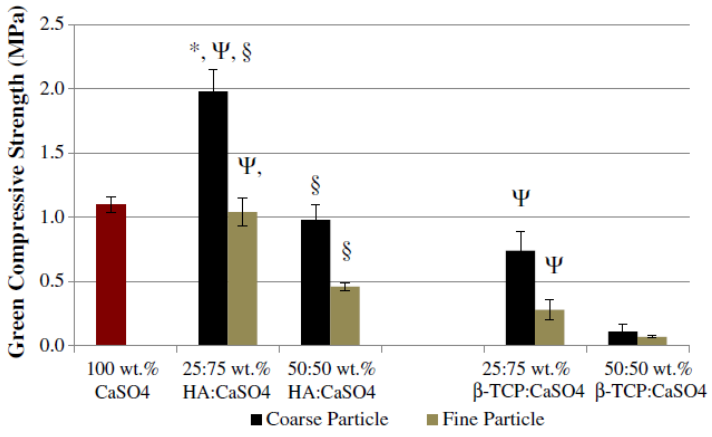

Figure 3-20: Green Compressive Strength of Components with Different Powder Combinations [34]

* denotes p-values < 0.05, indicating a significant difference between a CaP (coarse): $CaSO_4$ powder and a CaP (fine): $CaSO_4$ powder; Ψ denotes p-values < 0.05, indicating a significant difference between powders having differing CaP: CaSO4 ratios; § denotes p-values < 0.05, indicating a significant difference between HA: $CaSO_4$ and the β-TCP: $CaSO_4$ powder combinations

The coarser powder size resulted in a higher packing bed density and packing ratio when compared to the finer blends. This increased flowability which increased print resolution. It also led to favorable powder-binder reactivity and wettability. CaP:$CaSO_4$ powder composites at 25:75 wt.% had a higher green strength that those at 50:50 wt.%.

SEM demonstrated macropores in the heterogeneously distributed powder bed with finer grain size, which decreased printability [34].

Influence of Grain Size and Grain-Size Distribution on Workability of Granules with 3D Printing

Refer to

Table 3-9 for the laser granulometry testing.

Table 3-9: Results from Particle Size Analysis [35]

	D10 (µm)	D50 (µm)	D90 (µm)	Span
<32	8.8	20.3	31.0	1.1
32-45	11.4	28.3	43.7	1.1
45-63	15.1	40.2	59.2	1.1
63-80	45.0	63.8	88.3	0.7
80-100	60.0	80.2	108.4	0.6
100-125	72.4	97.7	132.8	0.6
>125	82.9	125.5	178.8	0.8
EG	22.5	58.8	107.4	1.4
>125+15%	40.2	122.3	173.2	1.1
>135+25%	36.9	119.9	174.6	1.2

Refer to Figure 3-21a and Figure 3-21b, and Figure 3-22a and Figure 3-22b for SEM test results.

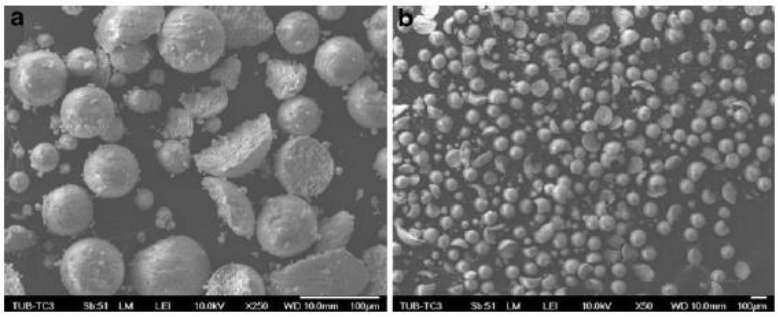

Figure 3-21: SEM Images of Broken HA Granules [35]

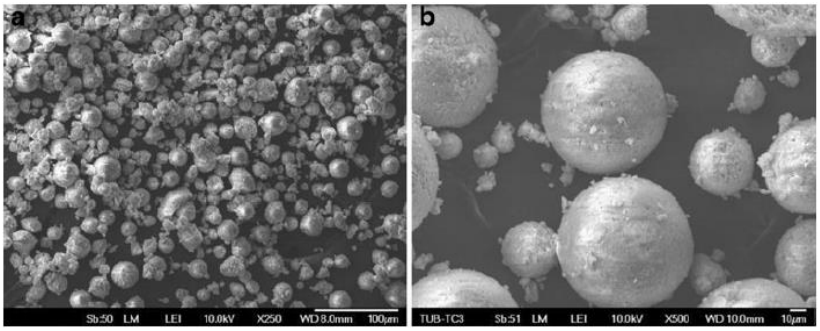

Figure 3-22: SEM Test Results

a) Irregularly Shaped Granules in Fraction <32

b) Spherical Particles in EG [35]

Refer to Table 3-10 for qualitative results from the powder granule recoating testing.

Table 3-10: Qualitative Results from Powder Recoating [35]

	FiB	FiR	RotR
<32	○	○	◔
32-45	◔	◔	◑
45-63	◔	◑	◑
63-80	◑	◑	◕
80-100	◑	◕	●
100-125	◕	◕	●
>125	◕	◕	●
EG	◕	◕	●
>125+15%	◕	◕	●
>135+25%	◕	◕	●

The smallest size fraction to show permissible surface recoating with the fixed blade was the 80-100 group. The 45-63 group produced acceptable results with the rotating roll mechanism, while the 63-80 fraction was the first section coated by the fixed roll to become passable [35].

Refer to Table 3-11 for HR, CI, BD, TD and AoR values.

Table 3-11: Bulk density (BD), Tapped density (TD), Hausner ration (HR), Carr's index (CI), Funnel diameter (FD) and Angle of repose (AoR) [35]

	BD (kg/m^3)	TD (kg/m^3)	HR	CI	FD (mm)	AoR (^{o})
32	399.1	512.4	1.28	22.1	18	58.5
32-45	429.3	547.9	1.28	21.6	16	55.2
45-63	452.3	549.6	1.21	17.7	14	53.9
63-80	462.5	550.9	1.19	16.1	8	48.7
80-100	466.3	540.5	1.16	13.7	4	48.4
100-125	470.9	541.9	1.15	13.1	4	47.6
>125	478.2	552.2	1.15	13.4	2	45.2
EG	480	599.4	1.25	19.9	8	55.5
>125 + 15%	497.2	602.4	1.21	17.5	4	51.3
>125 + 25%	496.8	604.6	1.22	17.8	10	54.7

Recoating methods are analyzed with respect to flowability as indicated by HR (refer to Figure 3-23).

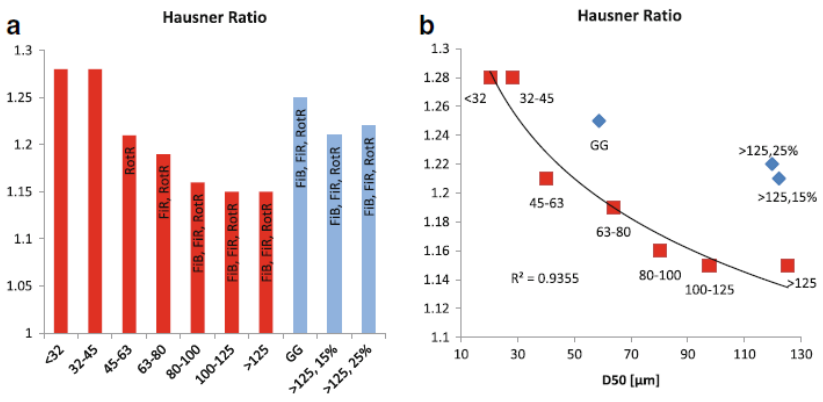

Figure 3-23: HR Plots

a) HR and Ideal Recoating Mechanism

b) Dependency of HR on Median Particle Size [35]

Recoating methods are analyzed with respect to flowability as indicated by CI (refer to Figure 3-24).

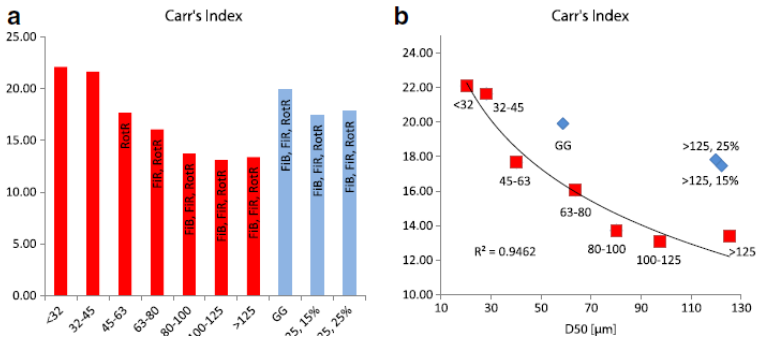

Figure 3-24: CI Plots

a) CI and Ideal Recoating Mechanism

b) Dependency of CI on Medium Particle Size [35]

Given the results from the CI and HR data, flowability may not be determined from HR and CI alone, and grain size distribution must be taken into account. Naturally, the required funnel diameter for uniform flow decreased with grain size (refer to Figure 3-25).

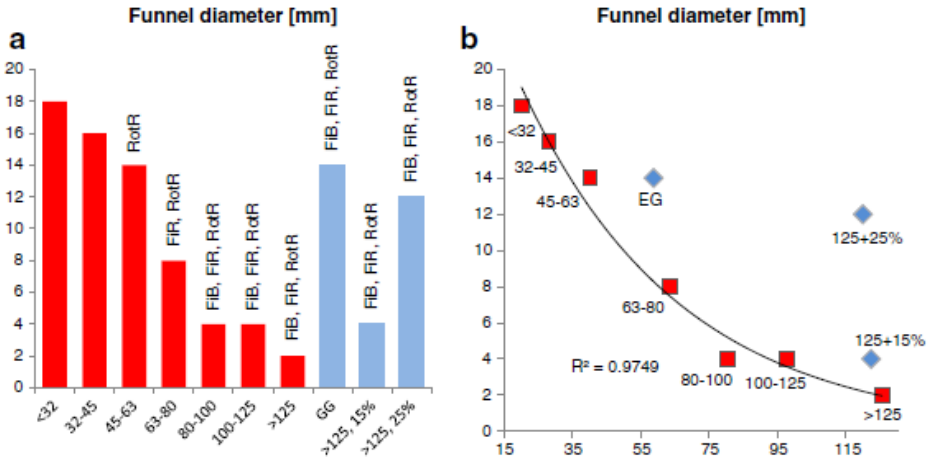

Figure 3-25: Funnel Diameter Plots

a) Funnel Diameter (mm)

b) FD Dependency on Median Particle Size [35]

The angle of repose graphs are similar to those of HR, CI and FD (refer to Figure 3-26).

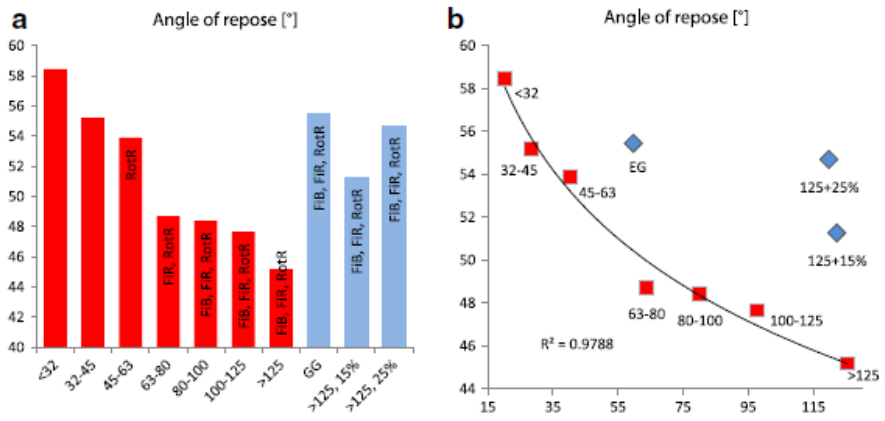

Figure 3-26: Angle of Repose Plots

a) Angle of Repose

b) AoR Dependency on Median Particle Size [35]

The flow rate increased with particle size (refer to Figure 3-27).

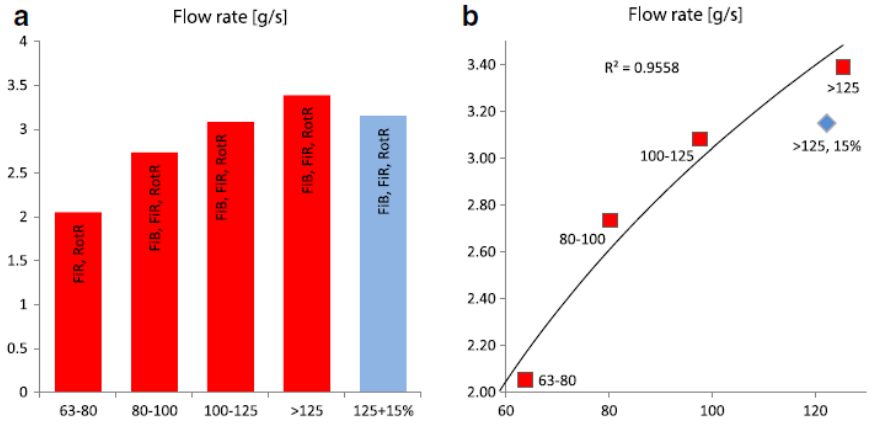

Figure 3-27: Flow Rate Plots

a) Flow Rate (g/s)

b) Flow Rate Dependence on Median Particle Size [35]

For the minimum flow rate suitable for each recoating mechanism, see Table 10.

Table 3-12: Minimum FR for Different Recoating Mechanisms (single fractions)

	FiB	FiR	RotR
FR (g/s)	2.73	n.v.	n.v.

In Vivo Evaluation and Characterization of a Bio-Absorbable Drug-Coated Stent Fabricated using a 3D-printing System

The initial weight of the BVS was 25.021 mg, and rose to 25.720 mg after being sprayed with the drug coating. The thickness of PLGA-PEG with the sirolimus layer was 5 +/- 2.5 microns. Traditional BVS (without coating) have a rough surface but this 3D printed drug-coated BVS had a smooth and pristine finish. The drug coated BVS released its drugs slowly with only 50% gone at 31 days. The 3D printed BVS provided mechanical support to the artery for 31 days at minimum. Ideally, a structure would support the artery for 3 to 6 months before completely degrading. After 4 weeks in the pigs, restenosis coverage was at 20.7% for the drug coated BVS compared to a less desirable 35.9% from the non-coated BVS. After 4 weeks, the sirolimus coated BVS significantly reduced neointimal hyperplasia compared to the non-coated BVS [36].

3.3.5 Summary

Printability of Calcium Phosphate:

Calcium Sulfate Powders for the Application of Tissue Engineered Bone Scaffolds using the 3D Printing Technique

This study examined 3D printing using CaP:$CaSO_4$ blends and evaluated variables that affect the printing quality. Fine powders led to heterogeneously distributed powder beds, slow

drop speeds, low wetting ratios, lower green masses and strengths, but larger drop penetration depth. Coarse powders resulted in homogenously distributed powder bed, rapid drop speeds, high wetting ratios and greater strengths, but lower drop penetration. Coarser grain size with a 25:75 wt.% CaP:$CaSO_4$ was generally favourable and has potential for 3D printing in the medical industry [34].

Influence of Grain Size and Grain-Size Distribution on Workability of Granules with 3D Printing

The Hausner ratio, Carr's index, funnel diameter, angle of repose and flow rate of the tested calcium phosphate all produced similar graphical curves. The testing confirmed that increased grain size led to an increase in flowability and improved print quality. When recoating powder granules, it was important to compare grain size distribution when assessing flowability, as the HR, CI, FD, AoR and FR values suggested unacceptable levels of flowability when in fact is was passable. Future work should focus on conducting these studies in a technical setting that more closely mirrors the actual process of 3D printing. This should produce more accurate results on recoating mechanisms. The rotating roll method of recoating proved to be the best in achieving good surface finishes [35].

In Vivo Evaluation and Characterization of a Bio-Absorbable Drug-Coated Stent Fabricated using a 3D-printing System

The drug-coated BVS was successfully 3D printed. The sirolimus was released from the stent in a uniform and sustained fashion. It reduced neointimal hyperplasia. The study suggests that 3D printing should be used for fabricating drug-eluting stents [36].

3.4 Technology in Manufacturing

3D printing will offer invaluable advantages to manufacturing companies. The section reviews many studies surrounding the world of manufacturing.

3.4.1 Literature Review

Additive Manufacturing for Product Improvement at Red Bull Technology

This 2012 study by David E. Cooper examines the viability of manufacturing hydraulic components using direct metal laser sintering (DMLS) for the Red Bull Formula 1 racing team.

Property Enhancement of 3D-Printed Alumina Ceramics using Vacuum Infiltration

This 2014 study by S. Maleksaeedi, H. Eng, F. E. Wiria, T.M.H. Ha and Z. explores vacuum infiltrating 3D printed ceramics with alumina slurry to improve density in sintered 3DP components.

3D Printing of Cement Composites

This 2010 study, by G.J. Gibbons, R. Williams, P. Purnell and E. Farahi, examines the possibility of 3D printing rapid hardening Portland cement (RHPC).

Using Magnetite/Thermoplastic Composite in 3D Printing of Direct Replacements for Commercially Available Flow Sensors

This 2014 study by S.J. Leigh, C.P. Pursell, D.R. Billson and D.A. Hutchins uses a magnetic thermoplastic composite to 3D print a flow sensor.

3D-Printing of Lightweight Cellular Composites

This 2014 study, by Brett G. Compton and Jennifer A. Lewis, examines 3D printing lightweight cellular composites. 3D printing offers unparalleled flexibility and cellular composites have many high performance applications due to their physical attributes.

3.4.2 Theory and Purpose

Additive Manufacturing for Product Improvement at Red Bull Technology

DMLS allows for components to have increasingly complex internal structures compared to their traditionally moulded counterparts. DMLS techniques are conducive to implementing material removal as a weight saving measure. This makes DMLS an attractive technology for F1 racing, which places weight at a premium. In addition, due to the design flexibility afforded by DMLS, internal flow paths for hydraulic components may be enhanced. However, DMLS is largely unproven and there remains uncertainty surrounding the material's mechanical properties and the repeatability of the process. This study uses pressure testing, flow visualization, surface roughness, dimensional accuracy measurements, micro hardness testing and porosity measurements to assess DMLS's viability compared to traditionally fabricated components [37].

Property Enhancement of 3D-Printed Alumina Ceramics using Vacuum Infiltration

3D printing ceramics traditionally requires combining ceramic powder with a binder, with the result typically being very porous. This leads to a low green and sintered density. Other techniques for improving density have been tried with some success. The best results have

been achieved using vacuum infiltration. Correspondingly, this study has chosen to supplement sintering with an alumina vacuum infiltrate to increase density [38].

3D Printing of Cement Composites

Materials other than polymers are being assessed for their feasibility in additive manufacturing. Ceramics are of particular interest as they could be used to 3D print bone implants. However, 3D printed ceramics offer poor strength and water resistance. In addition, they require large amounts of post-processing operations. Post-processing often precludes the addition of bio-additives such as growth factors or pharmaceuticals. Hydraulic cement does not require these extra operations, is easily customized and is much cheaper than traditional 3D printed ceramics. This study attempts to establish a "proof-of-concept" of 3D printing using RHPC [39].

Using Magnetite/Thermoplastic Composite in 3D Printing of Direct Replacements for Commercially Available Flow Sensors

3D printing material with magnetic properties is useful in manufacturing functional devices. In order to demonstrate these capabilities, this study seeks to replicate a commercially available flow sensor through additive manufacturing. Liquid passes through the body of the flow sensor and forces the internal magnetic rotor to spin. Imbedded magnetic sensors analyze the moving magnetic fields and produce pulses. The frequency of the pulses is then proportional to the flow rate of the liquid (refer to Figure 3-28). The purpose of this project is to demonstrate that 3D printing is useful in manufacturing applications of already commercially available products and should not be solely considered as a RP technology [40].

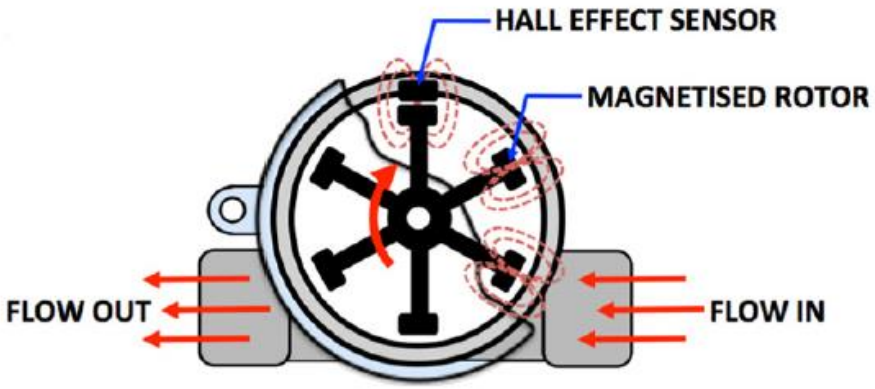

Figure 3-28: Commercially Available Flow Sensor Operation Technique [40]

3D-Printing of Lightweight Cellular Composites

Cellular composites are composed of an interconnected network of cells, and are desirable from an engineering perspective given their low density, high strength specific properties and multifunctionality. Carefully controlling the composition and structure of the cell pattern can yield exceptional bending stiffness and strength. This study reports on using a new epoxy-based 3D printing ink to form cellular composites with a high degree of controllability. The printing ink is concentrated and viscoelastic; it undergoes shear thinning so that it may be extruded relatively easily during printing. However, the ink also has a suitably high shear elastic modulus and shear yield strength in order to maintain the printed filamentary shape upon contact with the print surface. Epoxy resins do not solidify in the same manner as other 3D printed inks. Instead, these inks undergo thermal curing at high temperatures [41].

3.4.3 Method

Additive Manufacturing for Product Improvement at Red Bull Technology

DMLS hydraulic components are printed with wall thicknesses ranging from 0.5 mm to 2 mm with varying cross-sectional geometries. Theses DMLS components are tested against traditionally manufactured aluminum ones [37].

Pressure Testing:

Both sets of parts are pressure tested; they are inserted into an oven and connected to a hydraulic rig. The temperature is raised to 140°C at a rate of 10°C/min, while the pressure is raised 2.5 MPa every 2 minutes until 25 MPa (3 MPa over operating pressure in F1 car). Once validated at 25 MPa, the pressure is reduced to 24 MPa and held for 20 minutes. The thinnest walled 0.5 mm samples are subjected to an additional 30 minutes at 24 MPa [37].

Flow Visualization

Particle Image Velocimetry (PIV) is used to conduct a flow visualization study on DSLM components. The passage of glass particles in fluid is recorded by a high speed camera. Software is used to infer particle vectors.

Surface Roughness Measurements

A non-contact interferometer is used to measure the AM components' surface at several points.

Dimensional Accuracy Measurement

A dimensional accuracy measurement test is made before and after the pressure testing.

Micro hardness Testing

Samples are hot-mounted, polished to 1 micron and microhardness tested to obtain a Vicker's hardness rating.

Porosity Measurement

Samples are hot-mounted, polished to 3 microns and etched with hydrofluoric acid. A microscope and porosity imaging software is used to obtain a reading.

Property Enhancement of 3D-Printed Alumina Ceramics using Vacuum Infiltration

Ceramic printing powder is prepared to allow for a high degree of flowability. Ceramic spheres are 3D printed using the powder and handled in a manner to improve strength. Very concentrated alumina slurries with 30%-50% solid matter are then created. The parts are infiltrated using a vacuum process. Figure 3-29 outlines the vacuum infiltration technique. The components are then sintered.

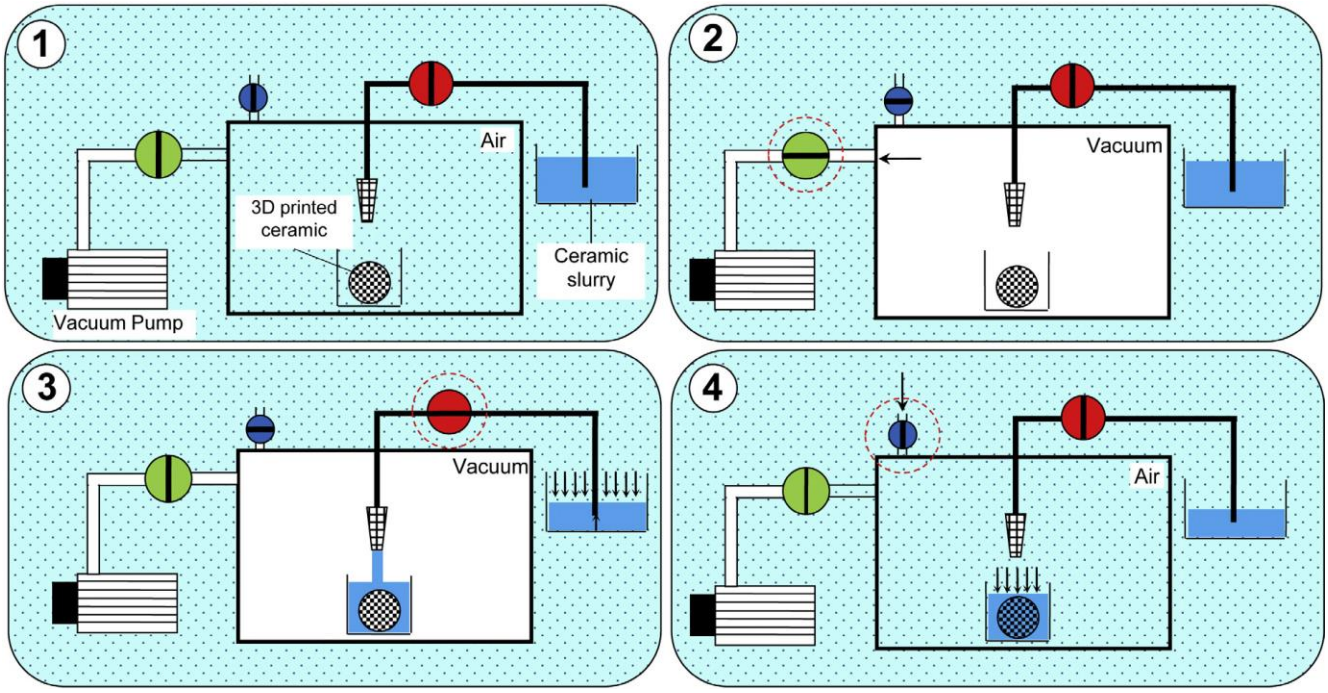

Figure 3-29: Vacuum Infiltration Method [38]

The printed and infiltrated parts are analyzed using a scanning electron microscope. The green and sintered densities are measured using several different techniques. The parts then undergo a 4 point bend test using an Instron machine, and the surface roughness is measured with a surface profiler [38].

3D Printing of Cement Composites

RHPC is 3D printed with demineralized water as the liquid binder. Small amounts of organic modifiers are also included in the RHPC powder at ratios of between 90:10 and 99:1. 3D printed components are then cured in water. The curing times and water temperatures are varied to determine optimal conditions. 12h, 24h and 26 day curing times are used with room temperature water, while 1 day is used with water at 80°C. Cured 3D printed parts are subjected to a 4-point flexural test. Parts are examined using a SEM [39].

Using Magnetite/Thermoplastic Composite in 3D Printing of Direct Replacements for Commercially Available Flow Sensors

A standard FDM 3D printer is used. Instead of making the entire impeller for the flow meter from a ferrous composite (as it is in the commercial sensor), only a small portion is magnetic. This is beneficial as it proves that 3D printing may be advantageous in reducing the amount of functional material required when costs are a concern. In addition, the typical ABS printing material can be used for the bulk of the impeller and will guarantee structural integrity. A composite magnetite thermoplastic is created for the FDM printer, and the flow sensor is subsequently printed [40].

SEM analysis to monitor the dispersion of the magnetite filler is conducted. Flow testing using air is carried out to prove the sensor is accurate and stable. It is important to monitor if the 3D printed material maintains its structure and does not deform during prolonged flow. The printed sensor will be compared to commercial sensors using trials with circulating water [40].

3D-Printing of Lightweight Cellular Composites

The ink is formulated with epoxy resin, nano-clay platelets, dimethyl methyl phosphonate (DMMP), silicon carbide whiskers and carbon fibers. An imidazole-based ionic fluid is used as a latent curing agent.

Rheological properties of the 3DP ink are analyzed using a rheometer. Samples are printed and subjected to tensile testing. The tensile testing uses samples with print paths in both the transverse and tensile directions. In addition, tensile samples made from only the base epoxy, free from carbon reinforcement, are tested for comparison. Strain measurements are also taken [41].

3.4.4 Simulation Results and Discussions

Additive Manufacturing for Product Improvement at Red Bull Technology

Pressure Testing

All samples, regardless of wall thickness, passed the pressure test. Except for the 3% initial pressure drop inherent to the system, pressure held constant.

Flow Visualization

There are areas of recirculation in traditional hydraulic geometry. The recirculation of fluid is caused by the manufacturing process which sees bores being blocked with Lee plugs. This causes abrupt changes in the flow direction and results in a reduction of flow velocity.

Refer to Figure 3-30 and Figure 3-31 for a flow vector field comparison between DSLM and traditional geometries. The 3D printed geometry allowed for a 250% increase and 160% increase in flow velocity at the end and center points respectively. A reduction in energy loses during transport requires less energy expenditure from the engine in the F1 car [37].

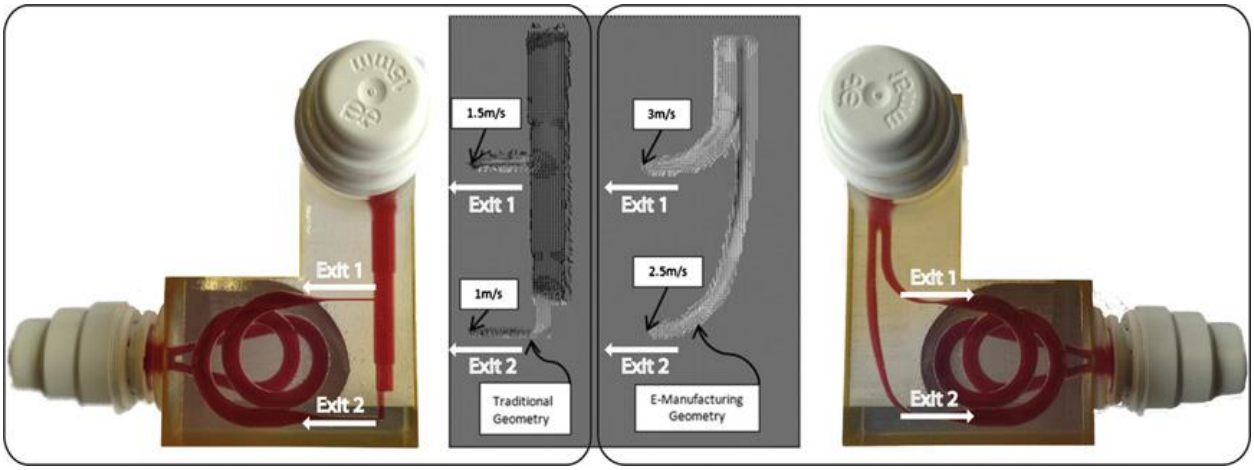

Figure 3-30: Vector Fields and Test Samples for Traditional and DSLM Components [37]

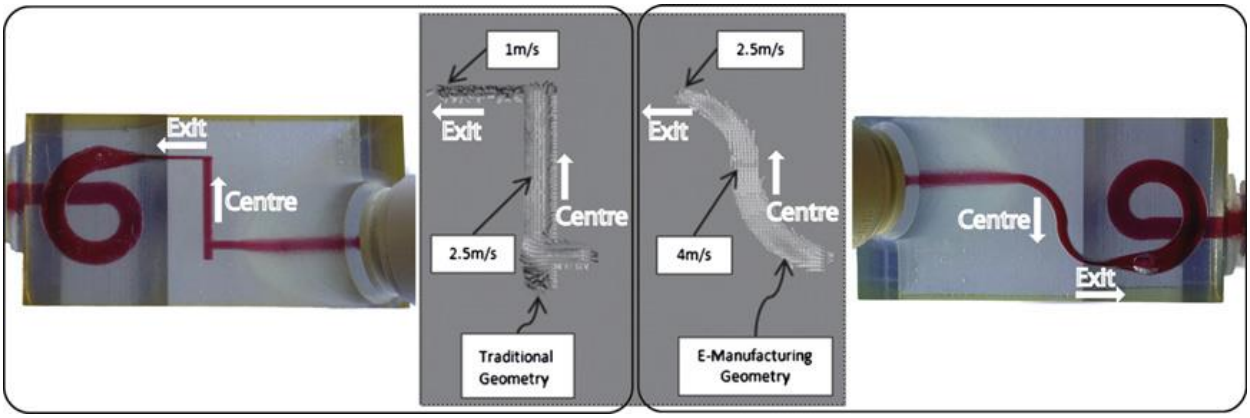

Figure 3-31: Vector Fields and Test Samples for Traditional and DSLM Components [37]

Surface Roughness

The machined components proved smoother than the 3D printed parts, which were not subjected to a finishing process. The roughest surfaces were faces where the structure was supporting during the DMLS build. For average surface roughness, refer

to Table 3-13.

Table 3-13: Surface Roughness Measurements for the DMLS Samples [37]

Position	R_a (μm)
Top Surface	3.96 ± 0.05
Upper facing sloping surface	8.95 ± 0.05
Lower facing sloping surface	17.50 ± 0.05
Supported surface	27.93 ± 0.05

Dimensional Accuracy

The pressure testing caused a minor change in the samples' dimensional accuracy. The highest deviation was seen in the thinnest section of the walls. These dimensional changes are largely attributed to the process of fitting samples onto the testing apparatus, and are not caused by pressure effects from the actual test [37].

Microhardness

DSLM parts yielded a Vicker's hardness of approximately 350 HV before heat treatment. This value climbed to roughly 500 HV post treatment [37].

Porosity

The areal density porosity of AM components was 0.28%+/- 0.05%. This is within the range usually present in an ALM processed Titanium alloy [37]

Property Enhancement of 3D-Printed Alumina Ceramics using Vacuum Infiltration

Refer to Figure 3-32 for a comparison of relative green densities, before and after infiltration, using a slurry with varying amounts of solid matter (and varying alumina ball sizes within the slurry). The green density of the components before infiltration is less than 25% (of

theoretical density). As the solid matter in the slurry approaches 30%-50%, the green density improves substantially. The 1.0 and 1.5 cm alumina spheres increase green density as their presence in the infiltrate increases. The 2.0 cm alumina balls improve density up to 30% by volume in the slurry, but after that, overall density decreases.

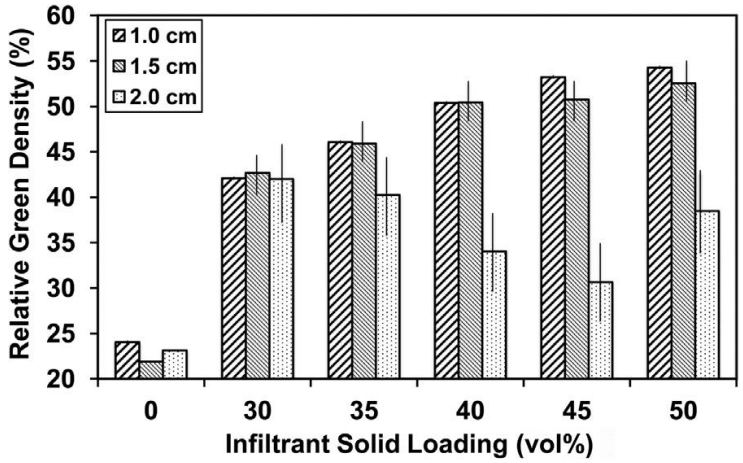

Figure 3-32: Relative Green Density vs Infiltrant Solid Loading [38]

Refer to Figure 3-33 for a comparison of relative sintered densities before and after infiltration using slurry with varying amounts of solid matter (and varying alumina ball sizes within the slurry). Similar trends between the sintered and green densities exist when compared to the amount of solid infiltrant present. Up to 85% relative density can be achieved under optimal conditions.

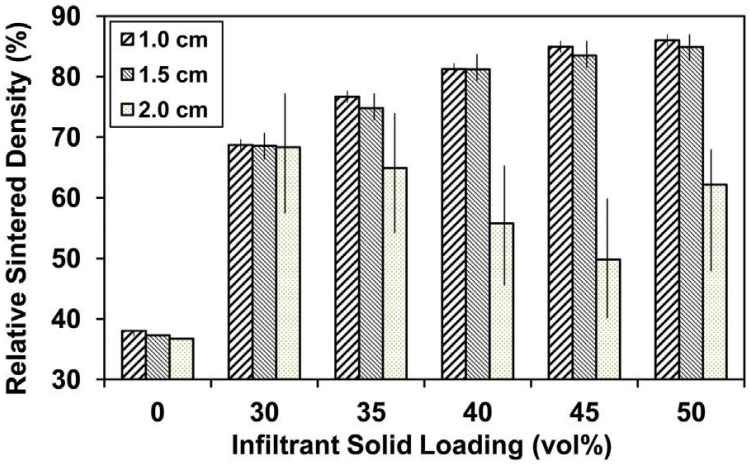

Figure 3-33: Relative Sintered Density vs Infiltrant Solid Loading

Refer to Figure 3-34 for the pore size distribution of the 1.0 cm spheres. It is desirable to eliminate inter-agglomerate pores, which reduce density (refer to Figure 3-35). Infiltrating components reduces inter agglomerate pores (see Figure 3-36).

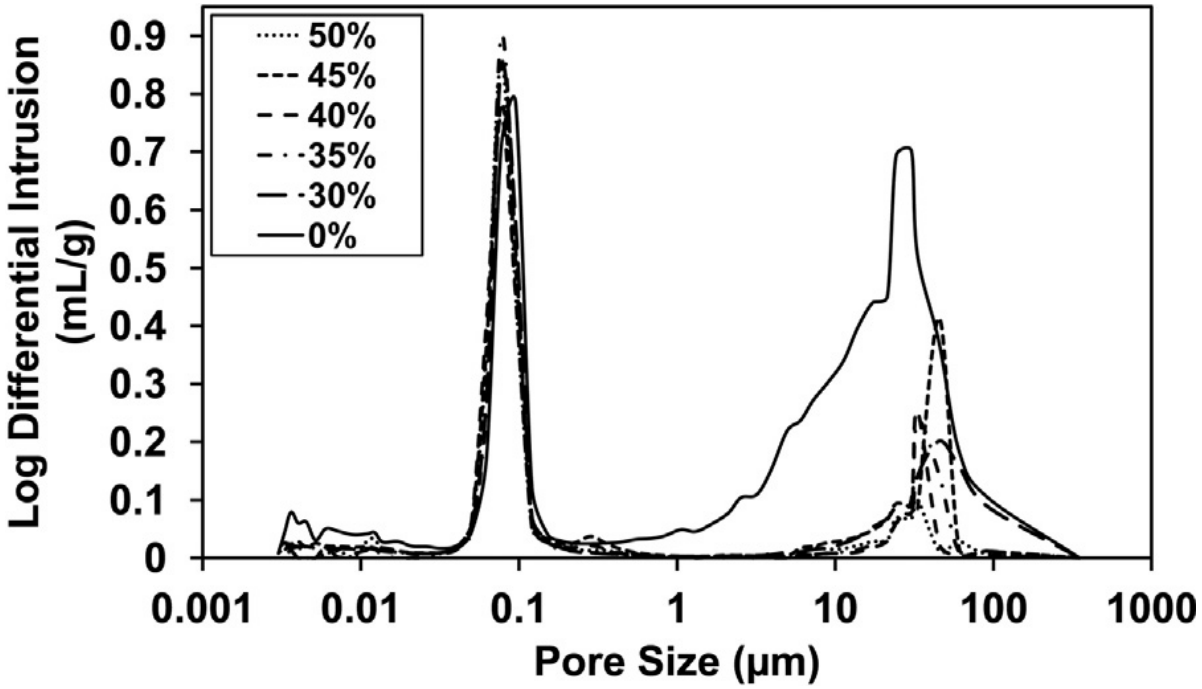

Figure 3-34: Pore Size Distribution of 1.0 cm Green Alumina Spheres [38]

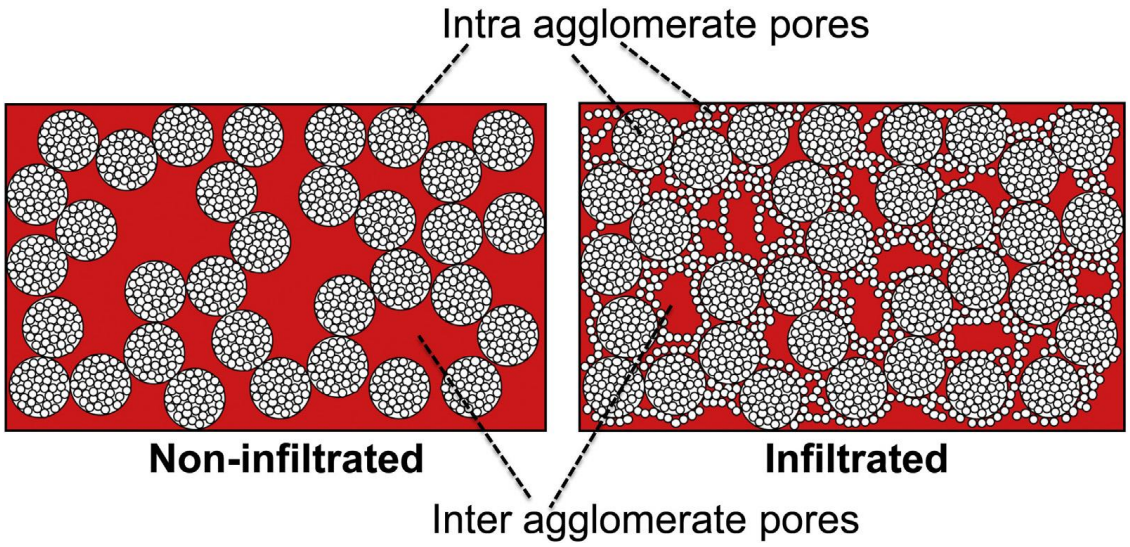

Figure 3-35: Inter and Intra Agglomerate Pores in Infiltrated and Non-Infiltrated Parts [38]

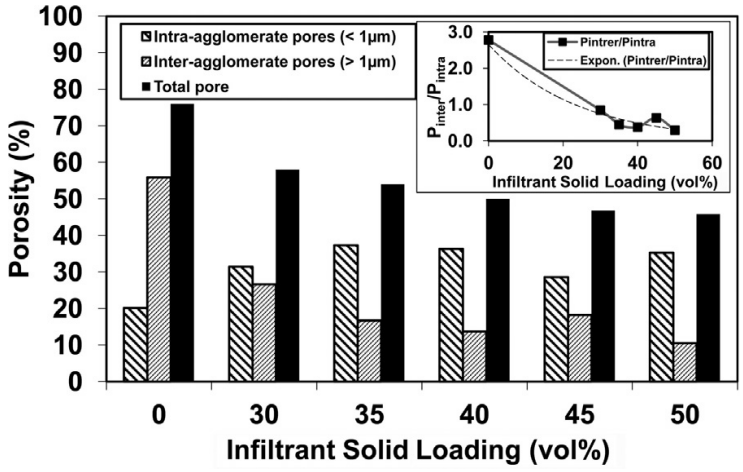

Figure 3-36: Inter and Intra Agglomerate Porosity in Infiltrated and Non-Infiltrated Parts [38]

Higher levels of infiltrant result in better surface finishes (refer to Figure 3-37).

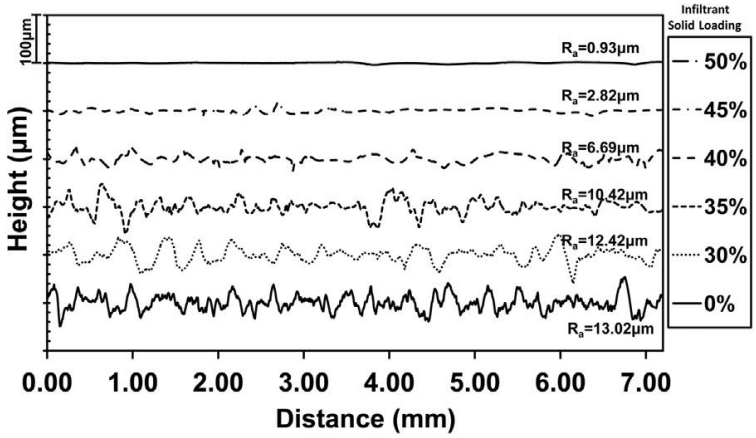

Figure 3-37: Surface Finish Results with Infiltrant Solid Levels [38]

The results from the 4 point fracture test may be seen in Figure 3-38.

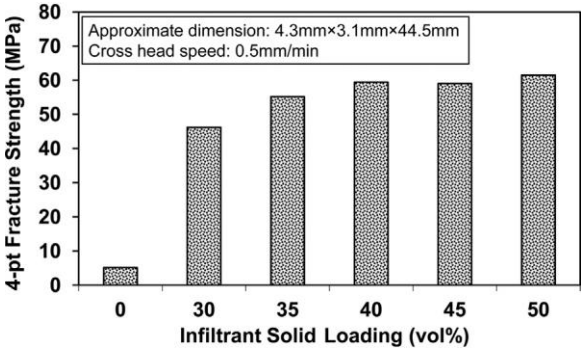

Figure 3-38: 4 Point Fracture Strength of 3D Printed Bars with Infiltrant Solid Loading [38]

3D Printing of Cement Composites

A RHPC powder with a PVA organic modifier at a ratio of 97:3 produced the strongest components. Refer to Figure 3-39 for some of the 3D printed parts.

Figure 3-39: 3D Printed Cement Parts – Large Bracket is 125 mm High [39]

The study produced complex features with internal cavities, offset holes, overhangs and undercuts, which are not easily created using simple moulds.

Curing for 1 day at 80°C water (which is similar to curing in water at room temperature for 50 days) produced only slightly greater strengths than curing for 26 days. Refer to Figure 3-40 for flexural testing results.

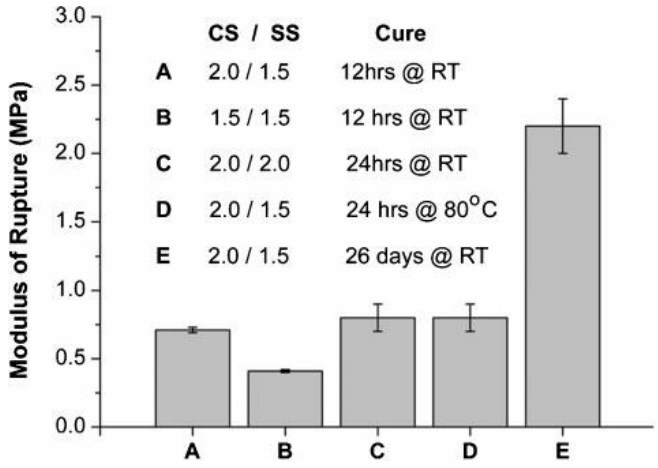

Figure 3-40: Flexural Strength vs Build Parameters and Curing Regime [39]

The flexural strength of the sample that was cured for 26 days was similar to traditionally compression moulded cement components, even though the 3D printed samples have much lower densities. 3D printed cement densities were 960 kg m^{-3} and 1300 kg m^{-3} before and after curing. Typical ceramic 3D prints are also roughly 1300 kg m^{-3}. However, densities usually reach 1800 kg m^{-3} in compression moulded composites [39].

Using Magnetite/Thermoplastic Composite in 3D Printing of Direct Replacements for Commercially Available Flow Sensors

The flow gauge was successfully 3D printed in approximately 4 hours (refer to Figure 3-41).

Figure 3-41: Completed Flow Sensor (note: black portion of impeller is magnetite composite) [40]

SEM image analysis showed that the magnetite filler was spread evenly throughout the polymer matrix and was not pushed to the edges during the printing process. A CT scan of the magnetite portion of the impeller revealed no spatial confinement, with good general dispersion of the magnetite particles.

The 3D printed sensor was tested using compressed air so as not to limit frictional heat degradation of the thermoplastic. Refer to Figure 3-42 for impeller frequency results. The

sensor appears to be stable and accurate. The 3D printed sensor was then tested alongside a commercial sensor with water as the fluid. The two displayed linear results with expected fluctuations due to typical fluid flow (refer to Figure 3-43). See Figure 3-44 for rotation speed of both sensors. After testing, the 3D printed sensor showed no signs of wear or plastic degradation.

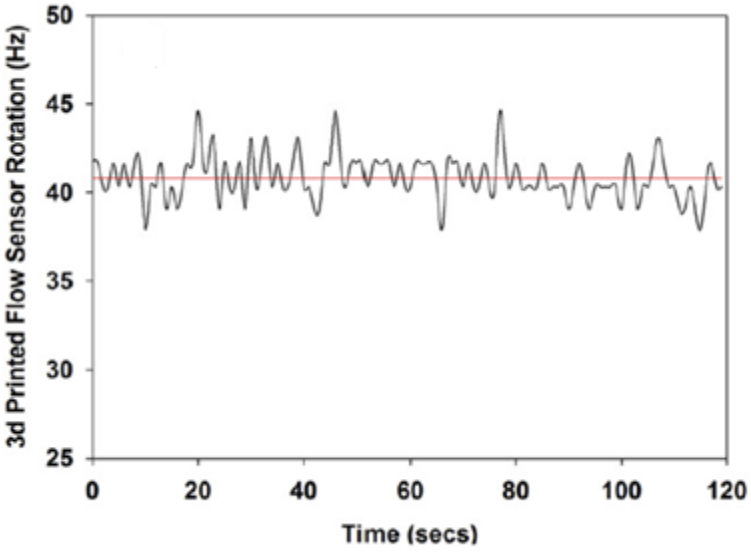

Figure 3-42: 3D Printed Flow Sensor Rotational Frequency [40]

Red Horizontal Line Indicates Mean Value

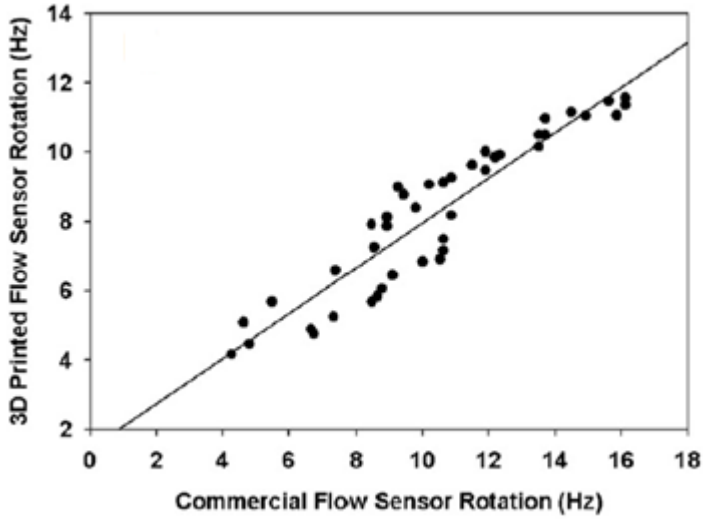

Figure 3-43: 3D Printed Flow Sensor Frequency and Commercial Slow Sensor Frequency [40]

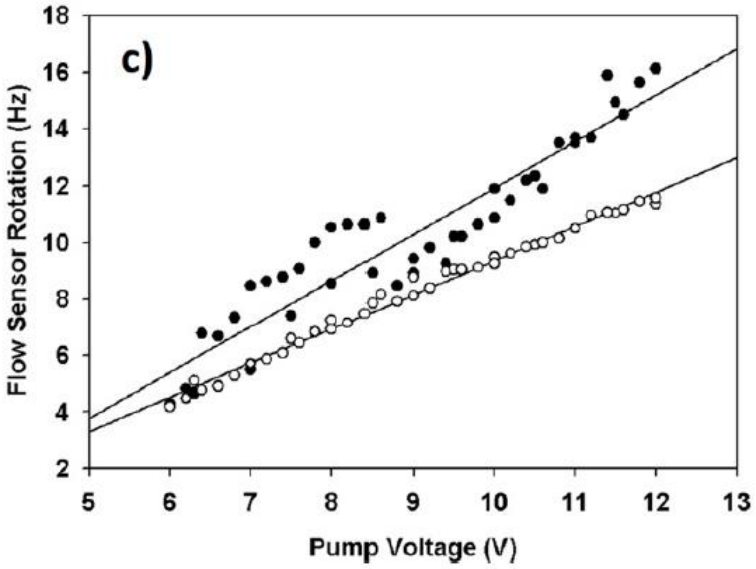

Figure 3-44: 3D Printed Flow Sensor Rotational Frequency (white dots) and Commercial Flow Sensor (black dots) vs Pump Rate [40]

3D-Printing of Lightweight Cellular Composites

Refer to Figure 3-45 and Figure 3-46 for rheological data from testing of epoxy based ink.

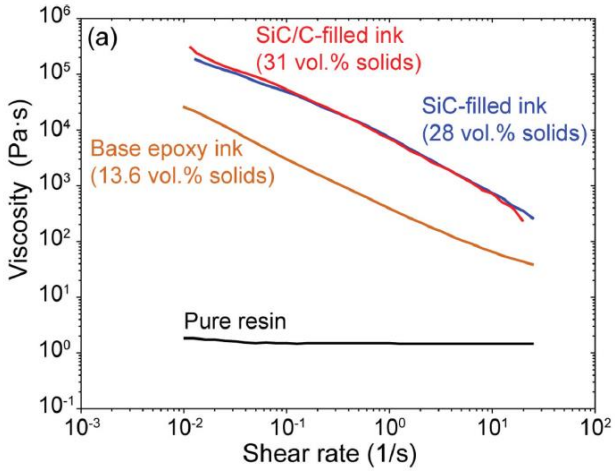

Figure 3-45: Log-Log Plot of Apparent Viscosity Related to Shear Rate for Various Epoxy-Based Inks [41]

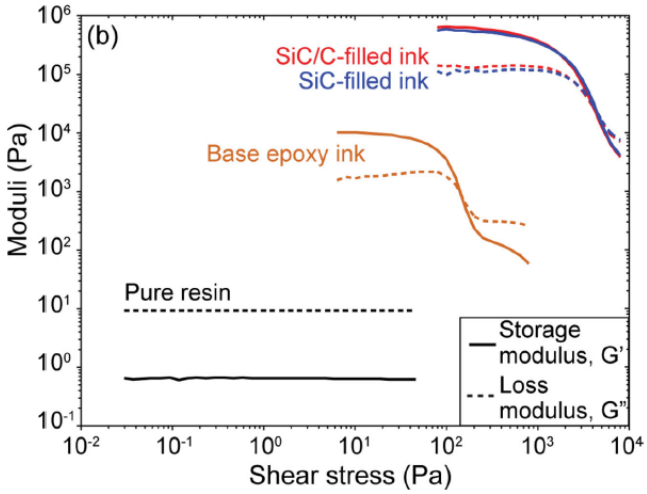

Figure 3-46: Log-Log Plot of Shear Storage and Loss Moduli Related for Shear Stress for Various Epoxy-Based Inks [41]

The nano-clay platelets turn the resin into a viscoelastic fluid. The SiC whiskers increase the viscosity of the ink, while the large carbon fibers increase the shear storage modulus. These inks have a high stiffness and yield stress and are ideal for the 3DP of cellular composites [41]. Refer to Figure 3-47 for tensile test results.

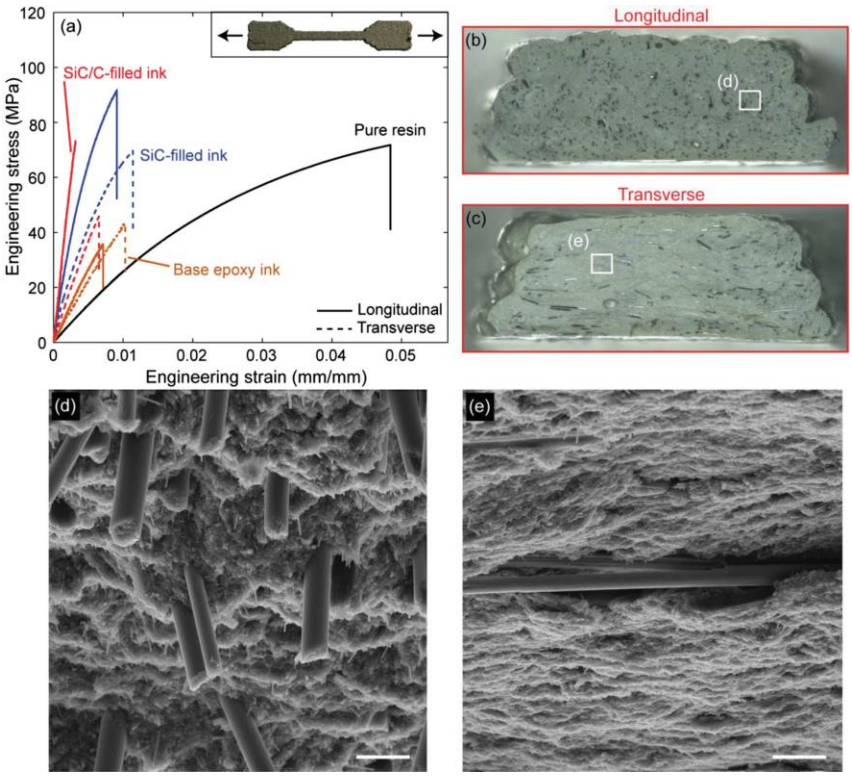

Figure 3-47: Tensile Test Results
a) Tensile Stress vs Strain Results
b) Tensile fracture surface of longitudinally printed sample (low magnification)
c) Tensile fracture surface of transversely printed sample (low magnification)
d) Tensile fracture surface of longitudinally printed sample (high magnification)
e) Tensile fracture surface of transversely printed sample (high magnification) [41]

Composites printed with silicon carbide and carbon fiber reinforcements had Young's modules 9 times higher than pure resin. In general, reinforced longitudinally printed samples yielded slightly better failure strengths than the transversely oriented ones. Samples printed with only the base epoxy ink behaved isotropically regardless of build direction [41].

The fracture surfaces from tensile testing appeared uniform and indicate an absence of deposition-related defects during the printing process. The anisotropic SiC and carbon fibers aligned with the print direction and can be manipulated to toughen the component by capitalizing on fiber pullout. See Figure 3-48 for 3D printed cellular composites.

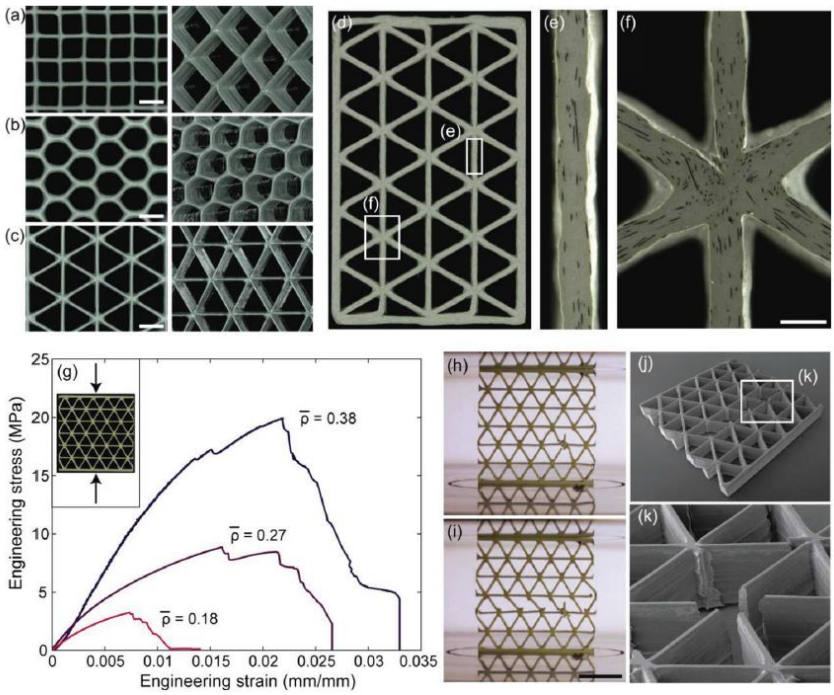

Figure 3-48: 3D Printed Cellular Composites
a) 3D printed SiC epoxy square honeycomb structure
b) 3D printed SiC epoxy hexagonal honeycomb structure
c) 3D printed SiC epoxy triangular honeycomb structure
(d-f) 3D printed SiC/C epoxy triangular images with carbon fibers oriented in print direction
g) Compressive stress strain curves for triangular honeycomb structures with various densities
h) Elastic wall buckling
i) Tensile fracture
(j-k) SEM images of failure locations [41]

See Figure 3-49 for Young's modulus and yield strength values. The dashed lines represent theoretical values for the SiC/C epoxy. Mechanical properties of 3D printed commercial polymers and polymer composites, balsa wood and wood cell walls are all compared.

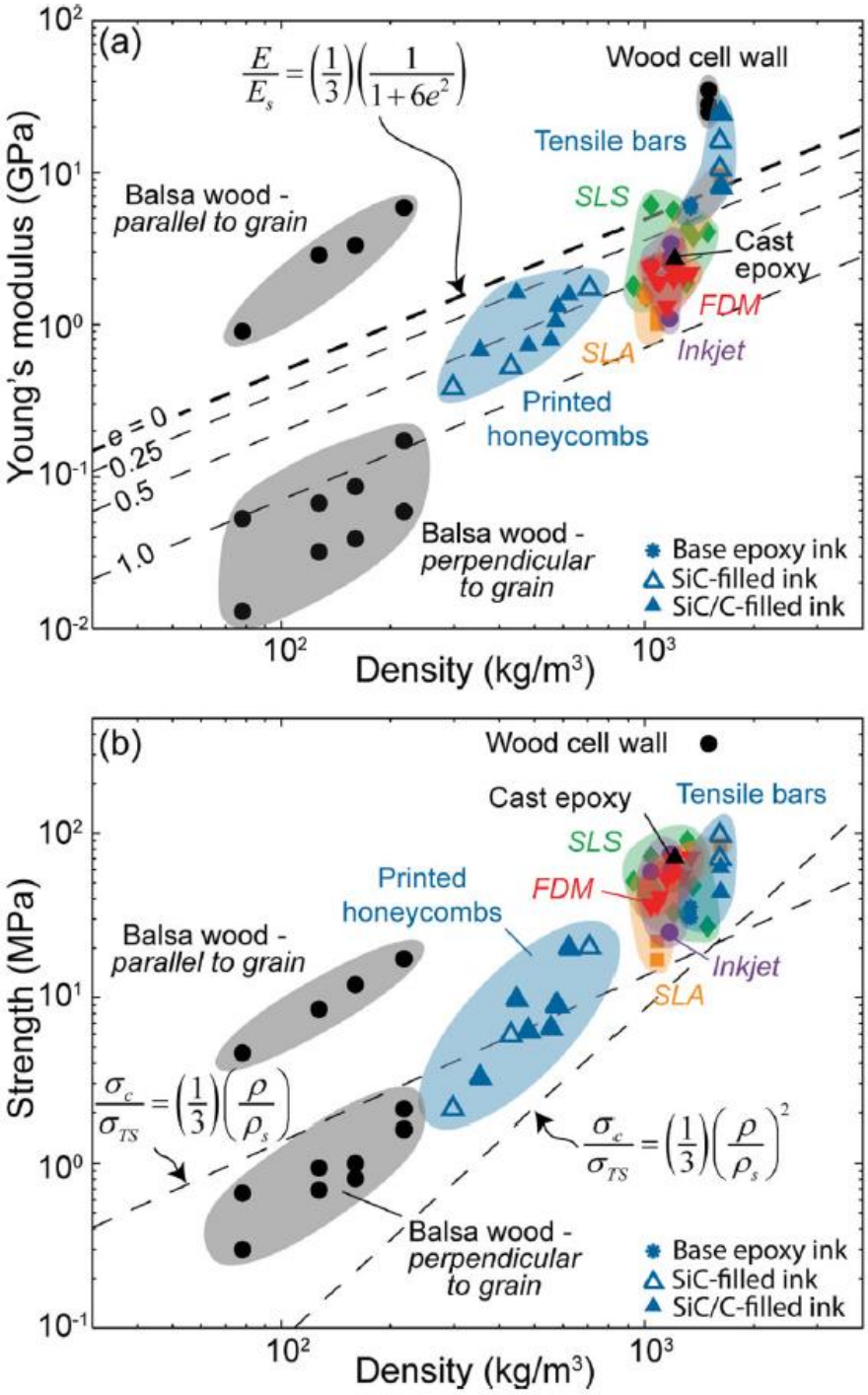

Figure 3-49: Young's Modulus and Yield Strength
a) Property space map of 3D printed epoxy Young's modulus correlated to density and compared to various materials
b) Property space map of 3D printed epoxy yield strength correlated to density and compared to various materials [41]

The SiC/C reinforced epoxy ink had a comparable longitudinal Young's modulus to wood cell walls. This value was 10 to 20 times greater than most available 3D printed polymers and 2 times greater than premier printed polymer composites. The cellular composites produced from the epoxy ink have 3 to 8 times stronger in-plane properties than a similar density balsa wood's transverse properties. The cellular composites have the added benefit of being isotropic [41].

3.4.5 Summary

Additive Manufacturing for Product Improvement at Red Bull Technology

The mechanical integrity of a 0.5 mm walled hydraulic part fabricated using DMLS has been proven in conditions simulating F1 applications. Components can be produced with a high degree of dimensional accuracy and achieve a required hardness. Post-processing surface finishing may be required. The use of DMLS is a strong choice given its ability to produce light weight components, as well as parts with up to 250% more efficient fluid flow compared to traditionally manufactured units. Its usefulness is increased by the small component batch size associated with elite motorsports [37].

Property Enhancement of 3D-Printed Alumina Ceramics using Vacuum Infiltration

The ceramic parts were successfully vacuum infiltrated. The infiltrate drastically increased density, lowered porosity and increased the strength of the parts. The density of a sintered component, infiltrated with 1 cm diameter spheres, increased by 49%. Infiltration reduced large inter-agglomerate porosity, which typically opposes densification of components. Higher solid content within the slurry yields greater overall density in the part. Larger infiltrant concentrations result in better surfaces of the finished 3D printed components. Elevated

infiltrant solid contents, up to 40% (where it plateaus), produced up to 15 times better strength in the 4 point bending test than without the infiltrate [38].

3D Printing of Cement Composite

This study successfully proves that components can be 3D printed with cement substrates. These parts have mechanical properties comparable to those produced with typical 3D printed ceramics before post-processing. This is surprising, given that cement samples have much lower density. These cements are inherently resistant to moisture and may be treated with pharmaceuticals for biomedical applications. Curing at 80°C is not a good method of expediting the curing process [39].

Using Magnetite/Thermoplastic Composite in 3D Printing of Direct Replacements for Commercially Available Flow Sensors

This study successfully proved that a commercially available flow sensor could be replicated using 3D printing with functional (magnetic) material. The 3D printed sensor held up during testing and was reliable and comparable to the commercial sensor. In addition, much less ferrous material was used than what would be found in a traditional sensor. This ability to print multiple materials and use just as much as needed illustrates 3D printing's usefulness as a viable means of manufacturing and demonstrates that it should not solely be considered as an RP technology [40].

3D-Printing of Lightweight Cellular Composites

3D printed cellular composites were successfully fabricated out of SiC/C laden epoxy. The material exhibited strong mechanical properties. The build direction of the 3D printing procedure was shown to affect the mechanical properties of the part, and this should be taken

into consideration in future 3D printing work. This parameter adds new possibilities to the rapidly expanding 3D printing technology. The cellular composites developed in this study behave similar and in some aspects better than the lauded balsa wood. 3D printed cellular composites are appealing for biomedical applications, due to the carefully controlled architecture and their mechanical properties [41].

4 3D Printing Implementation

The previous two sections discussed the effect of additive manufacturing on different industries as well as the technical components of 3D printing. This section will focus on the implementation of these technologies.

4.1 Printing Implementation Process

This section describes the procedure for 3D printing a CATIA part file. First, the part file needs to be converted to a format that is readable by the 3D printer. Then, the file has to be prepared for 3D printing and 3D printing parameters have to be defined.

First, the procedure to convert the CATIA part file is described,

1. Launch CATIA Software

2. Open the desired part file with .prt extension

3. Go to Start tab. See Appendix B-1: Catia Environment- Start

4. Select Machining option. See Appendix B-2: Catia Environment- Machining

5. Select STL rapid prototyping, this will open up a tool box. See Appendix B-2: Catia Environment- Machining

6. Select Tessellation from the right panel. See Appendix B-4: Catia Environment- Tessellation

7. Define the Sag Value; this is usually set to 0.2 mm. See Appendix B-5: Catia Environment- Tessellation Sag

8. Now the user is asked to select the desired section from the part tree on the top right panel. If the entire part is to be printed the parent part file needs to be selected from the tree. See Appendix B-6: Catia Environment- Selection Part for Tessellation

9. Click Apply button. See Appendix B-6: Catia Environment- Selection Part for Tessellation and Appendix B-7: Catia Environment- Applying Tessellation

10. From the top panel, select the Save option. See Appendix B-8: Catia Environment- Saving the File

11. Save the file with .stl extension. See Appendix B-9: Catia Environment- Saving File as .stl

At this point the CATIA .prt file has been converted to .stl which is readable by the 3D printer, see Appendix B-10: Catia Environment- .stl File. Now the 3D printer software has to be utilized to read the .stl file and define the printing parameters. For this exercise, Catalyst Ex has been selected as the 3D printing software. The procedure is described as follow,

1. Launch Catalyst Ex Software

2. Open the .stl file that was previously converted in the aforementioned steps

3. Select the Orientation tab

4. In this step, the user is given the option of orienting the part in the 3D plane; select the desired orientation.

4.2 Orientation

The orientation of the part is an important parameter which determines the path of the printer and consequently the speed of printing. Let's use an example to explain the importance of the orientation of part. Figure 50 shows a simple part in both vertical and horizontal orientations. Note that the 3D printer lays a bid of material layer by layer and therefore needs a structure to lay each layer on top of another. One can readily see that for the vertical option, the undercut section which is encircled in orange in Figure 51 has no support structure and therefore, the printer has to create extra support structure before laying the main layer for the part. This support structure is shown with red lines in Figure 52.

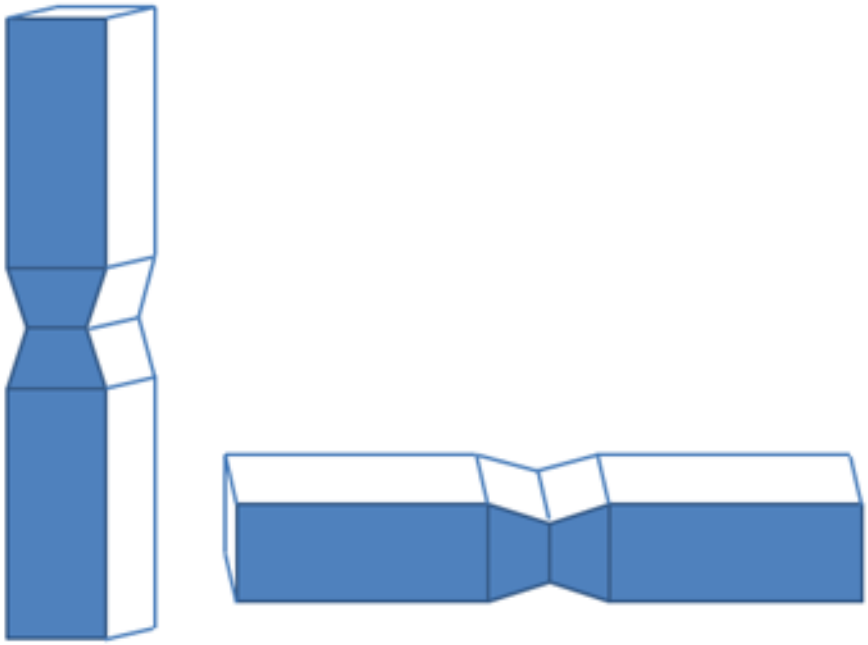

Figure 4-1: Test 3D Sample

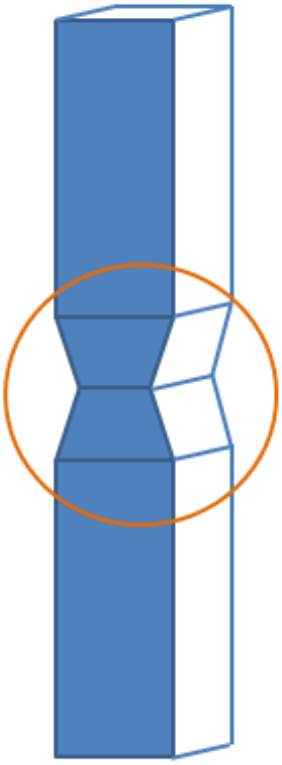

Figure 4-2: Vertical Sample with Undercut

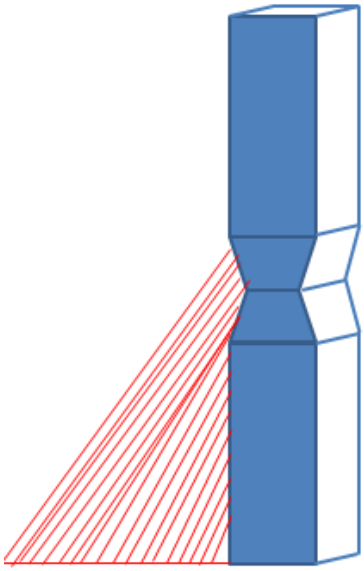

Figure 4-3: Vertical Sample with Support Structure for Undercut

This printer uses a different type of polymer for the support structure. Once the printing is completed, the part is soaked in a chemical bath which dissolves the support structure while the actual part remains intact. This does not mean that vertical orientation is always disadvantageous. There are examples, where the part needs to be oriented vertically due to complexity of its shape or in other cases where the part has to have better mechanical properties in a certain direction. Note that 3D printed parts are anisotropic due to their layered structure.

4.3 Effect of Part Orientation on Structural Integrity

The orientation of the part plays an important role in material usage, printing time and mechanical properties of the part. It was mentioned that due to the layered structure of the 3D printed components, they are anisotropic. This property is not always desirable when the component is to be subjected to mechanical testing since the results could be misleading. In order to demonstrate the effect of part orientation, the part shown in Figure 56 was utilized to perform an experiment. In this experiment the same part was printed in both horizontal and vertical orientation 5 times to create a total of ten samples. The samples were placed in a tensometer and were subjected to tensile testing. Table 14 and 15 shows the results of the tensile test on all ten samples. All samples were subjected to the same maximum load of 105 N with and extension rate of 50 mm/min. Given these conditions, it can be readily seen that the horizontally oriented samples have a maximum extension value of 5.2mm whereas the vertically oriented samples have a maximum extension of 15.2 mm. This difference comes from the orientation of the layers on in order words the plastic bids that create the layers.

Furthermore, it can be seen that there is a variation within the same group of samples, with a standard deviation of 0.61 and 0.64 for horizontal and vertical samples respectively. This variation is introduced by many different printed parameters such as slight variation in cooling rate of plastic due to room pressure and temperature changes. Overall, this study shows that in a fairly small and simple part, the orientation of printing can have a large effect on the part's performance. It is evident that this effect can be amplified when dealing with larger and more complex parts subjected to more rigorous mechanical tests such as fatigue.

4.4 3D Printing the Part

5. After orienting the part, user is given the option of selecting the printing resolution or layer thickness. Usually this parameter is set to 0.01'' inches.

6. Select density

7. Select process STL button

8. After processing STL, the layer and the nozzle path can be viewed. The red line is the periphery pf the part and the green is the center line of the bead.

9. When the printing starts, the printer first creates a base plate. In order to make the printer more efficient, the user can print multiple parts at the same time. For this option, select the Pack tab. This will allow for multiple parts to be placed on the same plate; step 1-8 has to be repeated if the part is different.

10. The created file has a .gz format. This will be the 3D printing file.

4.5 Design for 3D Printing

In terms of the dimensions, it is important to consider the thickness of the bead. The dimension perpendicular to the plane of printing is always a factor if the layer size. For instance, if he layer size if 0.01, the perpendicular dimension will be a factor of 0.01.

Furthermore, for determining the tolerances, the aforementioned layer thickness results in a total tolerance of 0.1 mm in the direction of printing. This means that for maximum material condition features such as the outside diameter of a circle, it will always be 0.1 mm larger than the actual dimension of the part file. Also, for minimum material condition features, the inside diameter of a circular feature such as a hole size, the dimension will always be 0.01 smaller. It is important to consider this fact when designing a part in order to accommodate for the tolerance of the 3D printing so the final part has the desired dimension.

Figure 53 is a 3D printed 3 in-lb torque wrench. Although this part has two moving components, Figure 54, it has been printed in one shot and there is no assembly of components. This is achieved by carefully considering the stack up tolerances between the moving parts. It was mentioned that the overall tolerance of the printed part, in the direction of printing is 0.1 mm; therefore, by considering this in the design and allowing the right clearance between the moving components, the entire part is printed as an assembly. Looking at Figure 55, it can be seen that the part was printed in the horizontal orientation, making sure the entire body is supported while building upwards and minimizing the amount of additional support structure. It is inevitable that the gear needs some additional support but it can be soaked in a chemical to dissolve or simply broken off once the wrench is rotated once.

Figure 4-4: 3D Printed Wrench

Figure 4-5: 3D Printed Wrench- Gear Assembly

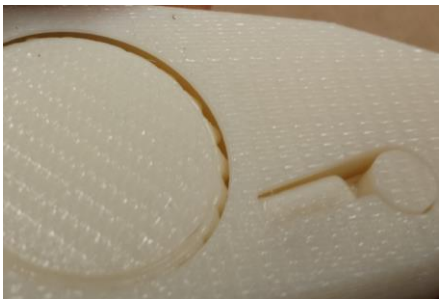

Figure 4-6: 3D Printed Wrench- Mechanism

Figure 56 to 58 are additional examples of 3D printed components with various complexities, illustrating the capability of 3D printing.

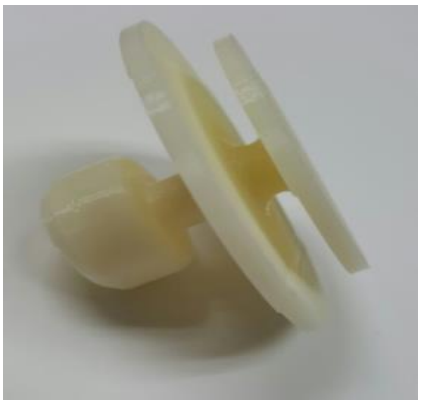

Figure 4-7: 3D Printed Knob

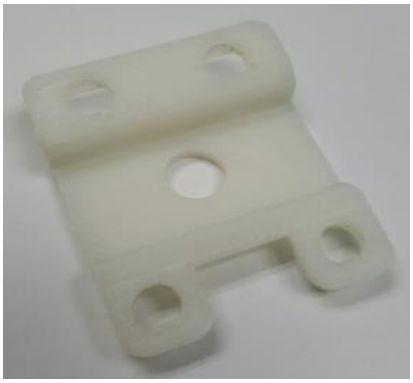

Figure 4-8: 3D Printed Bracket 1

Figure 4-9: 3D Printed Bracket

4.6 Tensile Testing 3D Printed Samples

4.6.1 Introduction

Injection molding is a conventional plastic processing technique widely used in the industry to manufacture plastic components. These components may be molded from a wide variety of plastics. While injection molding components on a moderate to large scale is both cost and time effective, there are instances in the prototyping and pre-production phases of programs where it is too slow when only a handful of components are needed. AM becomes particularly attractive when frequent design changes are made to components on nascent programs. It can also be effective at providing components very quickly for prototyping when traditional manufacturing methods have long lead times. In order to use 3D printed components as a substitute for their injection molded i.e. polypropylene counterparts they must have comparable properties. This study places particular emphasis on tensile strength given the loading pattern of certain plastic components.

The yield strength of components produced through additive manufacturing is controlled by several factors. Yield strength is a material property, but AM can produce components that are anisotropic. Obviously, the type of AM technology used is a major factor, as is material selection. Some materials are only compatible with certain AM methods. In addition, some AM techniques are dependent on the orientation of the component as it is being built. Correspondingly, sample geometry may also impact tensile properties.

The purpose of this report is to assess the impact of different additive manufacturing technologies, print orientation, sample geometry and material selection on tensile testing behavior. The goal is to establish a formula of parameters that will produce AM components that may be used instead of injection molded components when the need arises.

4.6.2 Sample Variables

Initially, the testing was supposed to be performed on test samples with hexagonal, triangular, rectangular and circular cross-sections. All samples were originally to be manufactured out of both polypropylene and ABS plastic, as these are most often used in injection molding. Also, print orientation will be taken into account where necessary. All combinations of these variables will be studied.

Further research reveals that there are no established tensile testing specifications for samples with hexagonal or triangular cross-sections; thus, these geometries are eliminated from the study. The material selection is then revised since there is no polypropylene material for FDM 3D printing. FDM printed samples will be produced from ABS plastic. Orientation is a factor for FDM and it will be considered when 3D printing tensile samples.

4.6.3 Method

Tensile testing is conducted using ASTM specification D638-14, which provides the procedure for tensile testing plastics. The ASTM standard, as well as the equivalent ISO 527 specification, is examined. However, the ASTM specification is chosen because it outlines testing for both traditional dog bone shaped samples with rectangular cross-sections and rod shaped samples with circular cross-sections. The ISO 527 specification for tensile testing plastics only covers dog bone shaped samples.

Rectangular dog bone samples are sized according to the ASTM D638-14 preferred sizing (Type I specimen dimensions). Refer to Figure 4-10 for the dog bone tensile testing sample dimensions.

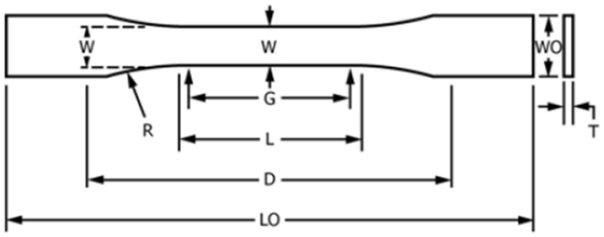

Dimensions	(mm)
W—Width of narrow section	13
L—Length of narrow section	57
WO—Width overall, min	19
LO—Length overall, min	165
G—Gage length	50
D—Distance between grips	115
R—Radius of fillet	76
T-Thickness	3.2

Figure 4-10: Dog Bone Specimen Dimensions

ASTM D638-14 only partially specifies dimensions for the circular rod shaped tensile samples. To maintain a degree of consistency between the circular and rectangular samples, the rod and dog bone samples have the same cross-sectional surface area at their narrowest points. ASTM D638-14 stipulates that the narrowest portion of the rod has a diameter that is 60% of the nominal diameter of the rod (the largest diameter at the ends). Using the cross-sectional area of the Type I dog bone samples, the smallest diameter in the middle of the rod may be calculated and therefore the largest nominal diameter of the rod may also be obtained. These values are then interpolated against a dimensional chart in ASTM D638-14 to obtain the final dimensions of the rod samples (Figure 4-11).

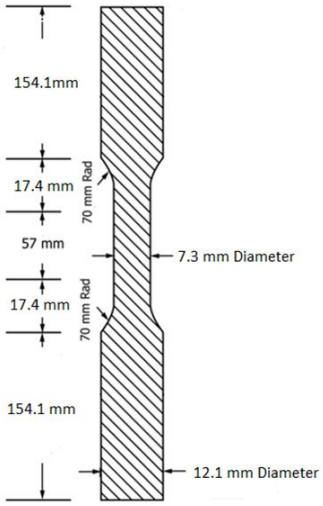

Figure 4-11: Rod Specimen Dimensions

As previously discussed, FDM sample orientation is important. Circular samples will be produced using two different print orientations. One orientation will yield vertical layers that are parallel to the tensile testing direction; while the other orientation will produce horizontal layers that are perpendicular to the testing direction (see Figure 4-12).

Figure 4-12: Rod Specimen Vertical Layers (Left) and Rod Specimen Horizontal Layers (Right)

Rectangular samples are printed using three different print orientations. The first orientation will have horizontal layers that are perpendicular to the tensile testing direction (Figure 4-13). There will then be two different orientations that will have vertical layers. These are referred to as print directions vertical-1 and vertical-2 (Figure 4-14 and Figure 4-15).

Figure 4-13: Dog Bone Specimen Horizontal Layers

Figure 4-14: Dog Bone Specimen Vertical-1 Layers

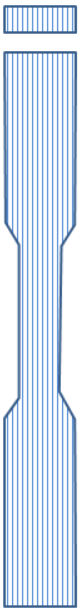

Figure 4-15: Dog Bone Specimen Vertical-2 Layers

The following configurations are set to be produced for tensile testing:

5 FDM rod samples using ABS with horizontal print orientation

5 FDM rod samples using ABS with vertical print orientation

5 FDM dog bone samples using ABS with horizontal print orientation

5 FDM dog bone samples using ABS with vertical-1 print orientation

5 FDM dog bone samples using ABS with vertical-2 print orientation

The samples are then to be tested using ASTM D638-14 procedures. As per the specification, all samples are strained at 50 mm/min. The tensile stress at yield, elongation at yield, tensile stress at break, elongation at break and Young's modulus are all measured.

4.6.4 Results

The dog bone samples were successfully printed using FDM as specified. Refer to Figure 5 and Figure 6 for FDM 3D printed rod samples. Refer to Figure 7 for FDM 3D printed dog bone samples. The surface finish on the samples was fair. The rod with the horizontal print orientation could not be completed as the FDM build is done with the rod standing upright for this orientation. The rod is too thin and vibrates during the printing as the last 50 mm are layered. This causes the print quality to become unacceptable. In order to combat this, the rod samples with the horizontal layers are shortened by 50.8 mm on either side. The total length of the rod samples in this orientation are therefore shortened by 101.6 mm. This alteration did not impact results because the extra material on the rod samples with vertical layers is simply the portion of the rod where the grippers would hold it during testing. Decreasing the length of rod in the grippers does not affect tensile behavior as long as there is enough material for the grippers to properly hold the specimen.

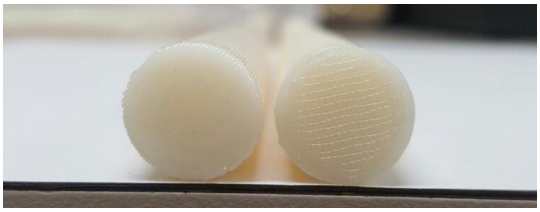

Figure 4-16: FDM Vertical Layers Rod (left) and FDM Horizontal Layers Rod (right)

Figure 4-17: FDM Vertical Layers Rod (bottom) and FDM Horizontal Layers Rod (top)

Figure 4-18: FDM Dog Bone Vertical -1 Layers (left), FDM Dog Bone Vertical-2 Layers (middle) and FDM Dog Bone Horizontal Layers (right)

The tensile testing was carried out as planned. Refer to Table 4-1 and Table 4-2 for tensile testing results of the ABS rod specimens FDM 3D printed with vertical and horizontal layers respectively.

Table 4-1: Tensile Testing Results of ABS Rods FDM 3D Printed with Vertical Layers

Vertical Rods					
Sample	Tensile Stress at Yield (MPa)	Elongation at Yield (%)	Tensile Stress at Break (MPa)	Elongation at Break (%)	Tensile Modulus (MPa)
1	31.9	2.35	30.2	6.44	2100
2	31.7	3.19	30.3	6.15	2050
3	32.6	2.28	29.6	7.42	2160
4	31.6	2.32	27.7	7.95	2080
5	32.7	2.35	30.4	6.33	2080

Table 4-2: Tensile Testing Results of ABS Rods FDM 3D Printed with Horizontal Layers

Horizontal Rods					
Sample	Tensile Stress at Yield (MPa)	Elongation at Yield (%)	Tensile Stress at Break (MPa)	Elongation at Break (%)	Tensile Modulus (MPa)
1	33.2	1.83	29.7	1.98	2380
2	31.2	1.68	28.7	1.79	2230
3	32.8	1.87	29.0	1.91	2280
4	32.7	1.83	30.3	1.93	2280
5	34.0	1.85	31.2	1.83	2370

Refer to Table 4-3, Table 4-4 and Table 4-5 for tensile testing results of the ABS rectangular dog bone specimens FDM 3D printed with vertical-1, vertical-2 and horizontal layers respectively.

Table 4-3: Tensile Testing Results of ABS Dog Bones FDM 3D Printed with Vertical-1 Layers

ASTM Bars: Vertical-1					
Sample	Tensile Stress at Yield (MPa)	Elongation at Yield (%)	Tensile Stress at Break (MPa)	Elongation at Break (%)	Tensile Modulus (MPa)
1	25.4	2.80	20.3	5.16	1770
2	25.4	3.09	24.3	7.58	1750
3	25.3	3.00	23.8	8.63	1750
4	26.4	2.90	24.7	7.50	1860
5	25.9	3.24	19.1	6.79	1800

Table 4-4: Tensile Testing Results of ABS Dog Bones FDM 3D Printed with Vertical-2 Layers

ASTM Bars: Vertical-2					
Sample	Tensile Stress at Yield (MPa)	Elongation at Yield (%)	Tensile Stress at Break (MPa)	Elongation at Break (%)	Tensile Modulus (MPa)
1	34.7	2.03	29.5	7.15	2160
2	34.5	2.03	24.3	5.64	2130
3	34.2	2.08	29.1	5.92	2140
4	33.5	2.04	27.0	9.91	2120
5	35.0	2.03	29.8	10.86	2200

Table 4-5: Tensile Testing Results of ABS Dog Bones FDM 3D Printed with Horizontal Layers

ASTM Bars: Horizontal					
Sample	Tensile Stress at Yield (MPa)	Elongation at Yield (%)	Tensile Stress at Break (MPa)	Elongation at Break (%)	Tensile Modulus (MPa)
1	26.6	1.64	*N/A	*N/A	2010
2	26.5	1.71	*N/A	*N/A	2110
3	26.5	1.63	10.82	3.21	2120
4	26.9	1.67	9.57	3.58	2170
5	26.0	1.55	4.11	2.09	2100

The testing data was used to create stress-strain curves for all rod and dog bone samples (refer to Figure 4-19 through Figure 4-23).

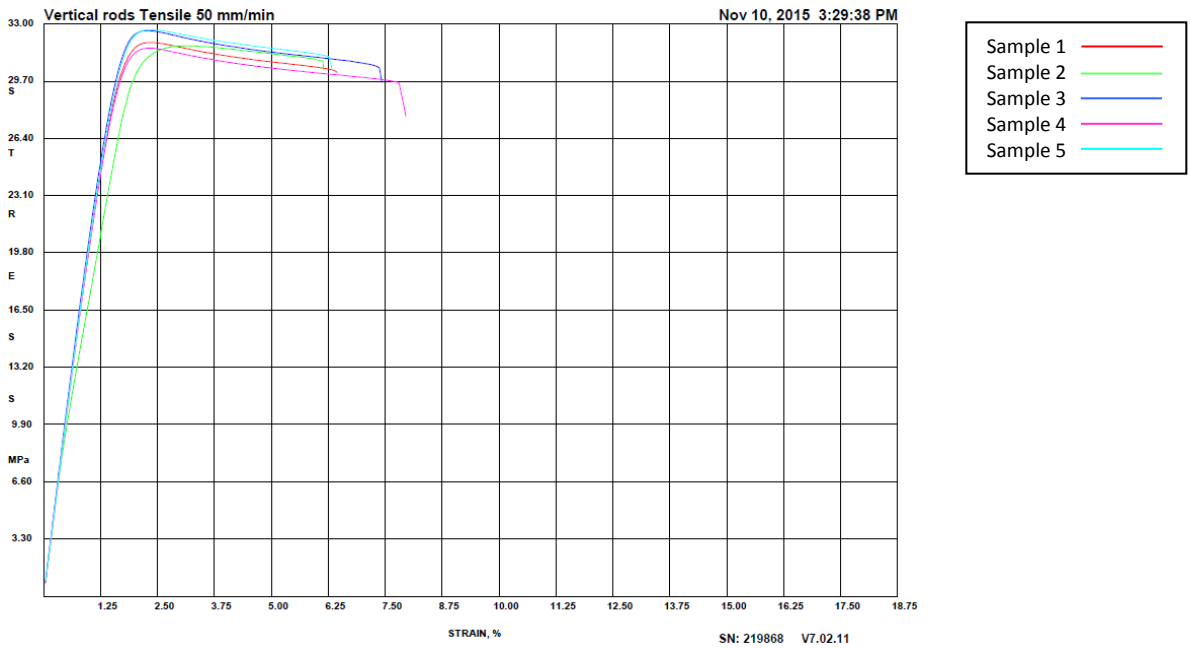

Figure 4-19: Stress-Strain ABS Rods FDM 3D Printed with Vertical Layers

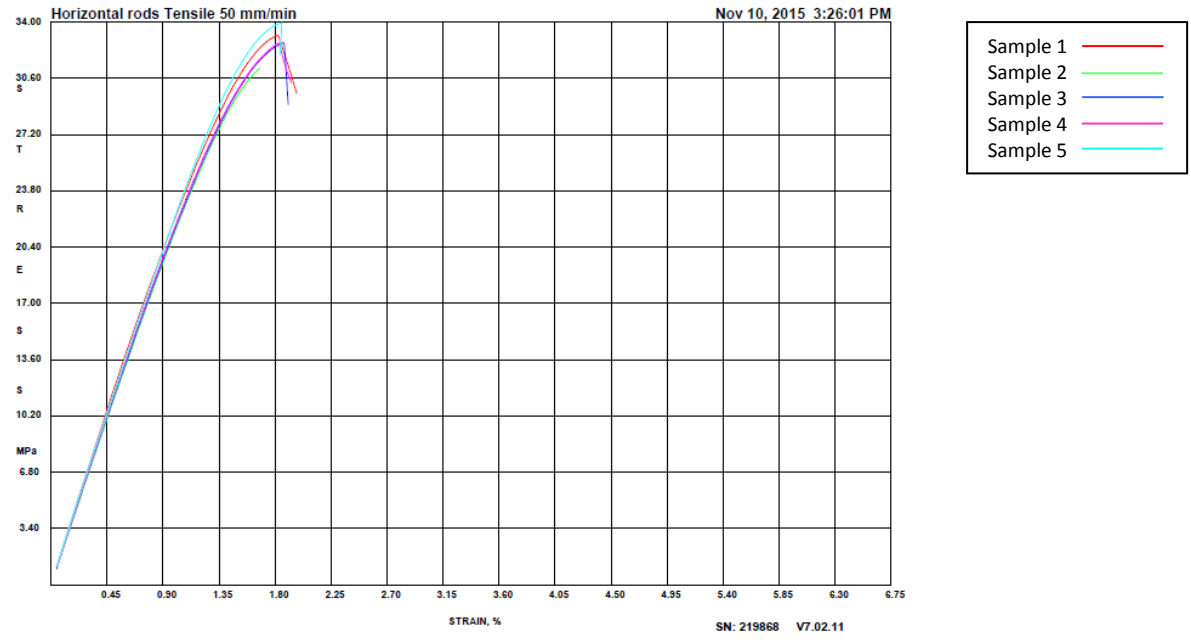

Figure 4-20: Stress-Strain ABS Rods FDM 3D Printed with Horizontal Layers

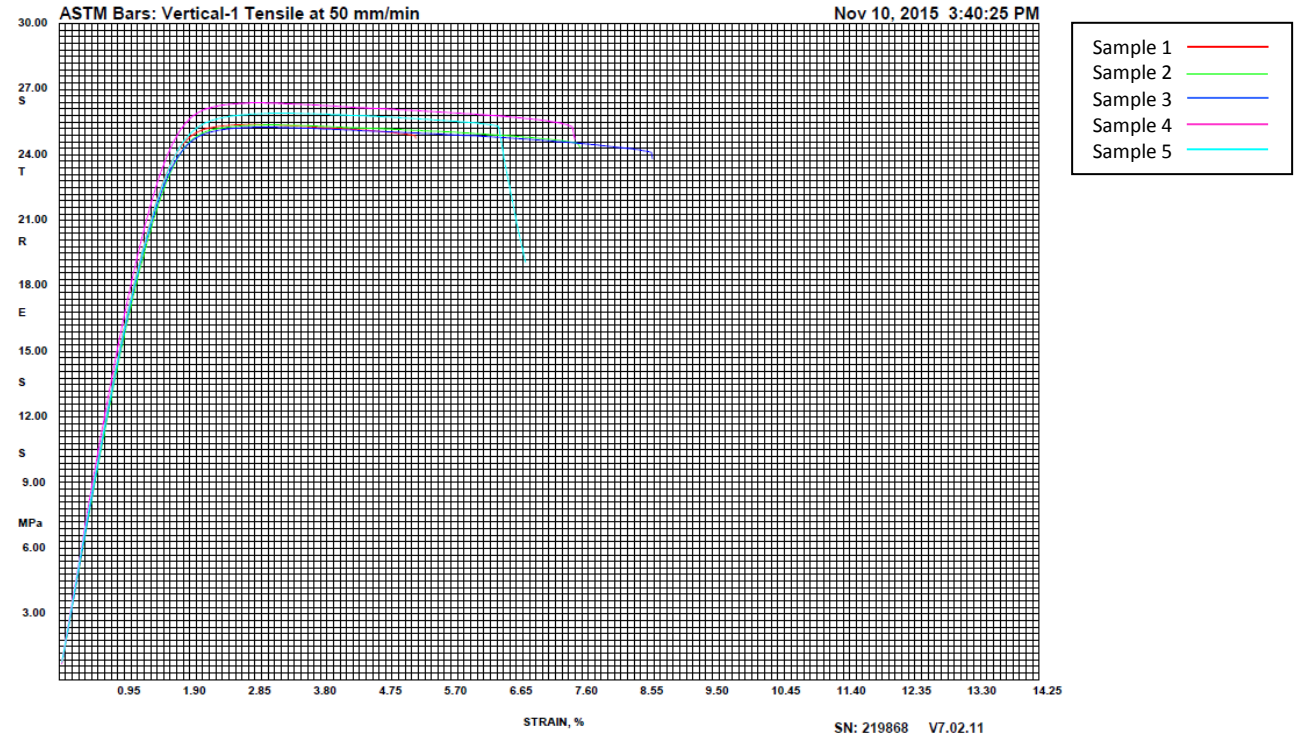

Figure 4-21: Stress-Strain ABS Dog Bones FDM 3D Printed with Vertical-1 Layers

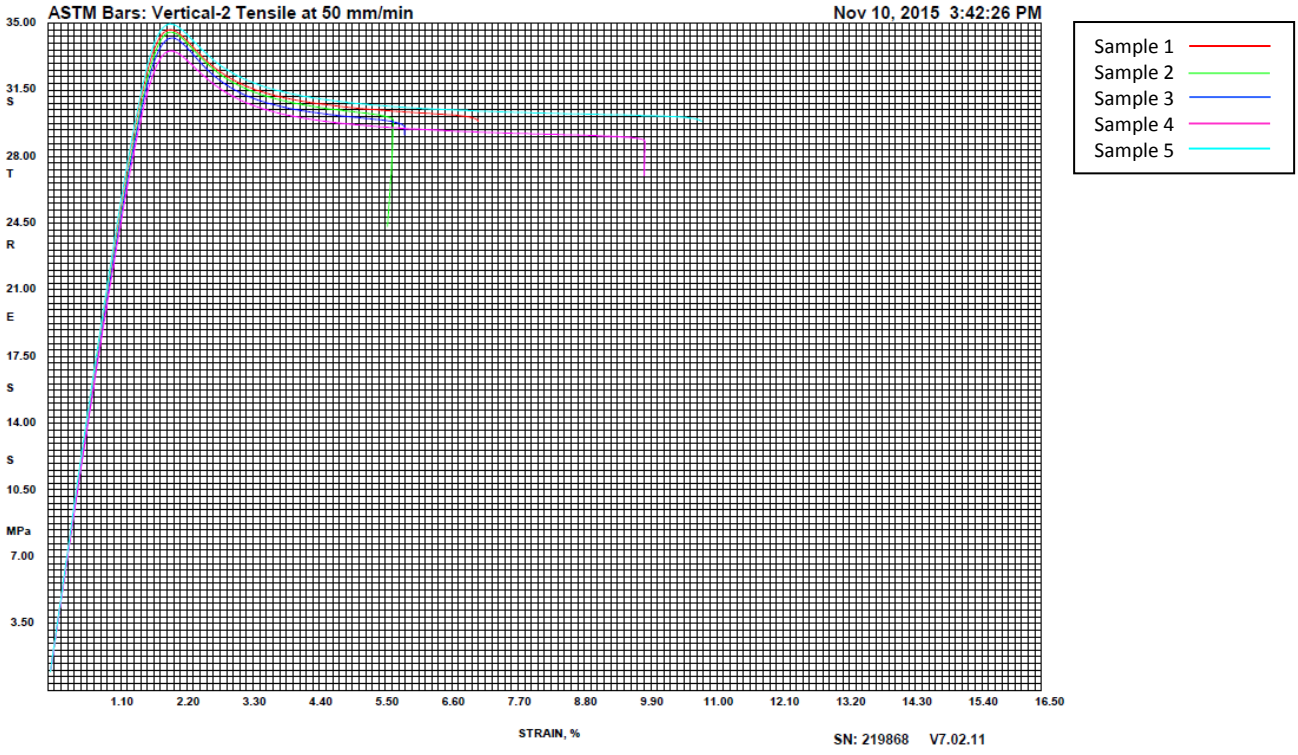

Figure 4-22: Stress-Strain ABS Dog Bones FDM 3D Printed with Vertical-2 Layers

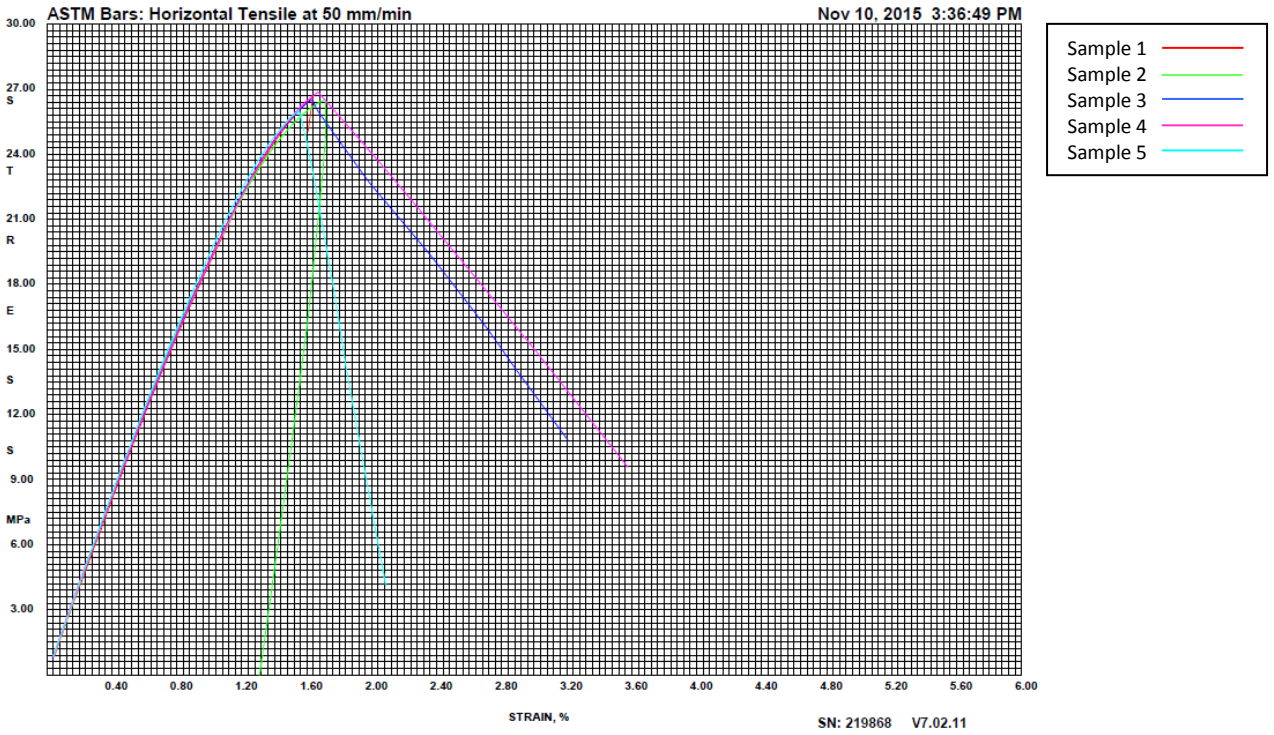

Figure 4-23: Stress-Strain ABS Dog Bones FDM 3D Printed with Horizontal Layers

See Figure 4-24 through Figure 4-28 for images of the samples immediately after fracture.

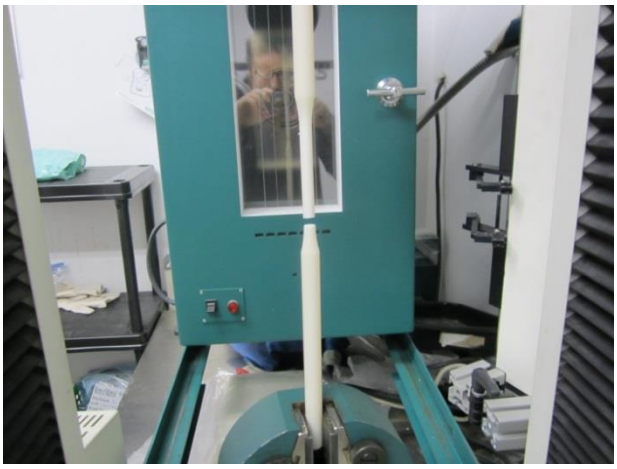

Figure 4-24: FDM Rod with Vertical Layers – Fracture after Testing

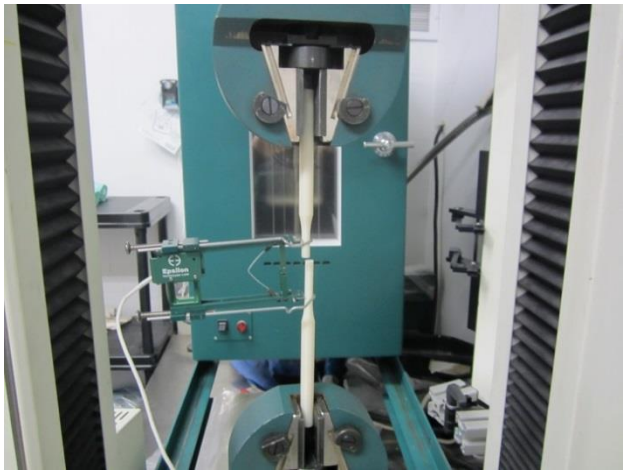

Figure 4-25: FDM Rod with Horizontal Layers – Fracture after Testing

Figure 4-26: FDM Dog Bone with Vertical-1 Layers – Fracture after Testing

Figure 4-27: FDM Dog Bone with Vertical-2 Layers – Fracture after Testing

Figure 4-28: FDM Dog Bone with Horizontal Layers – Fracture after Testing

4.6.5 Discussion

The average tensile strength of the rods with horizontal layers was 32.78 MPa; 0.68 MPa higher than the average tensile strength of the rods with vertical layers. The vertically layered rods also exhibited much higher elongation both at yield and at fracture. For the vertical rods, the mean elongation at yield and break were 2.5% and 6.86% respectively. Conversely, the horizontally layered rods had an average elongation at yield and break of only 1.81% and 1.9%. The vertical rod displayed much higher levels of plastic deformation between yield and fracture; increasing the specimen elongation on average by approximately 4.36%, compared to only 0.08% for horizontally layered rods. For the circular cross-sectional geometry, when the FDM layers are perpendicular to the tensile stress, the material is stronger but also more brittle. The Young's modulus of the horizontal rods was slightly higher than that of the vertical rods. The mean tensile modulus of the horizontal rod was 2.3 GPa compared to 2.1 GPa for the vertical

rod. Given the results of the testing, the bonds between FDM layers are stronger than the inter-layer bonds within the strands.

Unlike the circular samples, horizontal layers were not the strongest printing orientation for the dog bone specimens. For the rectangular dog bone samples, the vertical-2 print direction was stronger than both the vertical-1 print direction and horizontal layers. The vertical-1 was the weakest with a mean yield strength of 25.68 MPa, but was only slightly weaker than the average 26.5 MPa provided by the horizontal layers. These values are both substantially lower than the average yield strength of vertical-2 layers of 34.38 MPa. The Young's modulus of the bars with horizontal and with vertical-2 layers were comparable (refer to Tables 4 and 5). Both the Young's modulus of the horizontal bars and the vertical-2 bars were higher than that of the vertical-1 bars. The horizontal bars had the lowest elongation profile for the rectangular samples, while the vertical-2 and vertical-1 specimens both possessed larger amounts of elongation. The vertical-2 bars elongated slightly less than the vertical-1 bars at yield, but displayed slightly more plastic deformation at failure (see Tables 3 and 4).

It is difficult to directly compare the circular rod and rectangular dog bone samples because the print orientation has proven itself to be very important in determining tensile properties. The overall strongest samples tested were rectangular dog bone specimens printed with vertical-2 layers (see Table 4). However, this configuration also exhibited the most elongation at failure. After the dog bone with vertical-2 layers, the order of strongest to weakest was: rods with horizontal layers, rods with vertical layers, dog bones with horizontal layers and dog bones with vertical-1 layers.

The trend with both the dog bones and rod samples indicates that vertical layers oriented parallel to the tensile stress elongate more than specimens with layers perpendicular to the testing direction.

4.6.6 Applications

The application for this tensile testing is using the results to select a combination of parameters to simulate the injection molded ABS components that are subjected to tensile load. Given that yield strength of the ABS resin is approximately 53 MPa and the rod samples have yield strengths of approximately 32 MPa, the FDM ABS is obviously not an appropriate substitute given the same cross section; however, the cross section of the printed part can now be optimized so the yield strength is now the same as an injection molded part. Consequently, the new part will be representative of the actual injection molded component and can be used in prototyping and validation testing.

4.6.7 Summary

No polypropylene currently exists for FDM printing, and no standards exist for tensile stress testing samples with cross-sectional geometries that are not either circular or rectangular.

It is difficult to produce long and thin samples in the vertical orientation with FDM technology. The component has a tendency vibrate and distort the print quality.

The combination of variables used in FDM printing tensile samples greatly impacts the yield strength. The sample geometry and print orientation both affected the Young's modulus, yield strength, strain at yield and strain at failure.

The strongest sample with the highest yield strength was the dog bone geometry with vertical-2 layers. The rods with horizontal layers had the highest average Young's modulus at 2.3 GPa.

Tensile samples with vertical layers elongated much more at yield and at fracture than samples with horizontal layers. The elongation at fracture for vertically layered samples was substantially higher than horizontal, indicating much a much higher degree of plastic deformation.

4.6.8 Future Works

Further work will involve tensile testing samples using SLS instead of FDM. In SLS AM, print orientation is not a factor. In addition, there is neither polypropylene nor ABS blends for SLS printing. Tensile testing trials with SLS will focus on different powder blends and geometry. Further studies will benchmark SLS technology and will aim to characterize the material property of SLS powder mixtures.

5 Conclusion

Additive manufacturing is a rapidly expanding technology, with many applications across a breadth of different industries. Part one of this literature review looked at 3D printing implementation and future opportunities in manufacturing, civil engineering and biomedical sectors. Prominent themes include 3D printing's suitability for rapid prototyping of low volume components, altering supply chains, and increasing design flexibility. The literature review also examined legal issues surrounding patents and open source designs.

The second part of this literature review summarized varied and ongoing research into 3D printing. The majority of the compiled studies examined AM with non-conventional materials. Other studies used advanced 3DP techniques to print medical stents with unique properties. Several articles touched on 3D printing control parameters, such as grain size and distribution. These reports focused on improving 3D print quality to achieve stronger parts with better surface finishes. A better understanding of printing parameters is crucial to propel AM forward and increase its range of applications.

The third section described 3D printing implementation and guidelines. In this section printing steps were explained in detail and in order to further enhance the study an experiment was conducted to show the effects of part orientation on mechanical properties of the 3D printed parts.

This paper provided a sampling of current trends, ideas and research in additive manufacturing. This is a dynamic and exciting field, and it should be monitored closely for important and useful developments.

6 References

[1] J. Coykendall, M. Cotteleer, J. Holdowsky and M. Mahto, "3D Opportunity in Aerospace and Defense," 2014. [Online]. Available: http://www2.deloitte.com/content/dam/Deloitte/nl/Documents/manufacturing/deloitte-nl-mer-3d-opportunity-aerospace-defense.pdf. [Accessed September 2014].

[2] C. A. Giffi, B. Gangula and P. Illinda, "3D Opportunity in the Automotive Industry," 2014. [Online]. Available: http://www2.deloitte.com/content/dam/Deloitte/nl/Documents/manufacturing/deloitte-nl-manufacturing-3d-opportunity-in-tooling-additive-manufacturing-shapes-the-future.pdf. [Accessed September 2014].

[3] "3D printing: A potential game changer for aerospace and defense," *Gaining Altitude,* no. 7, pp. 1-5, 2013.

[4] "3D Printing and the Future of Manufacturing," 2012. [Online]. Available: http://assets1.csc.com/innovation/downloads/LEF_20123DPrinting.pdf. [Accessed October 2014].

[5] T. Ghawana and S. Zlatanova, "3D printing for urban planning: A physical enhancement of spatial perspective," in *UDMS Anuual 2013*, London , CRCpress, 2013, pp. 211-224.

[6] Y. Tadjdeh, "3D Printing Promises to Revolutionize Defense, Aerospace Industries," March 2014. [Online]. Available: http://www.nationaldefensemagazine.org/archive/2014/March/Pages/3DPrintingPromisestoRevolutionizeDefense,AerospaceIndustries.aspx. [Accessed October 2014].

[7] UK Intellectual Property Office Patent Informatics Team, "3D Printing: patent overview," November 2013. [Online]. Available: https://www.gov.uk/government/uploads/system/uploads/attachment_data/file/312699/informatics-3d-printing.pdf. [Accessed November 2014].

[8] J. Cali, D. A. Calian, C. Amati, R. Kleinberger, A. Steed, J. Kautz and T. Weyrich, "3D-Printing of Non-Assembly, Articulated Models," *ACM Transactions on Graphics (TOG) ,* vol. 31, no. 6, pp. 50-58, 2012.

[9] N. Herbert, D. Simpson, W. Spence and W. Ion, "A preliminary investigation into the development of 3-D printing of prosthetic sockets," *Journal of Rehabilitation Research and Development,* vol. 42, no. 2, pp. 141-146, 2005.

[10] E. Anderson, "Additive Manufacturing in China: Aviation and Aerospace Applications (Part 2)," *Journal of International Commerce and Economics,* vol. 6, no. 1, pp. 40-75, 2014.

[11] J. Hiemenz, "Additive Manufacturing Trends in Aerospace," 2014. [Online]. Available: http://web.stratasys.com/rs/objet/images/SSYS-WP-AeroTrends-03-13-FINAL.pdf. [Accessed November 2014].

[12] M. Gou, X. Qu, W. Zhu, M. Xiang, J. Yang, K. Zhang, Y. Wei and S. Chen, "Bio-inspired detoxification using 3D-printed hydrogel nanocomposites," *Nature Communications ,* pp. 1-9, 8 May 2014.

[13] T. Galeta, M. Kljajin and M. Karakšić, "Cost Evaluation of Shell and Compact Models in 3D Printing," 2008. [Online]. Available: https://bib.irb.hr/datoteka/331032.3-str-27-29.pdf. [Accessed December 2014].

[14] B. Grynol, "Disruptive Manufacturing - The Effects of 3D Printing," 2013. [Online]. Available: https://www2.deloitte.com/content/dam/Deloitte/ca/Documents/insights-and-issues/ca-en-insights-issues-disruptive-manufacturing.pdf. [Accessed December 2014].

[15] D. Dohetry, "Downloading Infringement: Patent Law as a Roadblock to the 3D Printing Revolution," *Harvard Journal of Law and Technology,* vol. 26, no. 1, pp. 354-373, 2012.

[16] S. H. Irsen, B. Leukers, B. Bruckschen, C. Tille, H. Seitz, F. Beckmann and B. Müller, "Image-based analysis of the internal microstructure of bone," in *SPIE*, 2006.

[17] L. MacEachern, A. Baytekin, A. Erfani and N. Levasseur, "3D Printed Prosthetic Hand with Intelligent EMG Control," 10 April 2013. [Online]. Available: http://www.doe.carleton.ca/Courses/4th_year_projects/Am4_Inglis_Timothy_2013.pdf-.pdf. [Accessed November 2014].

[18] S. E. Hudson, "Printing Teddy Bears: A Technique for 3D Printing of Soft Interactive Objects," in *Proceedings of the SIGCHI Conference on Human Factors in Computing Systems*, New York , 2014.

[19] H. Lipson and M. Kurman, "The printer of youth," in *Fabricated: The New World of 3D Printing*, Wiley, 2013, pp. 105-111.

[20] M. H. N., M. S. N. and M. S. Nagabhushan, "The Scope of Rapid Prototyping in Civil Engineering," *International Journal of Engineering Trends and Technology (IJETT),* vol. 4, no. 8, pp. 3506-3508, 2013.

[21] U. o. Sheffield, "Titanium powder used to 3D print," Phys Org., 10 December 2013. [Online]. Available: http://phys.org/news/2013-12-titanium-powder-3d-automotive.html. [Accessed 21 November 2014].

[22] Q. Ge, H. J. Qi and M. L. Dunn, "Active materials by four-dimension printing," *Applied Physics Letters ,* vol. 103, no. 23, 2013.

[23] C. C. Seepersad, "Challenges and Opportunities in Design for Additive Manufacturing," *3D Printing and Additive Manufacturing,* vol. 1, no. 1, pp. 10-13, 2014.

[24] D. R. F. Mohamed and D. A. S. Mahmoud, "Emphasizing the advantage of 3d printing technology in packaging design," *International Design Journal - Helwan University,* vol. 1, no. 1, pp. 111-119.

[25] M. Alimardani, "Multi-Physics Analysis of Laser Solid Freeform Fabrication," 2009. [Online]. Available: https://uwspace.uwaterloo.ca/bitstream/handle/10012/4297/Alimardani_Masoud.pdf?sequence=1. [Accessed November 2014].

[26] E. C. D. L. M. M. Nancy Bota, "An in-depth analysis of 3DP'S Potential Impact on Health Care," 2011. [Online]. Available: http://www.mirrrroring.net/DUMP/BIET_Final.docx. [Accessed December 2014].

[27] S. S. Sujata K. Bhatia, "3D-Printed Prosthetics Roll of the Presses," 2014. [Online]. Available: http://www.aiche.org/sites/default/files/cep/051428.pdf. [Accessed October 2014].

[28] H. H. David Moinina, "A Variable-Impedance Prosthetic Socket for a Transtibial Amputee Designed from Magnetic Resonance Imaging Data," *Journal of Prosthetics and Orthotics,* vol. 25, no. 3, pp. 129-137, 2013.

[29] Z. Zhou, F. Buchanan, C. Mitchell and N. Dunne, "Printability of Calcium Phosphate: Calcium Sulfate Powders for the Application of Tissue Engineered Bond Scaffolds using the 3D Printing Technique," *Materials Science and Engineering C,* no. 38, pp. 1-10, 2014.

[30] D. E. Cooper, M. Stanford, K. A. Kibble and G. J. Gibbons, "Additive Manufacturing for Product Improvementat Red Bull Technology," *Materials and Design,* no. 21, pp. 226-230, 2012.

[31] S. Maleksaeedi, H. Eng, F. Wiria, T. Ha and Z. He, "Property Enhancement of 3D-Printed Alumina Ceramics using Vacuum Infiltration," *Journal of Materials Processing Technology,* no. 214, pp. 1301-1306, 2014.

[32] L. Wang and J. Liu, "Liquid Phase 3D Printing for Quickly Manufacturing Conductive Metal Objects with Low Melting Point Alloy Ink," *Science China Technological Studies,* vol. 57, no. 9, pp. 1721-1728, 2014.

[33] G. Gibbons, R. Williams, P. Purnell and E. Farahi, "3D Printing of Cement Composites," *Advances in Applied Ceramics,* vol. 109, pp. 287-290, 2010.

[34] E. Kroll and D. Artzi, "Enhancing Aerospace Engineering Students' Learning with 3D Printing Wind-Tunnel Models," *Rapid Prototyping Journal ,* vol. 13, no. 4, pp. 196-203, 2007.

[35] S. Spath and H. Seitz, "Influence of Grain Size and Grain-Size Distribution on Workability of Granules with 3D Printing," *International Journal of Advanced Manufacturing Technology,* no. 70, pp. 135-144, 2013.

[36] S. Leigh, C. Purssell, D. Billson and D. Hutchins, "Using Magnetite/Thermoplastic Composite in 3D Printing of Direct Replacements for Commercially Available Flow Sensors," *Smart Materials and Structures ,* vol. 23, no. 9, 2014.

[37] J. T. Muth, D. M. Vogt, R. L. Truby, Y. Mengus, D. B. Kolesky, R. J. Wood and J. A. Lewis, "Embedded 3D Printing of Strain Sensors within Highly Stretchable Elastomers," *Advanced Materials,* no. 26, pp. 6307-6312, 2014.

[38] M. Vaezi and C. K. Chua, "Effects of Layer Thickness and Binder Saturation Level Parameters on 3D Printing Process," *International Journal of Advanced Manufacturing Technology,* no. 53, pp. 275-284, 2011.

[39] R. Shivpuri, X. Cheng, K. Agarwal and S. Babu, "Evaluation of 3D Printing for Dies in Low Volume Forging of 7075 Aluminum Helicopter Parts," *Rapid Prototyping Journal,* vol. 11, no. 5, pp. 272-277, 2005.

[40] B. G. Compton and J. A. Lewis, "3D-Printing of Lightweight Cellular Composites," *Advanced Materials ,* no. 26, pp. 5930-5935, 2014.

[41] S. A. Park, S. J. Lee, K. S. Lim, I. H. Bae, J. H. Lee, W. D. Kim, M. H. Jeong and J.-K. Park, "In Vivo Evaluation and Characterization of a Bio-Absorbable Drug-Coated Stent Fabricated using a 3D-Printing System," *Materials Letters,* no. 141, pp. 355-358, 2014.

Appendix A: Figures and Tables for Section 2

Path I: Companies do not seek radical alterations in either supply chains or products, but may explore AM technologies to improve value delivery for current products within existing supply chains.

Path II: Companies take advantage of scale economics offered by AM as a potential enabler of supply chain transformation for the products they offer.

Path III: Companies take advantage of the scope economics offered by AM technologies to achieve new levels of performance or innovation in the products they offer.

Path IV: Companies alter both supply chains and products in the pursuit of new business models.

Appendix A-1: Implementation Paths of AM [15]

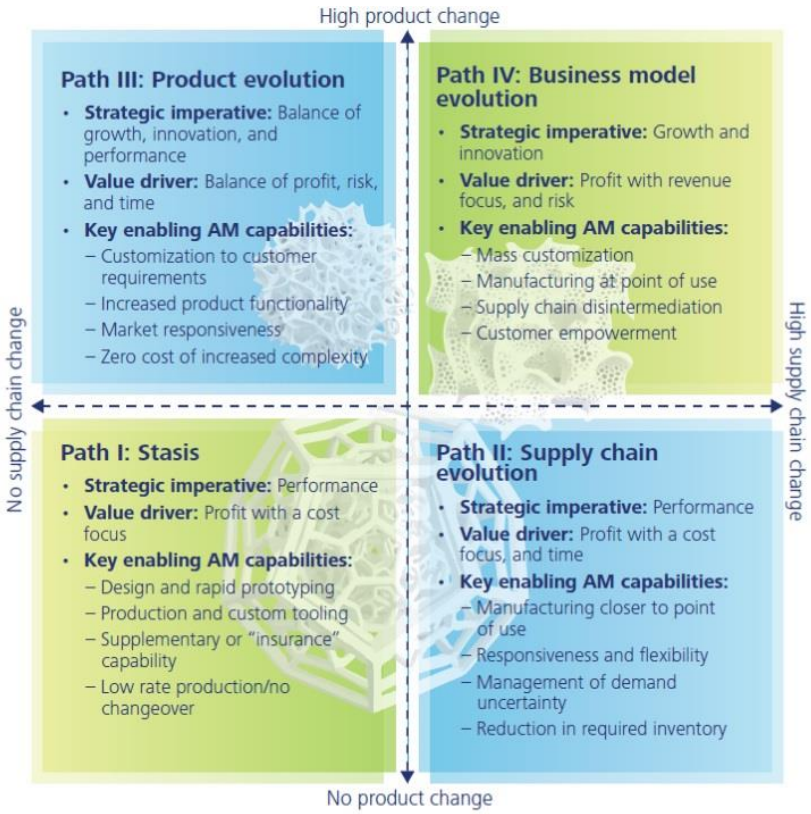

Source: Mark Cotteleer and Jim Joyce, "3D opportunity: Additive manufacturing paths to performance, innovation, and growth," *Deloitte Review* 14, January 2014.

Graphic: Deloitte University Press | DUPress.com

Appendix A-2: Framework for Better Understanding AM Paths and Values [15]

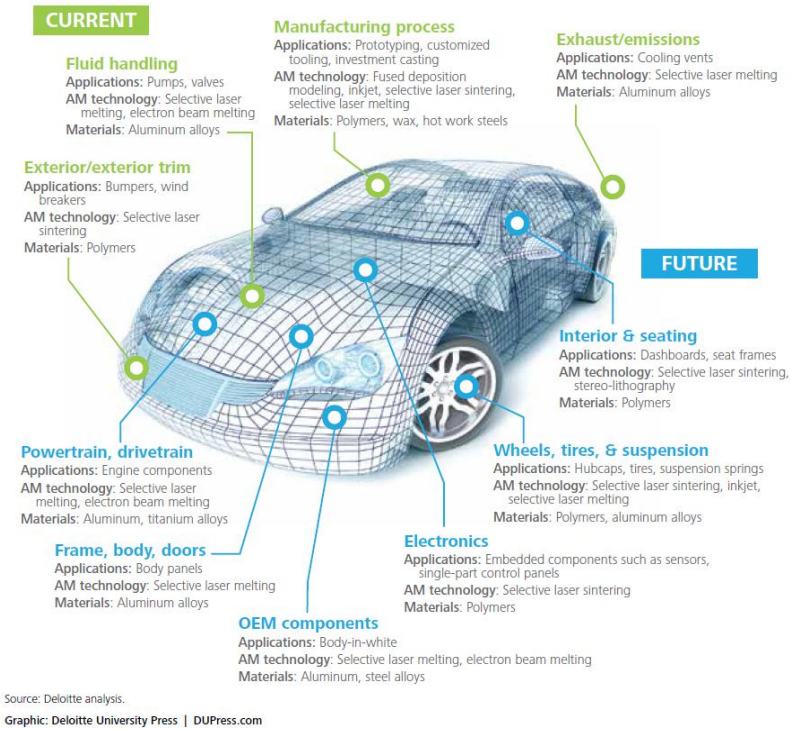

Appendix A-3: Potential Application of AM [15]

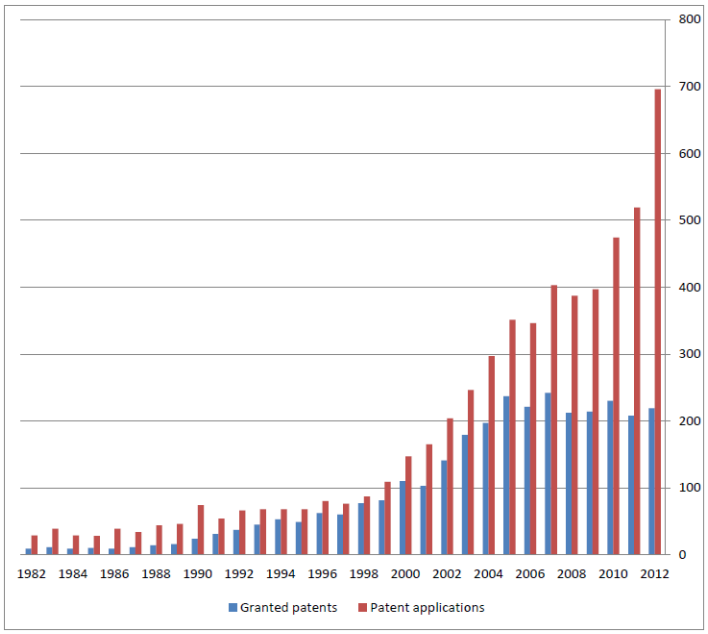

Appendix A-81: Comparison of Granted Patents and Published Patent Applications by Publication Year [27]

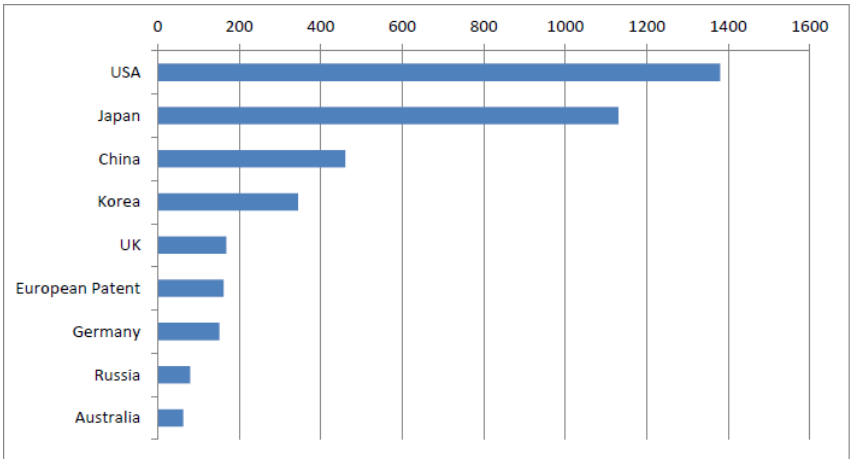

Appendix A-82: Priority Country Distribution for Top Countries [27]

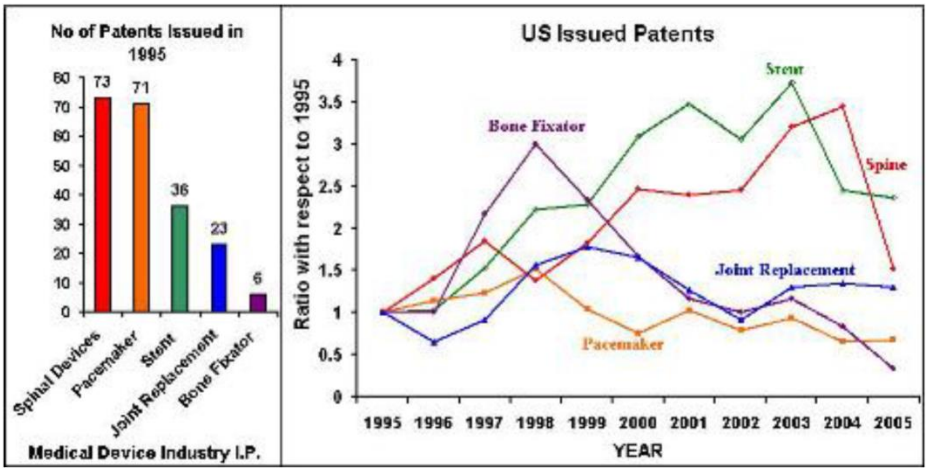

Appendix A-6: Patents in the Medical Device Industry [12]

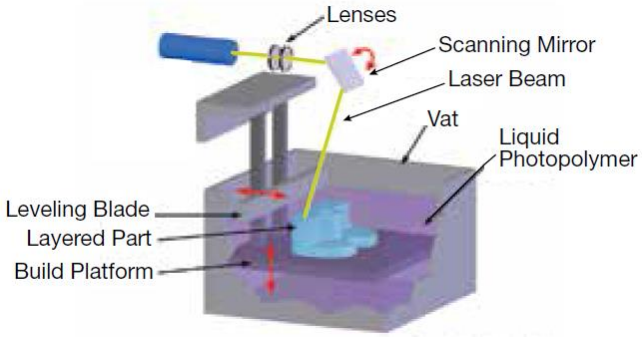

Appendix A-7: Stereolithography AM Method [13]

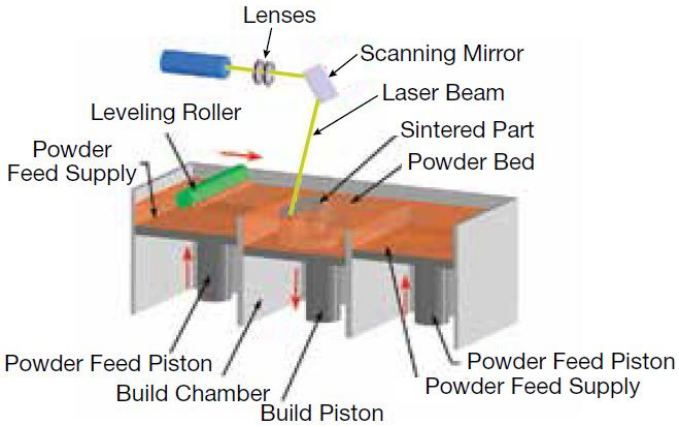

Appendix A-8: Selective Laser Sintering AM Method [13]

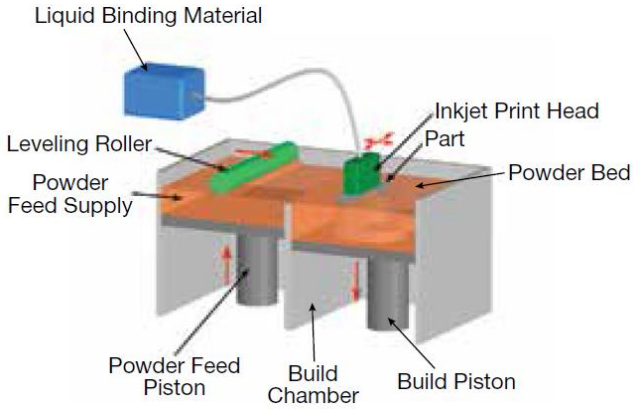

Appendix A-9: Inkjet (3DP) Printing AM Method [13]

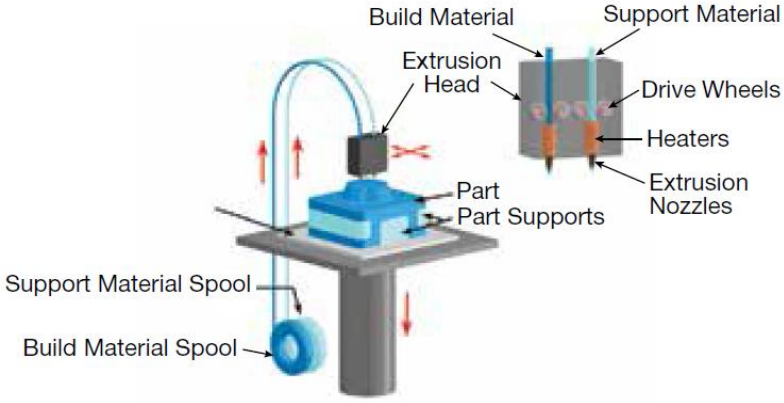

Appendix A-10: Fused Deposition Modeling AM Method [13]

Appendix B: How to 3D print a Catia File

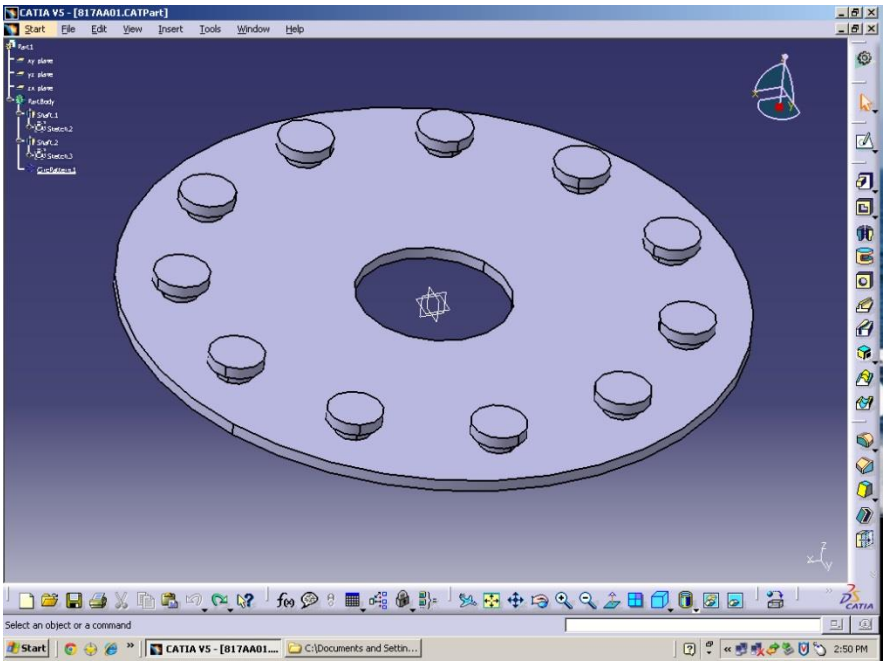

Appendix B-1: Catia Environment- Start

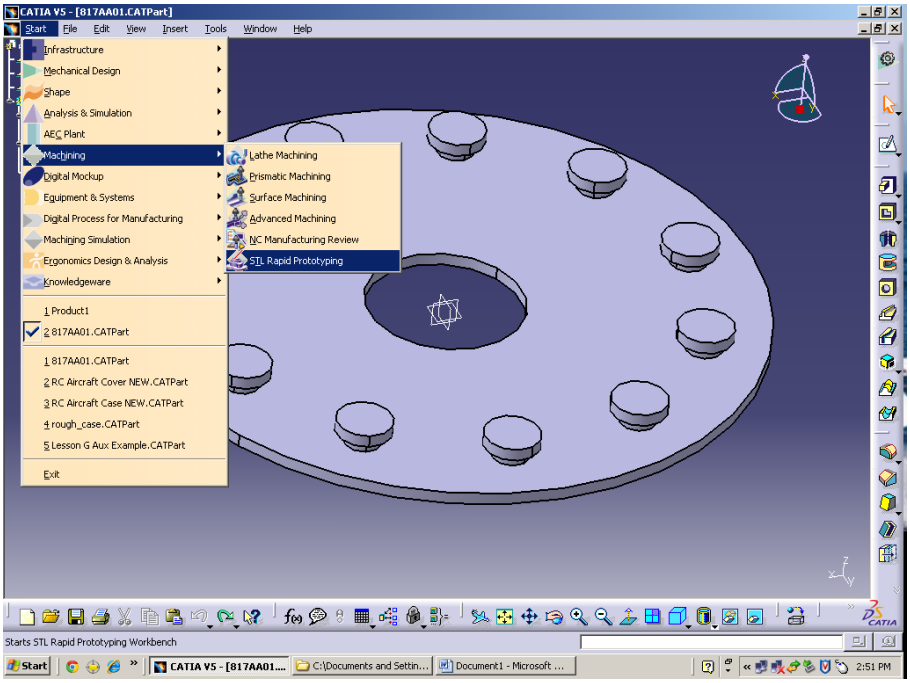

Appendix B-2: Catia Environment- Machining

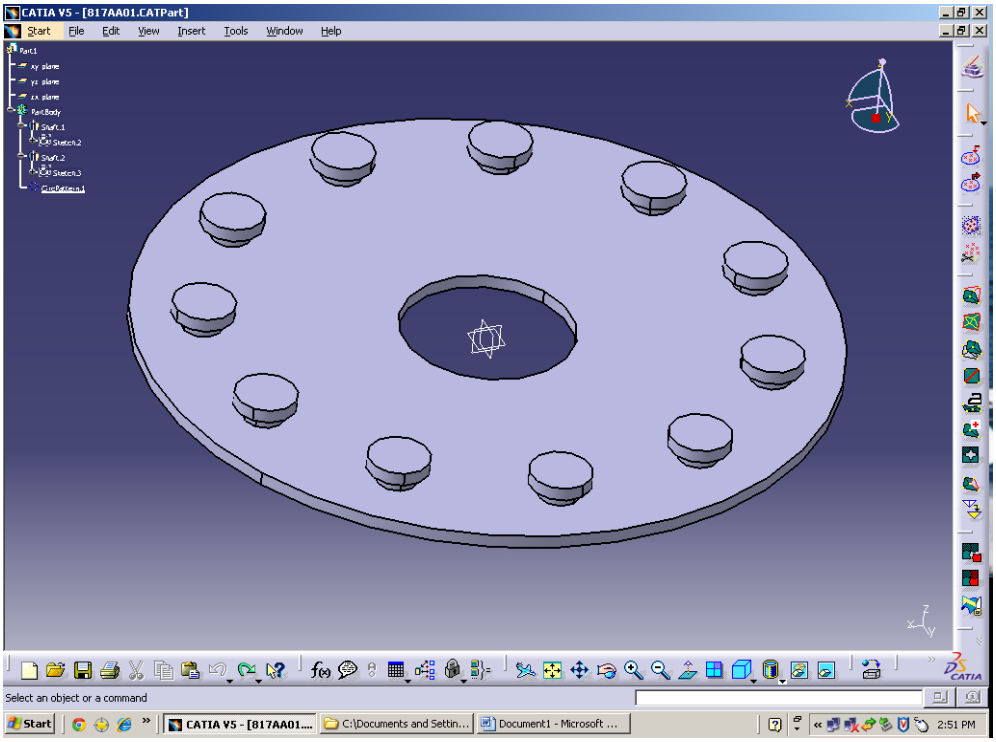

Appendix B-3: Catia Environment- Part

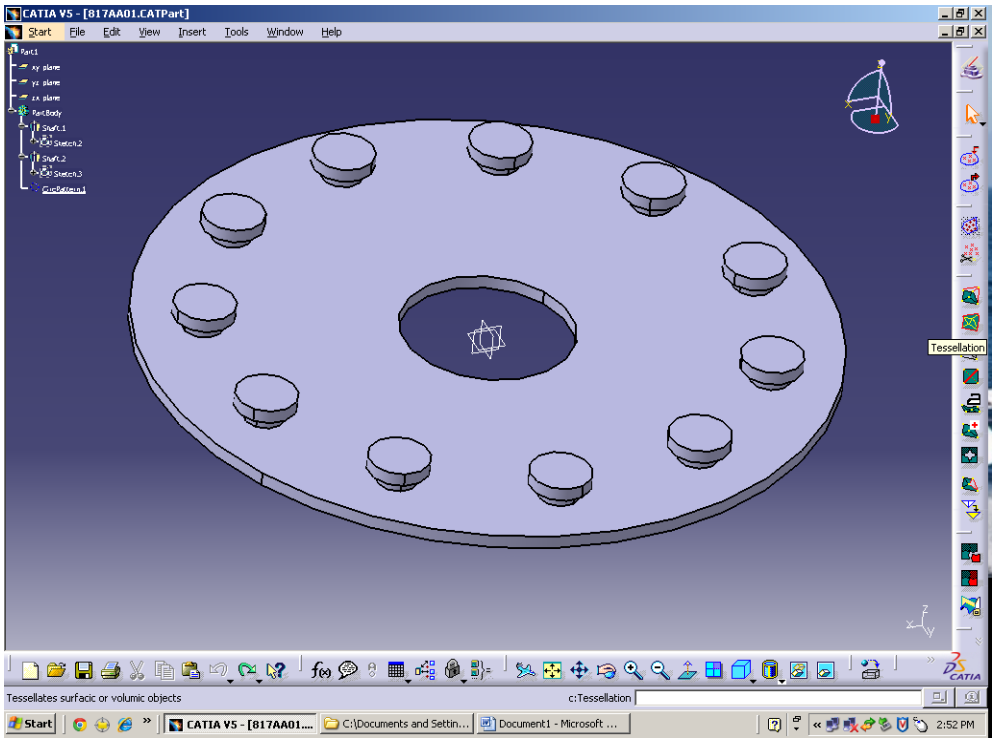

Appendix B-4: Catia Environment- Tessellation

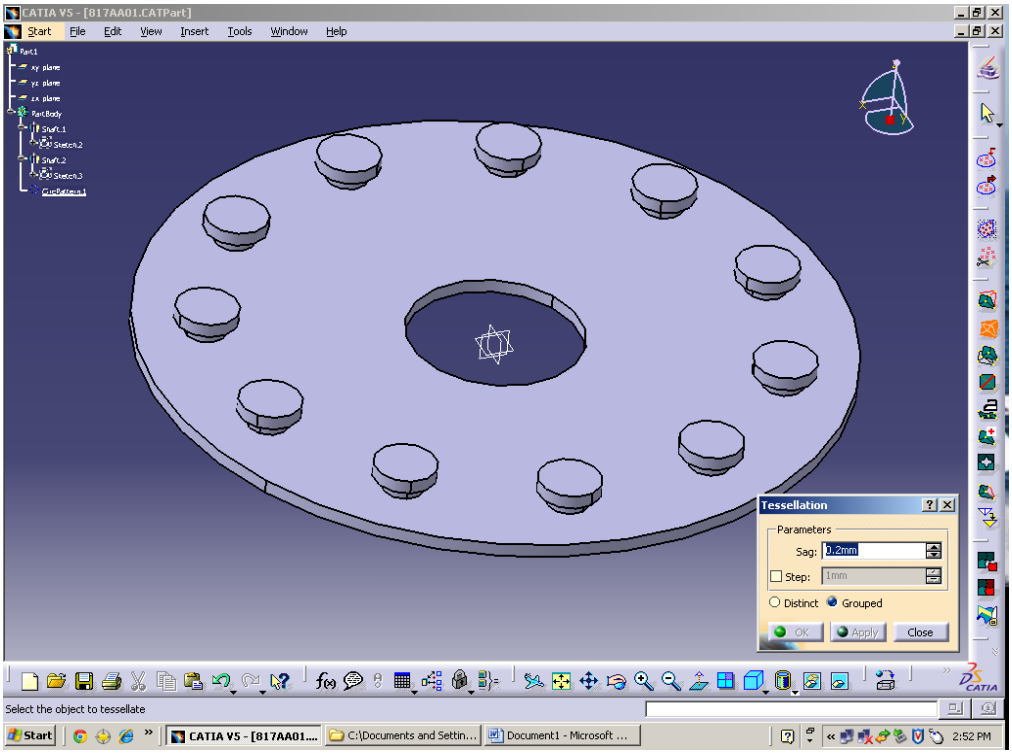

Appendix B-5: Catia Environment- Tessellation Sag

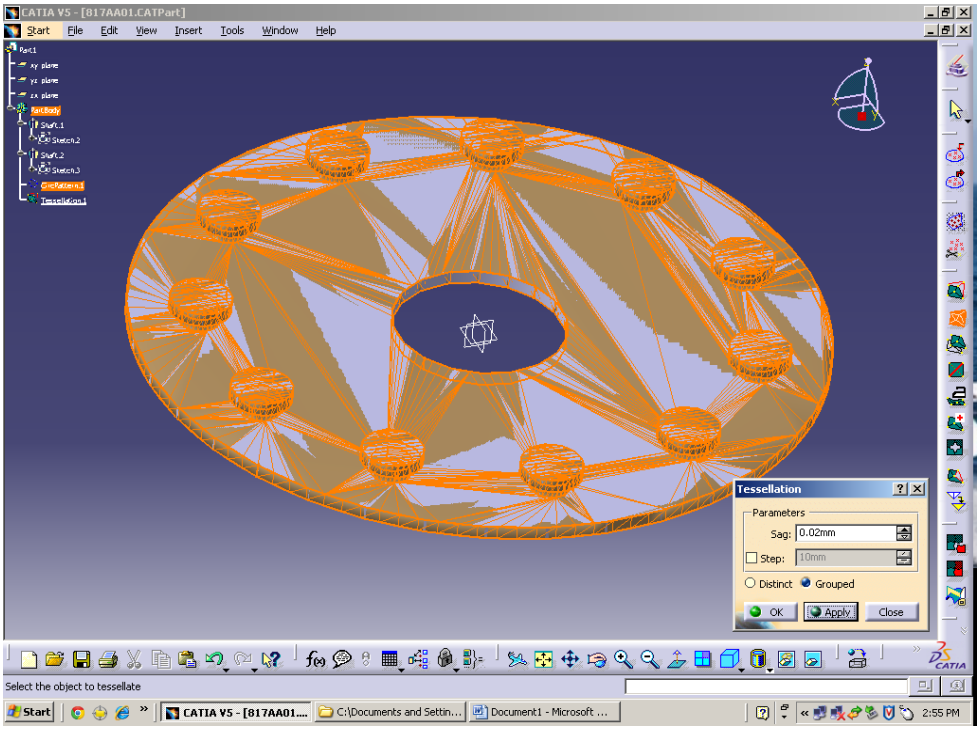

Appendix B-6: Catia Environment- Selection Part for Tessellation

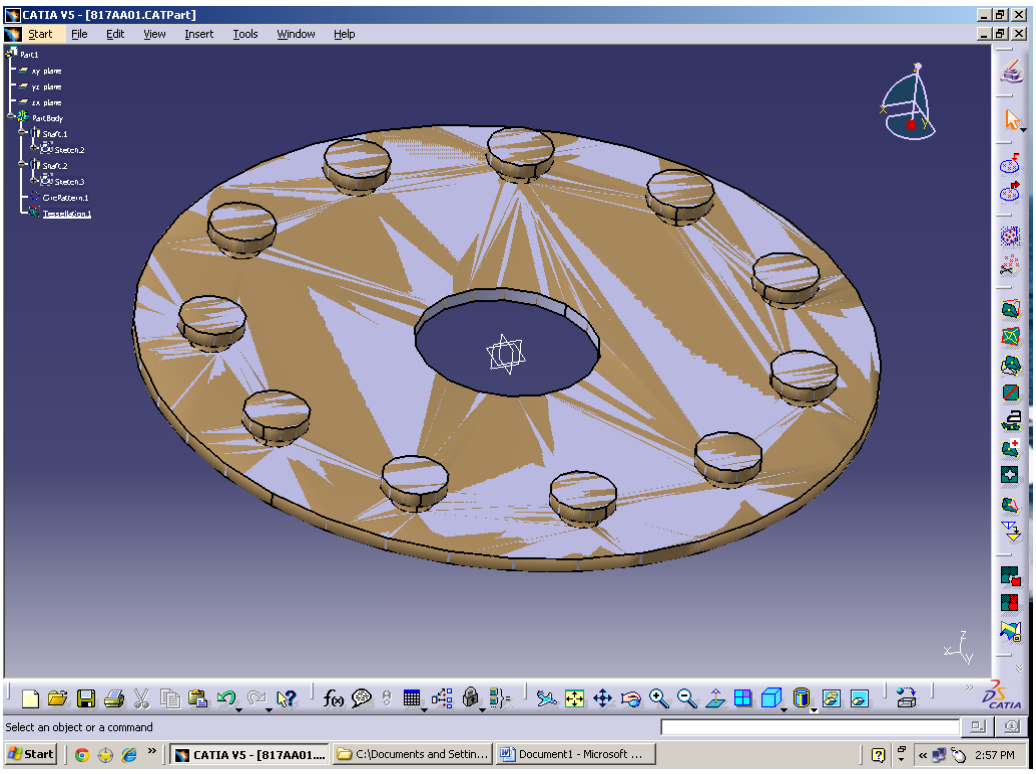

Appendix B-7: Catia Environment- Applying Tessellation

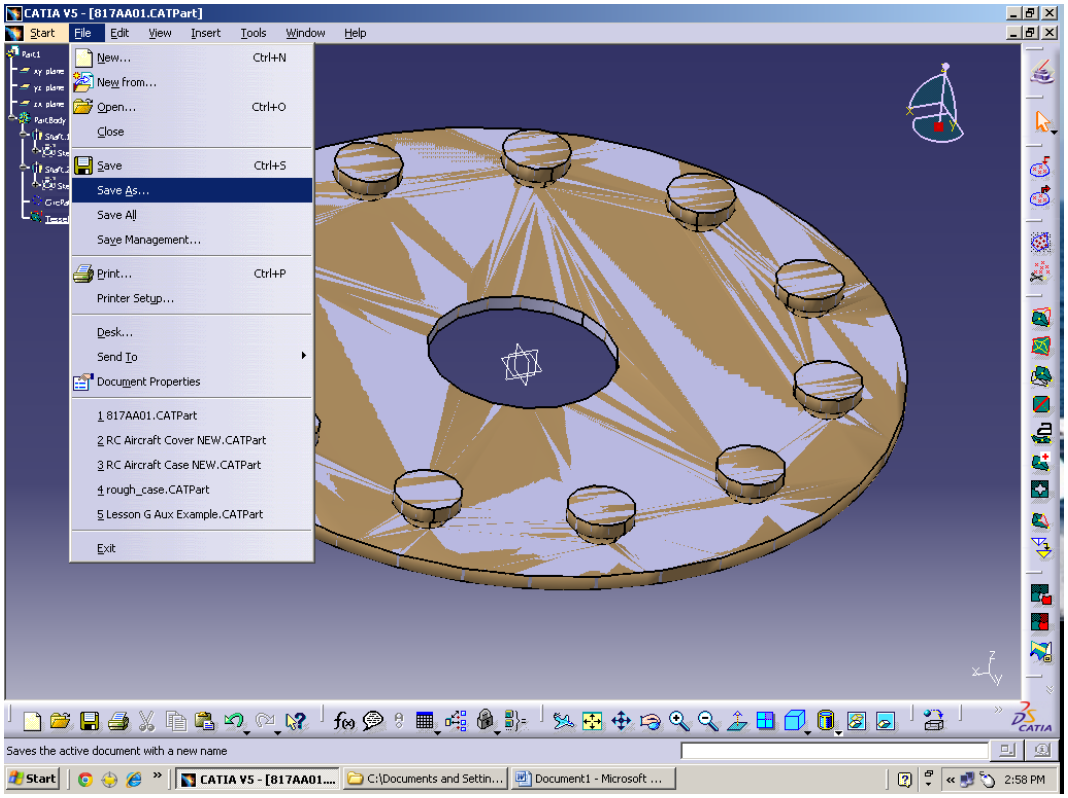

Appendix B-8: Catia Environment- Saving the File

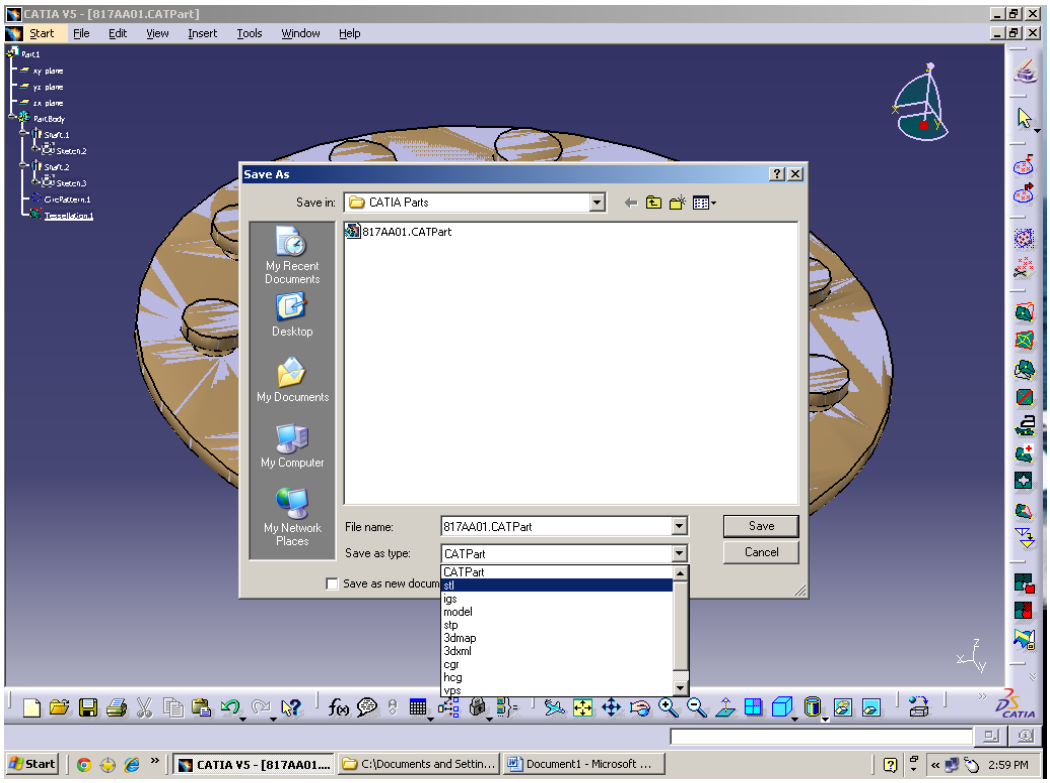

Appendix B-9: Catia Environment- Saving File as .stl

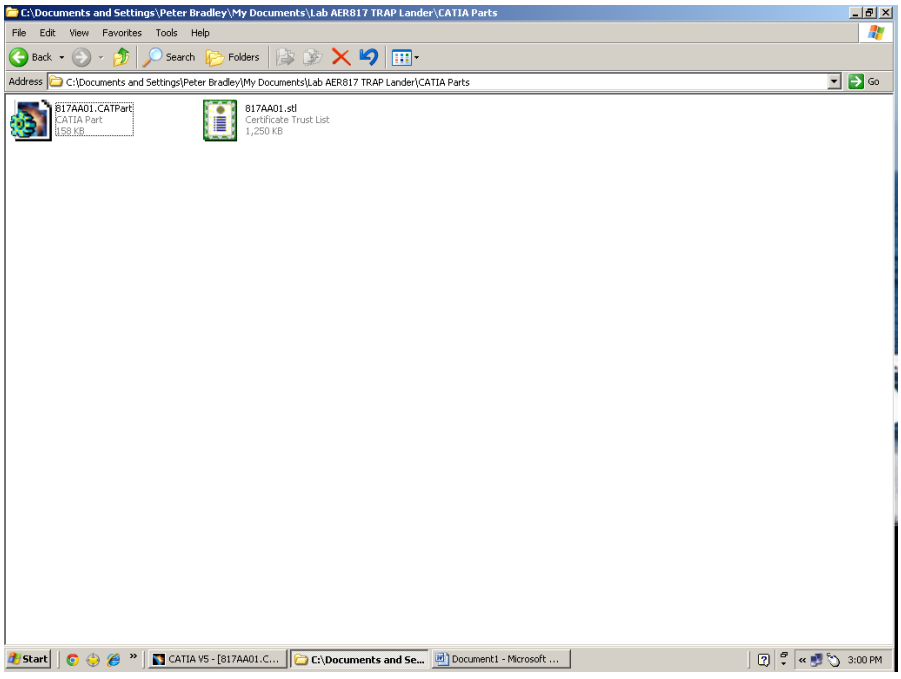

Appendix B-10: Catia Environment- .stl File